

**SYNTHESIS OF NOVEL THIAZOLINONE DERIVATIVES AND  
INVESTIGATION OF THEIR EFFECTS ON AROMATASE ENZYME**

**Master's Degree Thesis**

**Anfal Abdalla Awadelgeed ABDALLA**

**Eskişehir 2022**

**SYNTHESIS OF NOVEL THIAZOLINONE DERIVATIVES AND  
INVESTIGATION OF THEIR EFFECTS ON AROMATASE ENZYME**

**Anfal Abdalla Awadelgeed ABDALLA**

**Master's Degree Thesis**

**Department of Pharmaceutical Chemistry**

**Supervisor: Prof. Dr. Ahmet Çağrı KARABURUN**

**Eskişehir**

**Anadolu University**

**Graduate School of Health Sciences**

**June 2022**

## FINAL APPROVAL FOR THESIS

This thesis titled "Synthesis of novel thiazolinone derivatives and investigation of their effects on aromatase enzyme" has been prepared and submitted by Anfal Abdalla awadelgeed ABDALLA in partial fulfillment of the requirements in "Anadolu University Directive on Graduate Education and Examination" for the degree of Master of Science (MS) in Pharmaceutical Chemistry Department has been examined and approved on 28/06/2022.

### Committee Members

### Signature

Member (Supervisor): Prof. Dr. Ahmet Çağrı KARABURUN	.....
Member : Assoc. Prof. Dr. Murat DURAN	.....
Member : Prof. Dr. Nalan GÜNDOĞDU-KARABURUN	.....

Prof. Dr. Gülşen Akalın ÇİFTÇİ  
Director of Graduate School of Health Sciences

## ABSTRACT

### SYNTHESIS OF NOVEL THIAZOLINONE DERIVATIVES AND INVESTIGATION OF THEIR EFFECTS ON AROMATASE ENZYME

Anfal Abdalla Awadelgeed ABDALLA

Department of Pharmaceutical Chemistry

Anadolu University, Graduate School of Health Sciences, June 2022

Supervisor: Prof. Dr. Ahmet Çağrı KARABURUN

Aromatase enzyme is an essential cytochrome P450 subtype. It is responsible for the rate-limiting steps in the biosynthesis of estrogen from androgen in human being and the synthesis of ergosterol from lanosterol in fungi by the (CYP19A1) and (CYP51) subtypes, respectively. Aromatase inhibitors interfere with these synthetic steps. Thus, they have been used for postmenopausal women with estrogen dependent breast cancer. However, hormonal therapy of estrogen-responsive malignancy has been used to prolong the disease-free time in females and to improve their quality of life. AIs additionally interfere with ergosterol biosynthesis, an essential part of the fungal cell membrane this explaining the usage of AIs as an antifungal agent. Although scientists have been focusing on finding a radical cure for these diseases, the emergence of resistance, and the side effects associated with drugs available in the market, boost the need for new selective non-steroidal AIs. Inspired by the previously mentioned facts and by using our practical information on rational drug design and synthesis, a series of new benzothiazole-based thiazolinone derivatives were synthesized and their structures were elucidated and confirmed by analytical methods. In general, the aims of our study were achieved, and the synthesized derivatives showed inhibition to aromatase enzyme. Compound **3b** is the most active analog with  $IC_{50}$   $0.041 \pm 0.002$  ( $\mu$ M) and letrozole drug used as positive control. The compound **3i** showed inhibition by more than 70% at  $10^{-3}$ M. The *in silico* studies were used to determine the possible interaction mode of the compound **3b** and receptor. The findings from this study will participate positively in discovering new, potent, and selective third generation NSAIs and will support future research on aromatase enzymes.

**Keywords:** Aromatase, Breast cancer, Antifungal, Thiazolinone, Benzothiazole

## ÖZET

### YENİ BAZI TİYAZOLİNON TÜREVLERİNİN SENTEZİ VE AROMATAZ ENZİMİ ÜZERİNE ETKİLERİNİN İNCELENMESİ

Anfal Abdalla Awadelgeed ABDALLA

Farmasötik Kimya Anabilim Dalı

Anadolu Üniversitesi, Sağlık Bilimleri Enstitüsü, Haziran 2022

Danışman: Prof. Dr. Ahmet Çağrı KARABURUN

Aromataz enzimi, temel bir sitokrom P450 alt tipidir. Sırasıyla (CYP19) ve (CYP51) alt tipleri ile insanda androjenden östrojen biyosentezindeki hız sınırlayıcı adımdan ve mantarlarda lanosterolden ergosterol sentezinden sorumludur. Aromataz inhibitörleri (Aİ) bu sentetik adımlara müdahale eder. Bu nedenle, hormona bağımlı meme kanseri olan postmenopozal kadınlar için kullanılmıştır. Bununla birlikte, östrojene duyarlı malignitenin hormonal tedavisi, kadınlarda hastalıksız süreyi uzatmak ve yaşam kalitelerini iyileştirmek için kullanılmıştır. Aİ'ler ayrıca mantar hücre zarının önemli bir parçası olan ergosterol biyosentezine de müdahale eder ve bu, Aİ'lerin antifungal etkinliklerini açıklar. Bilim adamları bu hastalıklar için radikal bir tedavi bulmaya odaklanmış olsalar da direncin ortaya çıkması ve piyasada bulunan ilaçlarla ilişkili yan etkiler, yeni seçici steroidal olmayan Aİ'lere olan ihtiyacı artırmaktadır. Daha önce bahsedilen gerçeklerden esinlenerek ve rasyonel ilaç tasarımı ve sentezi konusundaki pratik bilgilerimizden yararlanılarak bir dizi yeni benzotiyazol bazlı tiyazolinon türevi sentezlenmiş ve yapıları analitik yöntemlerle doğrulanmıştır. Genel olarak çalışmamız amaçlarına ulaşmış ve sentezlenen türevler aromataz enzimine karşı inhibisyon göstermiştir. Bileşik **3b**,  $IC_{50}$   $0.041 \pm 0.002$  ( $\mu$ M) değeri ile en aktif analogdur, letrozole ilacı pozitif kontrol olarak kullanılmış ve bileşik **3i** %70'in üzerinde inhibisyon göstermiştir. Bileşik **3b** ve reseptörün olası bağlanma şeklini belirlemek için *in silico* çalışmalar gerçekleştirilmiştir. Bu çalışmadan elde edilen bulgular, yeni, güçlü ve seçici üçüncü nesil NSAİ'lerin keşfedilmesine olumlu katkıda bulunacak ve aromataz enzimleri üzerine gelecekteki araştırmaları destekleyecektir.

**Anahtar Sözcükler:** Aromataz, Meme kanseri, Antifungal, Tiyazolinon, Benzotiyazol

*If you really want to do something, you will find a way if you do not you will find excuses. My goal is to realize my father's dream of seeing me as a master's degree and Ph.D. holder, and there are no excuses. The appropriate time has come for me to make good on my promise to make your dream come true.*

*You could not wait till today, my dearest dad. Please accept my apologies for not completing this earlier. May ALLAH grant you a place in Jannat Al Firdous. You are the inspiration for this thesis.*

## ACKNOWLEDGEMENTS

20/05/2022

In the start, I thank **ALLAH**, the omnipotent, for providing me this opportunity and equipping me with the patience and skills I need to go on and to succeed. There are many people who have supported and aided me during my master's journey; it is a pleasure for me that I can finally thank each of these people individually.

First of all, I would like to show my honest thanks to my supervisor **Prof. Dr. Ahmet Çağrı KARABURUN**, who listens to me carefully, urging me to try new things and guiding me through the process of learning, experiencing, and practicing. He increased my eagerness in medicinal chemistry and surrounded me with full support. I might not have dreamed of a better, more accessible, and more helpful master's supervisor than you.

The words of thanks would never reflect my gratefulness and my appreciation for the unlimited support since the first day I came to the laboratory, and I decided to work despite my health issue, to my nearer great mentor **M. Pharm. Asaf Evrim EVREN, Pharm. Chem.**, he taught me practical skills starting from the tiny things in the lab, prompting me to think, analyze, report, and write more thoughtfully and clearly from the beginning. He was not stingy in sharing any information or assistance I asked for. Moreover, he has motivated me to think positively and encouraged me to look on the bright side aspects of life.

I also appreciate his effort in doing docking studies. I am honestly indebted for everything you did for me.

I want to express my gratitude to **Prof. Dr. Leyla YURTTAŞ**, who helped me practically, and provided countless suggestions and ideas on how to go about each stage. And I appreciate her spiritual support for me during my research period.

I am also thankful to the respectful teachers at Anadolu University Department of Pharmaceutical Chemistry for accommodating time, patience, and kindness, **Assoc. Prof. Dr. Begüm Nurpelin SAĞLIK** for examining the biological activity of the newly synthesized compounds, **Res. Sci. Süleyman YUR** and **Lab. Tech. Betül AYDIN** for doing spectroscopic analysis, recording, and interpreting the spectral data.

I am very grateful to Turks Abroad and Related Communities (**YTB**) for giving me this opportunity to visit turkey and to start my postgraduate study here and for the financial support.

I would like to appreciate the spirit of the working environment made by the informative collaboration with colleges (**Demokrat, Sam, Amal, Sana, Shorouq, Abdalrahman...**), and I will never forget the moment we spent together in the Laboratory.

A sincere letter of thanks and appreciation to my lovely mother **Zainab**, who has always been my inspiration and motivation to do what I dreamed for, and to my dearest sister **Azza** for her ultimate moral support and their assistance to me hand by hand to complete my master's course while experiencing my first maternity period. And I would give special thanks to my sisters (**Alla, Amal, and Aliaa**) for standing beside me to do all my best. Nothing compensates for your heartfelt support.

To my small **FAMILY**, nothing compares to the unspoken support provided with love by my husband, **Modather Alwasela**. Without your help, I would not have been able to receive this degree. To my little son **Abdalla** I am blessed with support made by your small hands in the middle of my master's journey. You pushed me forward and encouraged me never to give up. With you both at my side, I don't have anything left to desire in this world. May Allah save you.

Last but not least, I might give exceptional thanks to my friends abroad (**Hind, Muhgat, Salma, Entissar, Mayada, Eman, and Abdalrahman**) because they have been a source of comfort and assistance in several ways, and because of their love and support have been a lifeboat for me.

20/05/2022

## **STATEMENT OF COMPLIANCE WITH ETHICAL PRINCIPLES AND RULES**

I hereby truthfully declare that this thesis is an original work prepared by me; that I have behaved in accordance with the scientific ethical principles and rules throughout the stages of preparation, data collection, analysis and presentation of my work; that I have cited the sources of all the data and information that could be obtained within the scope of this study, and included these sources in the references section; and that this study has been scanned for plagiarism with “scientific plagiarism detection program” used by Anadolu University, and that “it does not have any plagiarism” whatsoever. I also declare that, if a case contrary to my declaration is detected in my work at any time, I hereby express my consent to all the ethical and legal consequences that are involved.

Anfal Abdalla Awadelgeed ABDALLA

## LIST OF CONTENTS

	<u>Page</u>
TITLE .....	i
FINAL APPROVAL FOR THESIS .....	ii
ABSTRACT.....	iii
ÖZET .....	iv
ACKNOWLEDGEMENTS .....	vi
STATEMENT OF COMPLIANCE WITH ETHICAL PRINCIPLES AND RULES .....	viii
LIST OF CONTENTS.....	ix
LIST OF TABLES .....	xiii
LIST OF FIGURES.....	xiv
LIST OF ABBREVIATIONS .....	xviii
1. INTRODUCTION .....	1
1.1. Aromatase Inhibitors and Breast Cancer .....	2
1.2. Aromatase Inhibitors and Antifungal Activity .....	6
1.3. Aromatase Inhibitors and Prostate Cancer .....	6
1.4. Aromatase Inhibitor and Cognitive Impairment.....	7
2. LITERATURE REVIEW .....	8
2.1. General Information about Thiazolinone Ring.....	8
2.2. Synthesis Methods of The Thiazolinone Ring .....	8
2.2.1. Hantzsch method.....	8
2.2.2. Liebermann synthesis .....	9
2.2.3. Reeve’s synthesis .....	9
2.2.4. One pot synthesis.....	10
2.3. Thiazole/Thiazolinone Derivatives That have Anticancer /Aromatase Inhibitor Activity .....	10

2.4. Thiazole/Thiazolinone Derivatives That have Antifungal/Aromatase Inhibitor Activity .....	14
2.5. General Information about Benzothiazole Ring .....	15
2.6. Synthesis Methods of Benzothiazole Ring.....	16
2.6.1. Hofmann synthesis .....	16
2.6.2. Jacobson cyclization.....	16
2.6.3. Synthesis of benzothiazole mediated by iodine.....	16
2.7. Benzothiazole Derivatives That have Anticancer/ Aromatase Inhibitor Activity.....	17
2.8. Benzothiazole Derivatives That have Antifungal/ Aromatase Inhibitor Activity.....	18
2.9. Thiazolinone and Benzothiazole Hybrid That have Biological Activity ....	20
3. MATERIALS .....	22
3.1. Chemicals.....	22
3.2. Instruments and Tools .....	23
4. EXPERIMENTAL METHODS .....	24
4.1. Chemical Synthesis Methods.....	24
4.1.1. A general method for the synthesis of 2-chloro-N-(5-methylbenzothiazol-2-yl)acetamide (A).....	24
4.1.2. A general method for the synthesis of 2-[(5-methylbenzothiazol-2-yl)amino] thiazol-4(5 <i>H</i> )-one (B) .....	24
4.1.3. A general method for the synthesis of 2-[(5-methylbenzothiazol-2-yl)[2-oxo-2-(substituent)ethyl]amino]thiazol-4(5 <i>H</i> )-one (C).....	24
4.2. Monitoring the Chemical Reaction.....	25
4.2.1. Thin-layer chromatography .....	25
4.3. Melting Point Determination .....	25
4.4. Chemical Analysis .....	26
4.4.1. Infra-red (IR) spectrometry .....	26

4.4.2. High resolution mass spectrometry (HRMS) .....	26
4.4.3. Proton nuclear magnetic resonance ( <sup>1</sup> H-NMR) spectrometry.....	26
4.4.4. Carbon-13 nuclear magnetic resonance ( <sup>13</sup> C-NMR) spectrometry.....	26
4.5. Investigation of Aromatase Inhibition Activity (AI).....	26
4.6. Molecular Modeling Studies.....	27
<b>5. RESULTS AND DISCUSSIONS .....</b>	<b>28</b>
5.1. Synthesis of The Targeted Products.....	28
5.1.1. Synthesis of 2-chloro-N-(5-methylbenzothiazol-2-yl)acetamide .....	28
5.1.2. Synthesis of 2-[(5-methylbenzothiazol-2-yl)amino]thiazol-4(5 <i>H</i> )- one .....	29
5.1.3. Synthesis of 2-[(5-methylbenzothiazol-2-yl)[2-oxo-2- (substituent)ethyl]amino]thiazol-4(5 <i>H</i> )-one.....	30
5.1.3.1. 2-[(5-ethylbenzothiazol-2-yl)(2-oxo-2- phenylethyl)amino]thiazol-4(5 <i>H</i> )-one.....	31
5.1.3.2. 2-[(5-methylbenzothiazol-2-yl)[2-oxo-2-( <i>p</i> - tolyl)ethyl]amino]thiazol-4(5 <i>H</i> )-one .....	36
5.1.3.3. 2-[[2-(4-methoxyphenyl)-2-oxoethyl](5- methylbenzothiazol-2-yl)amino]thiazol-4(5 <i>H</i> )-one .....	41
5.1.3.4. 2-[(5-methylbenzothiazol-2-yl)[2-(naphthalen-2-yl)-2- oxoethyl]amino]thiazol-4(5 <i>H</i> )-one .....	46
5.1.3.5. 2-[[2-(4-fluorophenyl)-2-oxoethyl](5-methylbenzothiazol- 2-yl)amino]thiazol-4(5 <i>H</i> )-one .....	51
5.1.3.6. 2-[[2-(4-chlorophenyl)-2-oxoethyl](5-methylbenzothiazol- 2-yl)amino]thiazol-4(5 <i>H</i> )-one .....	56
5.1.3.7. 4-[N-(5-methylbenzothiazol-2-yl)-N-(4-oxo-4,5- dihydrothiazol-2-yl)glycyl]benzotrile .....	61
5.1.3.8. 2-[[2-(2,4-dichlorophenyl)-2-oxoethyl](5- methylbenzothiazol-2-yl)amino]thiazol-4(5 <i>H</i> )-one .....	66

5.1.3.9. 2-[[2-(3,4-dichlorophenyl)-2-oxoethyl](5-methylbenzothiazol-2-yl)amino}thiazol-4(5 <i>H</i> )-one .....	71
5.1.3.10. 2-[[2-(benzofuran-2-yl)-2-oxoethyl](5-methylbenzothiazol-2-yl)amino}thiazol-4(5 <i>H</i> )-one .....	76
<b>5.2. Chemical Analysis Results.....</b>	<b>81</b>
5.2.1. IR spectrometry.....	81
5.2.2. <sup>1</sup> H-NMR analysis results.....	81
5.2.3. <sup>13</sup> C-NMR analysis results.....	82
5.2.4. Mass spectrometry .....	82
<b>5.3. Results and Discussion of Aromatase Inhibition Activity .....</b>	<b>83</b>
<b>5.4. Pharmacokinetic Profile .....</b>	<b>83</b>
<b>5.5. Molecular Docking Analysis.....</b>	<b>85</b>
<b>5.6. Structure Activity Relationship Study .....</b>	<b>88</b>
<b>6. CONCLUSION AND RECOMMENDATIONS.....</b>	<b>90</b>
<b>RESUME</b>	

## LIST OF TABLES

	<u>Page</u>
<b>Table 1.1.</b> Classification of BC according to molecular subtype and its relation to immunohistochemical markers (ICMs) .....	<b>3</b>
<b>Table 5.1.</b> The % of inhibition of the synthesized compounds against aromatase enzyme at $10^{-3}$ and $10^{-4}$ M concentrations and $IC_{50}$ ( $\mu$ M) values .....	<b>83</b>
<b>Table 5.2.</b> The <i>in silico</i> physicochemical parameters .....	<b>84</b>

## LIST OF FIGURES

	<u>Page</u>
<b>Figure 1.1.</b> Aromatization of ring A by aromatase enzyme CYP19 .....	1
<b>Figure 1.2.</b> Function of aromatase enzyme CYP51 .....	1
<b>Figure 1.3.</b> Aromatase inhibitors .....	4
<b>Figure 1.4.</b> Optimization of aromatase inhibitory activities .....	5
<b>Figure 1.5.</b> First 2-phenyl benzothiazole derivative with interesting anticancer activity .....	6
<b>Figure 1.6.</b> Structure of anazole antifungal ketoconazole.....	6
<b>Figure 2.1.</b> 1,3 thiazole and 1,3-thiazolin-4-one structures and numbering system .....	8
<b>Figure 2.2.</b> (a) 2-amino-thiazolinone, (b) 2-imino-thiazolidinone (pseudothiohydantoin), (c) 1,3-thiazolidin-2,4-dione (glitazone), (d) 2-thioxo-1,3-thiazolidin-4-one (rhodanine) .....	8
<b>Figure 2.3.</b> Synthesis of 1,3-thiazolinone according to hantzsch method .....	9
<b>Figure 2.4.</b> Schematic representation for the original synthesis of N,N'- diphenyl-pseudothiohydantoin (Lange's diphenylsulfohydantoin) .....	9
<b>Figure 2.5.</b> Schematic representation for synthesis of 2-imino-4- thiazolidinone by reeve's method .....	10
<b>Figure 2.6.</b> Synthesis of 2-imino-4-thiazolidinone by one pot method .....	10
<b>Figure 2.7.</b> Compounds (7k) (S)-2-[(4-diethylaminophenyl)imino]-3- (thiophen-2-ylmethyl) thiazolidin-4one, (7m) (S)-2-[(4-propane-1- aminophenyl)imino]-3-(thiophen-2-ylmethyl) thiazolidin-4one, (7n) (S)-2-[(4-pyrrolidinophenyl)imino]-3-(thiophen-2-ylmethyl) thiazolidin- 4one.....	11
<b>Figure 2.8.</b> Compound (10) methyl 2-hydroxy-5-[(5-(4-bromobenzylidene)- 4-oxo-4,5-dihydro-1,3-thiazol-2-yl)-amino]benzoate.....	11
<b>Figure 2.9.</b> Compound (1) 4-(2-Hydroxyphenyl)-2-(pyrimidine-2-yl)thiazole .....	12
<b>Figure 2.10.</b> Compounds (HH3) methyl -2-hydroxy-5-[(5-(4-methylbenzylidene) -4-oxo-4,5-dihydrothiazol-2-yl)amino]benzoate, (HH13) methyl-5- [(5-(4-(dimethylamino)benzylidene)-4-oxo-4,5-dihydrothiazol- 2-yl)amino]-2-hydroxybenzoate .....	12
<b>Figure 2.11.</b> Compounds (2g) 4-(4-chlorophenyl)-2-[2-(2-methyldihy drofuran-3(2 <i>H</i> )-ylidene) hydrazineyl]thiazole, (21) 4-	

(2,4-dichlorophenyl)-2-[2-(2-methyldihydrofuran-3(2 <i>H</i> )-ylidene)hydrazineyl]thiazole .....	13
<b>Figure 2.12.</b> Compound (2q) Ethyl 2-(2-{2-[(6-methoxynaphthalen-2-yl)methylene]hydrazinyl}thiazol-4-yl)acetate.....	13
<b>Figure 2.13.</b> Compound (2e) 2-{2-[ ( <i>IH</i> -imidazol-4-yl)methylene]hydrazineyl}-4-(4-nitrophenyl)thiazole.....	13
<b>Figure 2.14.</b> Compounds named 2-[5-(2-chloro-6-methylquinolin-3-yl)-3-(aryl)-4,5-dihydro- <i>IH</i> -pyrazol-1-yl]thiazol-4(5 <i>H</i> )ones.....	14
<b>Figure 2.15.</b> Compounds (9b) 5-(2,4-Dichlorobenzylidene)-2-(naphthalen-1-ylamino)thiazol-4(5 <i>H</i> )-one, (10) 2-(methylamino)thiazol-4(5 <i>H</i> )-one .....	14
<b>Figure 2.16.</b> Compound (3) 2-[(2-(hexan-3-ylidene)hydrazo]-4-(4-chlorophenyl)-thiazole .....	15
<b>Figure 2.17.</b> Compound (5e) 3-ethyl-4-methyl-2-({1-[4-(quinolin-2-yloxy)phenyl]ethylidene}hydrazono)-2,3-dihydrothiazole.....	15
<b>Figure 2.18.</b> Structure and numbering of benzothiazole ring .....	15
<b>Figure 2.19.</b> Schematic representation for the synthesis of benzothiazoles from 2-aminothiophenol according to Hofmann.....	16
<b>Figure 2.20.</b> Benzothiazole synthesized by ipso substitution according to Jacobson....	16
<b>Figure 2.21.</b> Synthesis of benzothiazoles mediated by iodine .....	17
<b>Figure 2.22.</b> Compound (9a) 2-(4-amino-3-methylphenyl)benzothiazole.....	17
<b>Figure 2.23.</b> Compound (5e) 4-chloro-1-dimethylaminomethyl-3-(6-methylbenzothiazol-2-ylimino)-1,3-dihydroindol-2-one.....	17
<b>Figure 2.24.</b> (Phortress) 2,6-diamino- <i>N</i> -[4-(5-fluorobenzothiazol-2-yl)-2-methylphenyl]hexanamide.....	18
<b>Figure 2.25.</b> Compound (26)3-(benzothiazol-2-yl)-6-fluoro-2 <i>H</i> -chromen-2-one .....	18
<b>Figure 2.26.</b> Compound (14p) Isobutyl( <i>S</i> )-2-(6-bromobenzothiazole-2-carboxamido)-3-( <i>IH</i> -imidazol-1-yl)propanoate.....	19
<b>Figure 2.27.</b> Compound (6h) 1-[2-(benzothiazol-2-ylmethoxy)phenyl]ethanone .....	19
<b>Figure 2.28.</b> Compound (4f) 2-[(2-Chlorobenzyl)sulfonyl]benzothiazole, (4k) 2-[(4-Methylbenzyl)-sulfonyl]benzothiazole.....	20
<b>Figure 2.29.</b> Compound (6) 2-{2-[3-(Benzothiazol-2-ylamino)-4-oxo-2-thioxothiazolidin-5-ylidenemethyl]-4-chlorophenoxy}- <i>N</i> -(4-methoxyphenyl)-acetamide .....	20

<b>Figure 2.30.</b> Compound (PP2) 2-{3-[2-(4-Chlorophenyl)-4-oxothiazolidin-3-yl]phenyl} benzothiazole-6-carboxylic acid.....	<b>21</b>
<b>Figure 2.31.</b> Compound (5b) 2-[(6-fluorobenzothiazol-2-yl)imino]-5-[(4-isopropylpiperazin-1-yl)methylene]thiazolidin-4-one.....	<b>21</b>
<b>Figure 4.1.</b> The general synthesis method of compounds (3a-3j) .....	<b>25</b>
<b>Figure 5.1.</b> Mechanism of acetylation reaction of 5-methylbenzothiazol-2-amine .....	<b>28</b>
<b>Figure 5.2.</b> Mechanism of cyclization of thiazolinone ring [89] .....	<b>29</b>
<b>Figure 5.3.</b> Mechanism of reaction for the synthesis of the final derivatives .....	<b>30</b>
<b>Figure 5.4.</b> IR spectrum of the compound 3a .....	<b>32</b>
<b>Figure 5.5.</b> <sup>1</sup> H-NMR spectrum of the compound 3a.....	<b>33</b>
<b>Figure 5.6.</b> <sup>13</sup> C-NMR spectrum of the compound 3a.....	<b>34</b>
<b>Figure 5.7.</b> Mass spectrum of the compound 3a .....	<b>35</b>
<b>Figure 5.8.</b> IR spectrum of the compound 3b .....	<b>37</b>
<b>Figure 5.9.</b> <sup>1</sup> H-NMR spectrum of the compound 3b .....	<b>38</b>
<b>Figure 5.10.</b> <sup>13</sup> C-NMR spectrum of the compound 3b .....	<b>39</b>
<b>Figure 5.11.</b> Mass spectrum of the compound 3b.....	<b>40</b>
<b>Figure 5.12.</b> IR spectrum of the compound 3c.....	<b>42</b>
<b>Figure 5.13.</b> <sup>1</sup> H-NMR spectrum of the compound 3c.....	<b>43</b>
<b>Figure 5.14.</b> <sup>13</sup> C-NMR spectrum of the compound 3c.....	<b>44</b>
<b>Figure 5.15.</b> Mass spectrum of the compound 3c .....	<b>45</b>
<b>Figure 5.16.</b> IR spectrum of the compound 3d .....	<b>47</b>
<b>Figure 5.17.</b> <sup>1</sup> H-NMR spectrum of the compound 3d .....	<b>48</b>
<b>Figure 5.18.</b> <sup>13</sup> C-NMR spectrum of the compound 3d .....	<b>49</b>
<b>Figure 5.19.</b> Mass spectrum of the compound 3d.....	<b>50</b>
<b>Figure 5.20.</b> IR spectrum of the compound 3e.....	<b>52</b>
<b>Figure 5.21.</b> <sup>1</sup> H-NMR spectrum of the compound 3e.....	<b>53</b>
<b>Figure 5.22.</b> <sup>13</sup> C-NMR spectrum of the compound 3e .....	<b>54</b>
<b>Figure 5.23.</b> Mass spectrum of the compound 3e .....	<b>55</b>
<b>Figure 5.24.</b> IR spectrum of the compound 3f.....	<b>57</b>
<b>Figure 5.25.</b> <sup>1</sup> H-NMR spectrum of the compound 3f .....	<b>58</b>
<b>Figure 5.26.</b> <sup>13</sup> C-NMR spectrum of the compound 3f .....	<b>59</b>
<b>Figure 5.27.</b> Mass spectrum of the compound 3f.....	<b>60</b>
<b>Figure 5.28.</b> IR spectrum of the compound 3g .....	<b>62</b>

<b>Figure 5.29.</b> <sup>1</sup> H-NMR spectrum of the compound <b>3g</b> .....	<b>63</b>
<b>Figure 5.30.</b> <sup>13</sup> C-NMR spectrum of the compound <b>3g</b> .....	<b>64</b>
<b>Figure 5.31.</b> Mass spectrum of the compound <b>3g</b> .....	<b>65</b>
<b>Figure 5.32.</b> IR spectrum of the compound <b>3h</b> .....	<b>67</b>
<b>Figure 5.33.</b> <sup>1</sup> H-NMR spectrum of the compound <b>3h</b> .....	<b>68</b>
<b>Figure 5.34.</b> <sup>13</sup> C-NMR spectrum of the compound <b>3h</b> .....	<b>69</b>
<b>Figure 5.35.</b> Mass spectrum of the compound <b>3h</b> .....	<b>70</b>
<b>Figure 5.36.</b> IR spectrum of the compound <b>3i</b> .....	<b>72</b>
<b>Figure 5.37.</b> <sup>1</sup> H-NMR spectrum of the compound <b>3i</b> .....	<b>73</b>
<b>Figure 5.38.</b> <sup>13</sup> C-NMR spectrum of the compound <b>3i</b> .....	<b>74</b>
<b>Figure 5.39.</b> Mass spectrum of the compound <b>3i</b> .....	<b>75</b>
<b>Figure 5.40.</b> IR spectrum of the compound <b>3j</b> .....	<b>77</b>
<b>Figure 5.41.</b> <sup>1</sup> H-NMR spectrum of the compound <b>3j</b> .....	<b>78</b>
<b>Figure 5.42.</b> <sup>13</sup> C-NMR spectrum of the compound <b>3j</b> .....	<b>79</b>
<b>Figure 5.43.</b> Mass spectrum of the compound <b>3j</b> .....	<b>80</b>
<b>Figure 5.44.</b> The 2D pose of the compound <b>3b</b> with aromatase enzyme.....	<b>86</b>
<b>Figure 5.45.</b> The 3D pose of the compound <b>3b</b> with aromatase enzyme.....	<b>87</b>
<b>Figure 5.46.</b> The general requirements for aromatase inhibition activity.....	<b>89</b>

## LIST OF ABBREVIATIONS

BC	: Breast cancer
AIs	: Aromatase inhibitors
ER	: Estrogen receptor
PR	: Progesterone receptor
SERMs	: Selective estrogen receptor modulators
SERDs	: Selective estrogen receptor down regulators
HER-2	: Human epidermal growth factor receptor
NSAIs	: Non-steroidal aromatase inhibitors
SAIs	: Steroidal aromatase inhibitors
NADPH	: Nicotinamide adenine dinucleotide phosphate
IC <sub>50</sub>	: Inhibition concentration
TLC	: Thin layer chromatography
<sup>1</sup> H-NMR	: Proton nuclear magnetic resonance
<sup>13</sup> C-NMR	: Carbon nuclear magnetic resonance
HRMS	: High resolution mass spectroscopy
2D	: Two dimensions
3D	: Three dimensions
DMF	: Dimethyl formamide
THF	: Tetrahydro furan
TEA	: Triethyl amine
DMSO	: Dimethyl sulfoxide
RDD	: Rational drug design
SAR	: Structure activity relationship
ADME	: Absorption, distribution, metabolism, elimination
GI	: Gastrointestinal
HBA	: Hydrogen bond acceptor
HBD	: Hydrogen bond doner
DFS	: Disease free survival

## 1. INTRODUCTION

Aromatase enzymes belong to the family of cytochrome P450 monooxygenase, a human being (CYP19A1) subtype responsible for converting circulating testosterone and androstenedione to aromatic estrogens estradiol and estrone, respectively. This is done with the assistance of oxygen and (NADPH). Aromatase enzyme oxidizes the methyl group at C19 and converts the ketone group at C3 to hydroxyl leading to the aromatization of ring (A) **Figure 1.1**. However, aromatization is done in ovaries and peripheral tissues in premenopausal women and in peripheral tissues in postmenopausal women [1]. While the aromatase (CYP51) fungal subtype is responsible for converting lanosterol to ergosterol, an essential component in the fungal cell membrane **Figure 1.2** [2-4].

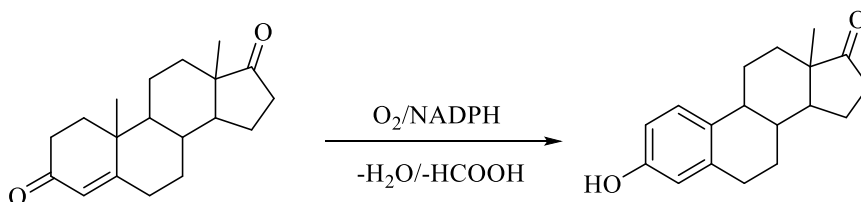


**Figure 1.1.** Aromatization of ring A by aromatase enzyme CYP19

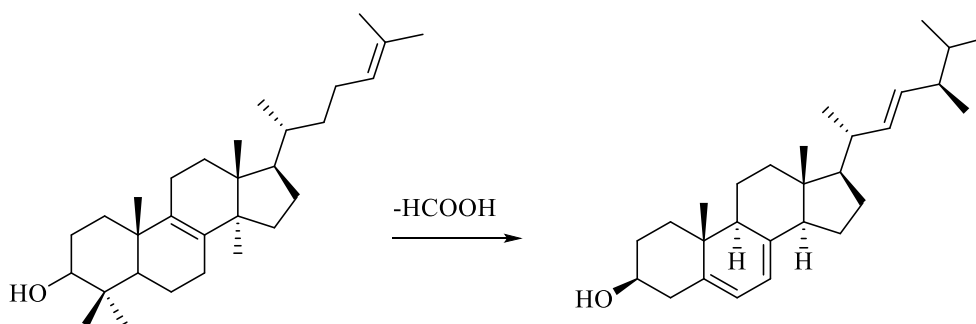


**Figure 1.2.** Function of aromatase enzyme CYP51

Aromatase inhibitors are class of drugs act by interfering with the action of aromatase enzymes. Thus, aromatase inhibitors interfere with the final steps that lead to estrogen biosynthesis and decrease the circulating estrogen level. As well as interfere with the synthesis of ergosterol, thus increasing cell membrane permeability, resulting in cell lysis and death [5].

Accordingly, aromatase inhibitors have been used as hormonal therapy for chemoprevention and the treatment of estrogen-responsive breast cancer, benign prostatic hyperplasia, and as antifungal agent [6].

From a chemical structure point of view, AIs can be classified as azoles, stilbene derivatives, and flavonoid analogs [7, 8].

### **1.1. Aromatase Inhibitors and Breast Cancer**

Breast cancer (BC) is the most common subtype of cancer that affects women and is the leading cause of mortality associated with cancer among females worldwide. Age, gender, and family history are the main risk factors for breast cancer [9, 10].

Like other malignancies, BC is a heterogeneous tumor with widely diverse molecular subtypes. Breast neoplasm can be subclassified according to molecular subtype identified by genetic profiling **Table 1.1**, according to the stage of disease (benign stage, atypical hyperplasia, preinvasive stage, metastatic carcinoma, and advanced stage), and according to the clinical therapeutic strategy, which in turn depend on the stage of diseases as well as the emergence of resistance (surgical, radiotherapy, and chemotherapeutic options) [11, 12].

Hormonal sensitive breast cancer is a subgroup of breast cancer in which the breast cancer cells have receptors for estrogen and progesterone hormones called (ER and PR) respectively. About two-thirds of the breast cancer among postmenopausal women fall under the subtype of hormonal-responsive breast cancer (or estrogen-sensitive); the circulating estrogen interacts with estrogen receptor in the cancer cell and stimulates the development and proliferation of the tumor. Thus, endocrine therapies that interfere with estrogen synthesis and interact with ER and block its action have been used for the treatment of and to prolong the disease-free period in affected females. Hormonal therapy can be classified to

1. Selective estrogen receptor modulators (SERMs), such as tamoxifen
2. Aromatase inhibitors (AIs), such as
  - i. Non-steroidal AIs; letrozole, anastrozole
  - ii. Steroidal AIs; exemestane
3. Selective estrogen receptor down-regulators (SERDs), such as fulvestran

SERMs act by interfering with the interaction of estrogen and its receptor that found in the cancer cell (estrogen agonist or antagonist). AIs block the interaction of estrogen with its receptor by interfering with its synthesis. While SERDs induce the degradation of the estrogen receptor [13, 14].

**Table 1.1.** Classification of BC according to molecular subtype and its relation to immunohistochemical markers (ICMs)

Molecular subtype	ER	PR	HER2
Luminal A	+	+	-
Luminal B	+	+	-
Luminal B	+	+	+
HER-2+	-	-	+
Basal like or triple negative	-	-	-

**ER:** estrogen receptor, **HER-2:** human epidermal growth factor receptor 2, **PR:** progesterone receptor

The concept of hormonal intervention in a patient with breast cancer was done by George Beatson in 1896, who tried estrogen deprivation to treat breast tumor by removing ovaries. Beatson’s idea developed with time, and over more than 70 years, Richard Santen and Alan Lipton tried the first aromatase inhibitor (aminoglutethimide) for malignant tumors [15].

The first-generation aromatase inhibitor (aminoglutethimide) is associated with side effects drowsiness and rashes limited its use, followed by the second-generation aromatase inhibitors (formestane and fadrozole) with higher selectivity. However, their clinical usage were arrested after the third generation emerged with potential activity, safety, and better pharmacokinetic properties **Figure 1.3** [16].

The third-generation aromatase inhibitors, non-steroidal AIs (letrozole and anastrozole), and steroidal AIs (exemestane) differ in the binding affinity to the aromatase enzyme as steroidal AIs bind irreversibly while non-steroidal AIs inhibit the enzyme reversibly. The third generation has been used in postmenopausal females with early-stage estrogen-responsive breast cancer according to 2018 guidelines from the American Society of Clinical Oncology (ASCO) as adjuvant therapy after 2-3 years of tamoxifen usage to be used for the next five years, and the next ten years after surgery to decrease recurrence and to prolong disease-free survival (DFS) equivalent to complete relieve [17, 18].

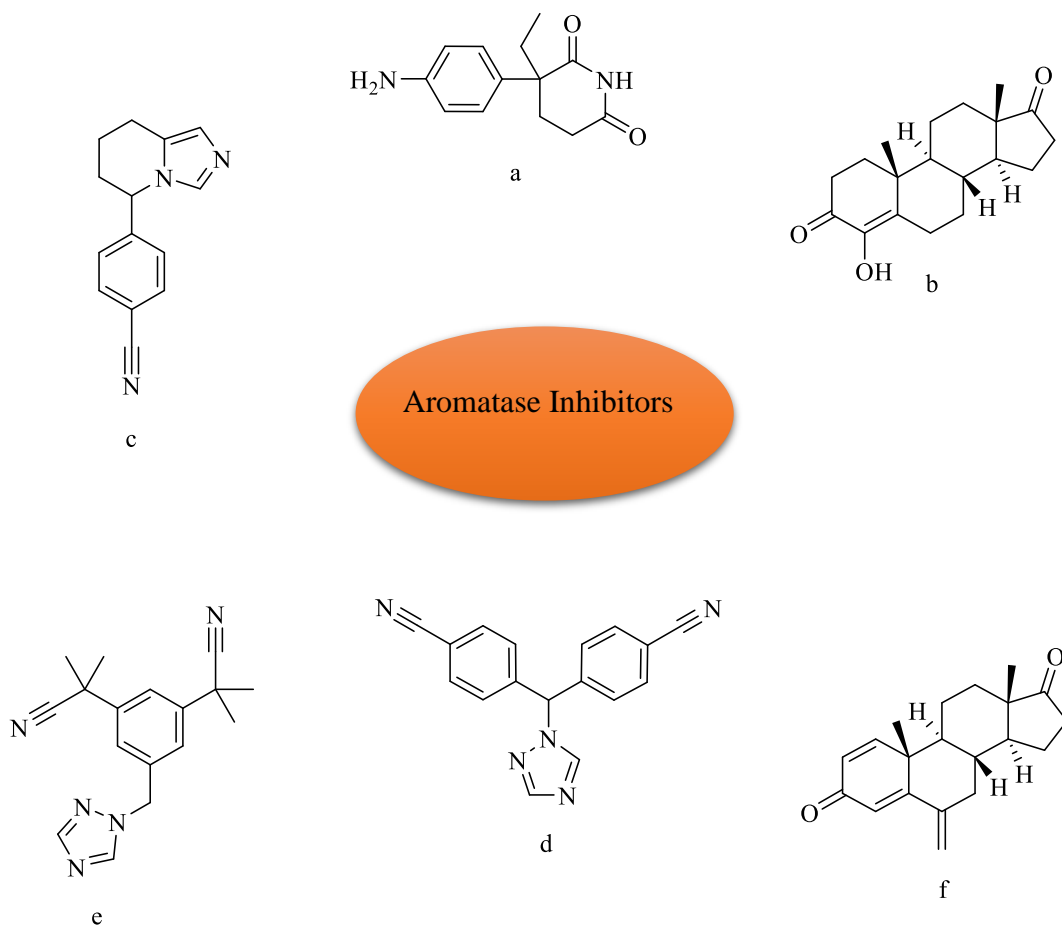


**Figure 1.3.** Aromatase inhibitors; a, aminoglutethimide, b, formestane, c, fadrozole, d, letrozole, e, anastrozole, f, exemestane

Azole containing heterocycles are of wide distribution naturally and synthetically and have a potential broad biological activity. Thiazole derivatives (thiazolinone and benzothiazole) have been intensely used in bio-isosteric replacements for designing and synthesizing new biological analogs as they are reported in the literature to have a broad spectrum of activity. 2-Amino thiazolinone and its tautomeric form 2-imino thiazolidin-4-one [19, 20] showed pharmacological activity as anticancer, anti-HIV, anti-influenza, anti-convulsant, antibacterial, antifungal, anti-diabetic, anti-inflammatory, analgesic and as aromatase inhibitors [21-32].

Synthesis of a new analog for the third-generation non-steroidal aromatase inhibitors according to the rational drug design (RDD) has been strongly recommended to produce a novel candidate with improved pharmacodynamic and pharmacokinetic activity. Synthesis of non-steroidal analogs is more beneficial than steroidal analogs

because SAIs are associated with severe adverse effects related to their similarity to androstenedione. According to the structure-activity relationship studies of the third-generation non-steroidal derivatives, the need for a hybrid of a nitrogen-containing heterocyclic ring and aromatic moiety separated by a particular distance is essential for activity because azole containing heterocycles make a coordination bond by its lone pair of electrons with ferrous ion ( $\text{Fe}^{+2}$ ) of the heme part of aromatase enzyme active binding site and this promoted the affinity of the product [33].

The incorporation of thiazole derivatives to improve aromatase inhibition was done in 2012 by Mayhoub et al., who replaced the ethylene bridge of resveratrol with an aromatic thiazole ring. Aromatase inhibition activity was reported to be improved by 6000-fold in a nanomolar  $\text{IC}_{50}$ . The hydrogen bonding with the receptor was also improved by replacing the phenyl with pyridine, thus the selectivity of analogs [7].

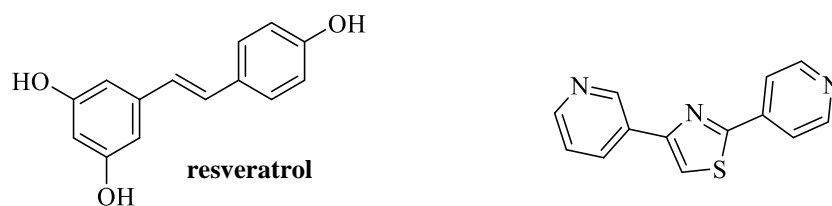


**Figure 1.4.** Optimization of aromatase inhibitory activities

The involvement of the bicyclic aromatic ring system was recommended from the structure-activity relationship studies of aromatase inhibitors because of the need for a bulky lipophilic group to interact with the hydrophobic portion of the enzyme and blocks estrogen synthesis. Benzothiazole ring is of particular interest because it has beamy evident pharmacological spectrum such as anti-microbial, anti-parasitic, anti-proliferative, anti-viral, sugar lowering, diuretic, anti-inflammatory, and many other activities [34-40].

The first cancer-fighting derivatives of the benzothiazole ring were synthesized in 1994 by Stevens et al., which are polyhydroxylated 2-phenyl benzothiazoles. The tested compounds against cancerous cell lines showed significant activity against breast cancer cell lines (MCF-7). These series were the triggering for the studies made on the benzothiazole ring system as anticancer [41].

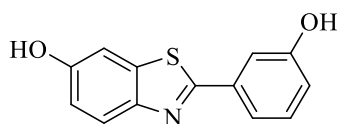


**Figure 1.5.** First 2-phenyl benzothiazole derivative with interesting anticancer activity

## 1.2. Aromatase Inhibitors and Antifungal Activity

Interference with the biosynthesis of sterol of the fungal cell membrane (called ergosterol) is the primary mechanism by which the azole antifungal available in the market (fluconazole, itraconazole, and ketoconazole) exert their actions [42].

The fungal aromatase enzyme lanosterol-14 $\alpha$ -demethylase (CYP51), which converts the lanosterol to ergosterol, simulates the human aromatase enzyme (CYP19) which is critical for estrogen biosynthesis. Both aromatases are inhibited by the same azole substrates that coordinate with the heme part of CYP450 subtypes and block their functions. This similarity explains the cross-sectional aromatase inhibition side effect of antifungal agents [43].

A study conducted in 1988 by W. Woljete et al. investigated the antifungal ketoconazole ability to inhibit human aromatase enzyme and compared it with aminoglutethimide as a positive control [6].

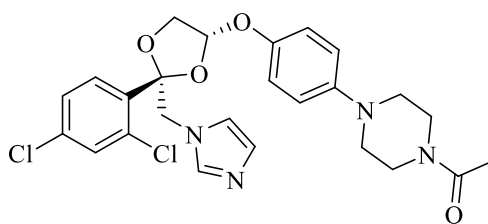


**Figure 1.6.** Structure of an azole antifungal ketoconazole

## 1.3. Aromatase Inhibitors and Prostate Cancer

The aromatase inhibitors have been tried to treat benign prostatic hyperplasia (BPH) and androgen-independent prostate cancer. Studies suggested that the prostate tissues are responsive to estrogen after being unresponsive to androgen, and aromatase enzyme synthesizes estrogen in the prostate tissue and stimulates prostatic hyperplasia. Despite the fact that estrogen contribution is mild, multiple studies have been conducted to investigate the effect of aromatase inhibitors in prostate cancer [44, 45].

The of-label usage of antifungal ketoconazole in resisting prostate cancer was explained by its non-selective inhibition of CYP450 subtypes and blocks the action of (CYP17A1) responsible for androgen biosynthesis [46, 47].

#### **1.4. Aromatase Inhibitor and Cognitive Impairment**

The role of estrogen in cognition and memory is still uncertain, but the cognition impairment and loss of short- and long-term memory in postmenopausal women aged >65 treated with hormonal therapy for the early-stage estrogen-responsive breast cancer was reported by the Women's Health Initiative Memory Study (WHIMS) [48].

The *in vitro* studies demonstrated a neuroprotection effect of estrogen and the presence of estrogen receptors in the brain, suggesting it promotes neuronal growth, in addition to the data supporting the usage of estrogen therapy for the prevention of dementia. All were supporting that blockage of estrogen biosynthesis in the brain by aromatase inhibitors may lead to cognitive impairment in postmenopausal women treated for breast cancer with other predisposing factors like age. However, aromatase inhibitors are also associated with side effects such as musculoskeletal syndrome and osteoporosis due to estrogen depletion [49, 50].

Owing to the need for synthesizing new analogs to the third-generation non-steroidal aromatase inhibitors to target multiple diseases, overcome resistance generated from a gene mutation in malignancies, and increase patient adherence by improving safety profile and the overall patient quality of life. Furthermore, in light of the above-mentioned interesting properties of thiazolinone and benzothiazole rings and their compliance with the requirement to block aromatase action (involvement of nitrogen atom and hydrophobicity), respectively, these are quite enough to encourage us to synthesize a novel series of hybrid structures of 1,3-thiazolinone and benzothiazole heterocyclic rings those are substituted differently, to elucidate and prove the structures using different analytical methods and to investigate them as aromatase inhibitors.

## 2. LITERATURE REVIEW

### 2.1. General Information about Thiazolinone Ring

Thiazoles are a unique heterocyclic ring system known to have significant biological activity and are found in many important clinically available molecules like penicillin, thiamine (vitamin B1), and diabetes type 2 sugar-lowering agents thiazolidinedione (TZD). Thiazolinone is a derivative of thiazole consisting of a five-membered ring system with two heteroatoms (S, N) occupying positions 1 and 3, respectively, and (C=O) group at position 4 named 1,3-thiazol-2-in-4-one **Figure 2.1**. 2-Amino-thiazolinone and its tautomeric form 2-imino-thiazolidinone (pseudothiohydantoin) are of great pharmacological interest as well as their classical isosteres, glitazone (1,3-thiazolidin-2,4-dione), and rhodanine (2-thioxo-1,3-thiazolidin-4-one) **Figure 2.2**. However, substitutions on positions 2 and 5 create the differences between them in the physicochemical properties, the way they interact with receptors, and the resultant pharmacological use [51, 52].

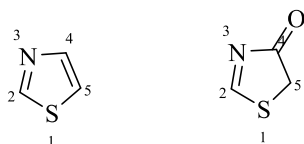


**Figure 2.1.** 1,3 thiazole and 1,3-thiazolin-4-one structures and numbering system

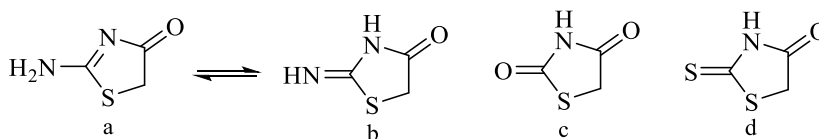


**Figure 2.2.** (a) 2-amino-thiazolinone, (b) 2-imino-thiazolidinone (pseudothiohydantoin), (c) 1,3-thiazolidin-2,4-dione (glitazone), (d) 2-thioxo-1,3-thiazolidin-4-one (rhodanine)

### 2.2. Synthesis Methods of The Thiazolinone Ring

#### 2.2.1. Hantzsch method

Thiazolinone is synthesized from molecules that show a nucleophilic structure (S-C=N) like thiocyanate, thioamide, thiourea, and thiosemicarbazide, which interact with  $\alpha$ -halo carbonyl compounds by refluxing in alcohol. This method gives 1,3-thiazole by

removing water with the assistance of acid and gives 1,3-thiazol-4-one by addition of base to the reaction mixture to stop acid-catalyzed dehydration [53]. Babadjamian et al. describe the mechanism of reaction [54].

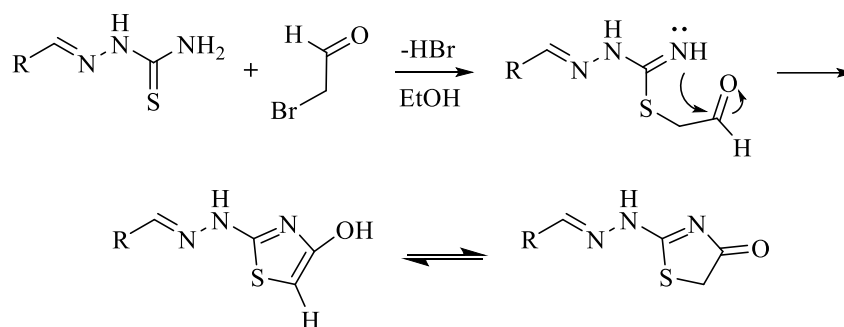


**Figure 2.3.** Synthesis of 1,3-thiazolinone according to hantzsch method

### 2.2.2. Liebermann synthesis

In 1879 Lange and Liebermann first reported the synthetic method of pseudothiohydantoins (2-imino-1,3-thiazolidin-4-one), the tautomeric form of 2-amino-1,3-thiazolin-4-one by reaction of diphenyl thiourea with monochloroacetic acid and reported as the following scheme [52].

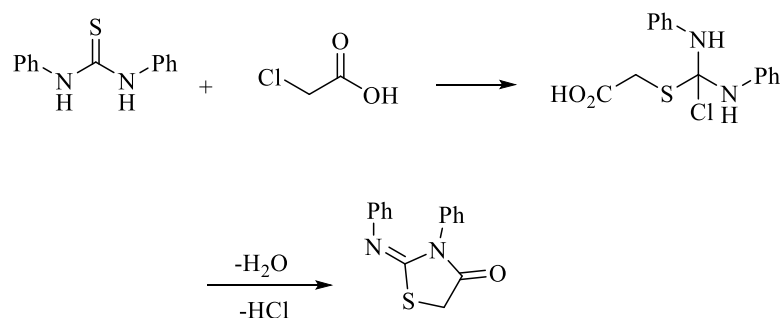


**Figure 2.4.** Schematic representation for the original synthesis of *N,N'*-diphenyl-pseudothiohydantoin (Lange's diphenylsulfhydantoin)

### 2.2.3. Reeve's synthesis

Synthesis of 2-imino-4-thiazolidinone tautomeric form of 2-amino-4-thiazolinone by Reeve's condition (MeOH, KOH, 50°C) with yield percent 30% from thioureas and alkyl (aryl) trichloromethyl carbinols and the general synthesis method in the following scheme [55].

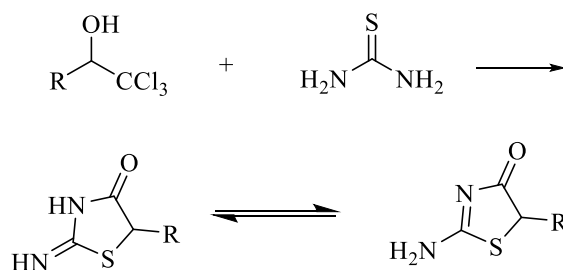


**Figure 2.5.** Schematic representation for synthesis of 2-imino-4-thiazolidinone by reeve's method

#### 2.2.4. One pot synthesis

By modifying Reeve and Nee's condition three-component one-pot synthesis of 2-imino-4-thiazolidinone from aldehyde, chloroform, and thiourea under basic condition was made with a 53% yield percent. Although it does not increase yield present dramatically, this method simplifies the synthesis [51].

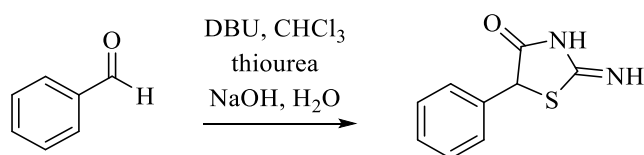


**Figure 2.6.** Synthesis of 2-imino-4-thiazolidinone by one pot method

### 2.3. Thiazole/Thiazolinone Derivatives That have Anticancer /Aromatase Inhibitor Activity

In 2016 novel derivatives of 2-imino-4-thiazolidinone were synthesized by Division et al., and investigated for their cytotoxic activity against (B16F10, A549, PANC-1) cell lines responsible for mouse melanoma, human lung cancer, and human pancreatic cancer, respectively, and tested for their effect on normal cell line (CHO). An  $IC_{50}$  from 3.4 to  $7\mu\text{M}$  by activation of apoptosis and DNA damage was reported against the cell line responsible for mouse melanoma by the **7k**, **7m**, and **7n** derivatives. These results were considered to be significant compared with doxorubicin [56].

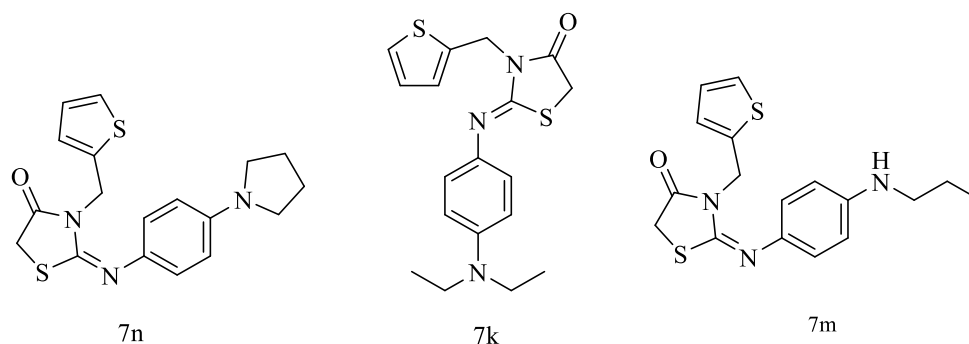


**Figure 2.7.** Compounds (7k) (S)-2-[(4-diethylaminophenyl)imino]-3-(thiophen-2-ylmethyl) thiazolidin-4-one, (7m) (S)-2-[(4-propylaminophenyl)imino]-3-(thiophen-2-ylmethyl) thiazolidin-4-one, (7n) (S)-2-[(4-pyrrolidinophenyl)imino]-3-(thiophen-2-ylmethyl) thiazolidin-4-one

Nineteen novel compounds with antiproliferative activity comparable to doxorubicin were synthesized by Abdu-Allah et al. in 2016. These compounds have a 5-aminosalicylate and 4-thiazolinone hybrid ring system in their structures and were investigated against four human cancer cell lines. However, compound **10** showed equipotent antiproliferative activity to doxorubicin against MCF-7, the cell line responsible for breast cancer, with an  $IC_{50}$  value of 70 nM and exhibited lower toxicity to the normal cell [57].

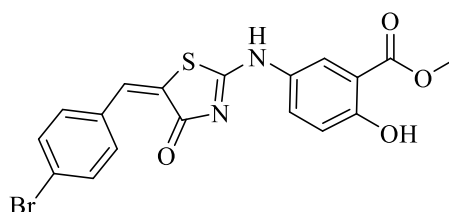


**Figure 2.8.** Compound (10) methyl 2-hydroxy-5-[(5-(4-bromobenzylidene)-4-oxo-4,5-dihydro-1,3-thiazol-2-yl)-amino]benzoate

Sahin et al. in 2018 synthesized 4-(aryl/heteroaryl)-2-(pyrimidin-2-yl) thiazole, a non-steroidal derivative to overcome the side effects of the steroidal aromatase inhibitors, to decrease the estrogen hormonal level by interfering with the final steps of its biosynthesis and blocking the aromatase enzyme activity. The rationale of this study has been dependent on synthesizing a planar aromatic ring connected to a ring system with a nitrogen atom. The synthesized compounds were also investigated for their antiproliferative activity against MCF-7, and HEK-293 cell lines using (MTT) assay.

Compound **1** has a potential inhibition activity of aromatase enzyme when compared to anastrozole and promising antiproliferative activity [58].

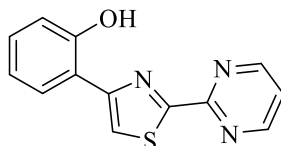


**Figure 2.9.** Compound (1) 4-(2-Hydroxyphenyl)-2-(pyrimidine-2-yl)thiazole

Another work on 5-aminosalicylate-4-thiazolinone hybrid-containing derivatives was made in 2020 by Ramadan et al., and the synthesized compounds were studied for their cytotoxic activity against seven different cancer cell lines included in breast cancer, cervical cancer, lung, and colon cancer. Compounds **HH3** and **HH13** showed results comparable to doxorubicin against SkBr3, HCT-116, and HeLa cell lines related to breast, colorectal, and cervical cancer, respectively, while the lung cancer cell line was considered to be resistant [59].

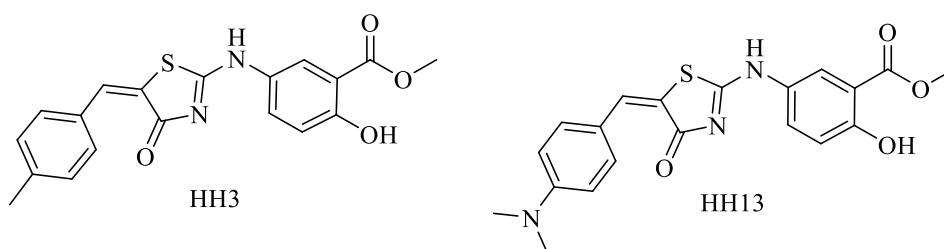


**Figure 2.10.** Compounds (HH3) methyl 2-hydroxy-5-[(5-(4-methylbenzylidene)-4-oxo-4,5-dihydrothiazol-2-yl)amino]benzoate, (HH13) methyl-5-[(5-(4-(dimethylamino)benzylidene)-4-oxo-4,5-dihydrothiazol-2-yl)amino]-2-hydroxybenzoate

In 2021 Osmaniye et al. synthesized thiazole-dihydrofuran derivatives and investigated their aromatase inhibition activity to decrease circulating estrogen, thus prolonging the disease-free period, and decreasing recurrence in postmenopausal women with hormonal-dependent breast cancer. Of these derivatives, **2g** and **21** showed to have  $IC_{50}$  of inhibition similar to that of letrozole, and the most active derivatives with a favorable safety profile [60].

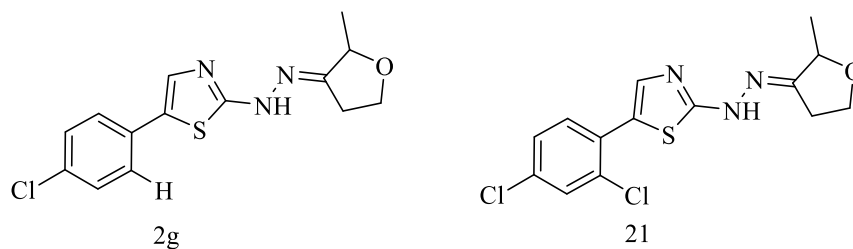


**Figure 2.11.** Compounds (2g) 4-(4-chlorophenyl)-2-[2-(2-methyldihydrofuran-3(2H)-ylidene)hydrazineyl]thiazole, (21) 4-(2,4-dichlorophenyl)-2-[2-(2-methyldihydrofuran-3(2H)-ylidene)hydrazineyl]thiazole

In 2022 Evren et al. synthesized novel 2-thiazolyl hydrazone derivatives and investigated their inhibition potency for both monoamine oxidase and aromatase enzymes because their chemical structures are hybrid containing the cores required to inhibit the two enzymes. Evren reported that compound **2q** inhibits both MAO-B and aromatase enzyme, it inhibits MAO-B quietly and selectively and showed high inhibitory effect on aromatase enzyme [61].

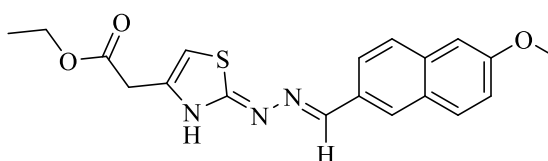


**Figure 2.12.** Compound (2q) Ethyl 2-(2-{2-[(6-methoxynaphthalen-2-yl)methylene]hydrazinyl}thiazol-4-yl)acetate

Osmaniye et al. in 2022, synthesized novel derivatives containing the imidazole ring and thiazolyl hydrazone structure and investigated their aromatase inhibition activity and MAO-B inhibition activity because the synthesized compounds have a hybrid skeleton known to have both activities. Compound **2e** showed aromatase inhibition activity similar to that of letrozole [62].

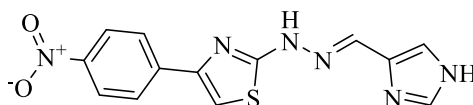


**Figure 2.13.** Compound (2e) 2-{2-[(1H-imidazol-4-yl)methylene]hydrazineyl}-4-(4-nitrophenyl)thiazole

## 2.4. Thiazole/Thiazolinone Derivatives That have Antifungal/Aromatase Inhibitor Activity

In 2012 new derivatives of quinoline-2-pyrazoline-based thiazolinone were designed and synthesized by Desai et al., and after their structures were confirmed by different analytical methods, they were tested for their antibacterial activity against gram-positive and gram-negative bacterial species and tested for their antifungal activity against (*Candida Albicans* and *Aspergillus* species). However, the compounds **4e**, **4f**, **4j**, **4i**, and **4l** have the most remarkable antimicrobial activity [63].

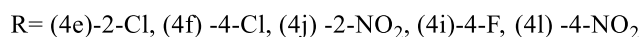
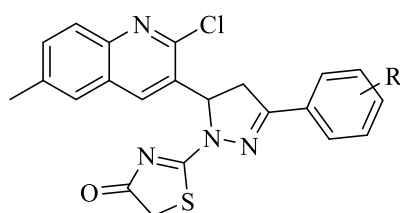


**Figure 2.14.** Compounds named 2-[5-(2-chloro-6-methylquinolin-3-yl)-3-(aryl)-4,5-dihydro-1H-pyrazol-1-yl]thiazol-4(5H)ones

In 2016 a series of new 2-(allyl-amino)-5-arylidene-thiazol-4(5H)-ones, 2-(phenyl-amino)-5-arylidene-thiazol-4(5H)-ones and 2-(1-naphthyl-amino)-5-arylidene-thiazol-4(5H)-ones were synthesized by Stana et al., and after their structures were validated by several spectroscopic methods, they were investigated for antifungal activity against different candida strains and compared with fluconazole. The compounds **9b** and **10** exhibited 500-fold inhibition of aromatase enzyme lanosterol 14 $\alpha$ -demethylase enzyme belonging to CYP450 family (CYP51) subtype more than the positive control [64].

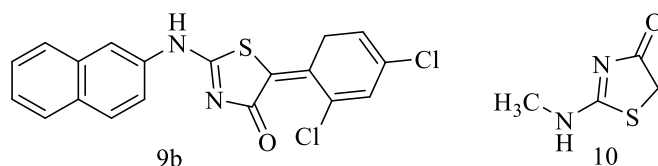


**Figure 2.15.** Compounds (9b) 5-(2,4-Dichlorobenzylidene)-2-(naphthalen-1-ylamino)thiazol-4(5H)-one, (10) 2-(methylamino)thiazol-4(5H)-one

In 2018 a series of novel derivatives of hydrazine-thiazole were synthesized by Lino et al. and examined against different fungal species including candida and compared with fluconazole and amphotericin B drugs. Authors reported that compound **3** was more active than fluconazole against all tested fungal strains [65].

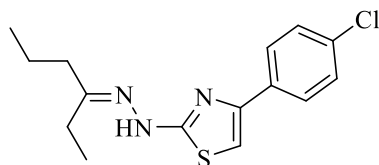


**Figure 2.16.** Compound (3) 2-[(2-(hexan-3-ylidene)hydrazo)-4-(4-chlorophenyl)-thiazole

In 2021 Eissa et al. designed and synthesized six quinoline-based thiazole derivatives, and the synthesized compounds were investigated for their antibacterial and antifungal activity. Of the synthesized compounds, compound **5e** showed the highest antifungal activity against *Aspergillus Fumigatus* compared to amphotericin B [66].

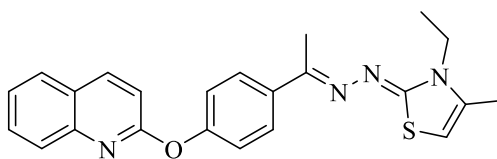


**Figure 2.17.** Compound (5e) 3-ethyl-4-methyl-2-({1-[4-(quinolin-2-yloxy)phenyl]ethylidene}hydrazono)-2,3-dihydrothiazole

## 2.5. General Information about Benzothiazole Ring

1,3-benzothiazole ring in which the 1,3-thiazole ring is fused with benzene ring at positions 4 and 5 of the thiazole ring **Figure 2.18**. This class of sulfur-nitrogen-containing heterocycles has a potential pharmacological activity as its derivatives constitute different xenobiotics. They are found naturally as part of firefly luciferin, an aroma of tea leaves and cranberries [67].

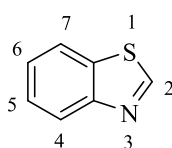


**Figure 2.18.** Structure and numbering of benzothiazole ring

## 2.6. Synthesis Methods of Benzothiazole Ring

### 2.6.1. Hofmann synthesis

In 1887 W. Hofmann first synthesized a 2-substituted benzothiazole ring from aldehyde and  $\alpha$ -amino thiophenol. This route is the most commonly used for simple cyclization. It is also applicable for synthesizing a 2-substituted benzothiazole ring from the other carbonyl-containing molecule such as carboxylic acid and its derivatives. The following scheme shows the general synthesis equation as reported by Hofmann [68].

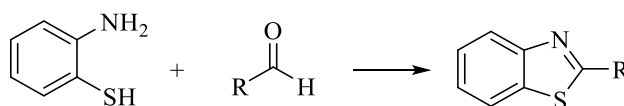


**Figure 2.19.** Schematic representation for the synthesis of benzothiazoles from 2-aminothiophenol according to Hofmann

### 2.6.2. Jacobson cyclization

This method was reported in 1886 for the synthesis of benzothiazoles. According to Jacobson, *o*-methoxy thiobenzamides were treated with potassium ferricyanide in an alkali medium, giving benzothiazole by *ipso* substitution of a methoxy group [69, 70].

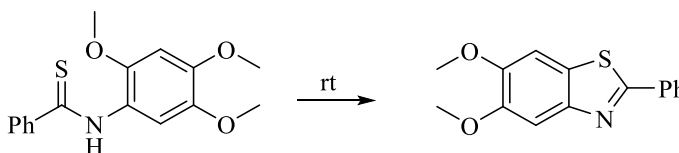


**Figure 2.20.** Benzothiazole synthesized by *ipso* substitution according to Jacobson

### 2.6.3. Synthesis of benzothiazole mediated by iodine

The same authors reported the synthesis of benzothiazole from thiobenzamide with the assistance of iodine. In this reaction, adding iodine follows the addition of thiobenzamide to the refluxing chlorobenzene or by adding NaH to the refluxing benzamide in benzene followed by iodine; however, this reaction favors the electron-donating group substitution on thiobenzamide ring and gives more than 80% yield [71].

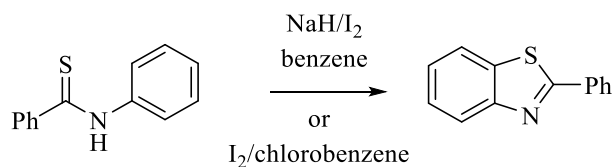


**Figure 2.21.** Synthesis of benzothiazoles mediated by iodine

## 2.7. Benzothiazole Derivatives That have Anticancer/ Aromatase Inhibitor Activity

In 1998 Shi et al. synthesized and reported the anticancer activity of 2-(4-aminophenyl)benzothiazole derivatives with different substitutions and related the structure of the molecules to their cytotoxic activity. Authors reported compound **9a** as the most potent candidate against ER<sup>+</sup> (MCF-7 and BO) and ER<sup>-</sup> (MT-1 and MT-3) breast cancer cell lines [72].

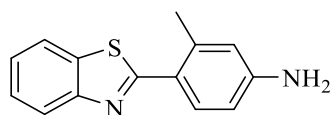


**Figure 2.22.** Compound (9a) 2-(4-amino-3-methylphenyl)benzothiazole

Solomon et al. in 2009, designed and synthesized a pharmacophoric hybrid of isatin and benzothiazole derivatives and investigated their cytotoxic activity on human cell lines, especially on those responsible for breast cancer (such as MDA-MB231, MDA-MB468, MCF7-). Of the tested compounds, compound **2I** showed a promising result as it killed the cancer cell (MCF7) 10-15 times more than the normal cell, which suggested it has lower side effects. While the concentration needed from compound **5e**, is approximately half of that of **2I** to exhibit the same cytotoxic effect [73].

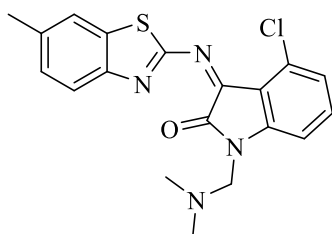


**Figure 2.23.** Compound (5e) 4-chloro-1-dimethylaminomethyl-3-(6-methyl-benzothiazol-2-ylimino)-1,3-dihydroindol-2-one

In 2010 Tzanopoulou et al. synthesized compounds that are a complex of 2-(4-amino-6-methyl phenyl) benzothiazole conjugated to  $M(I)(CO)_3(NNO)$  ( $M = Re, ^{99m}Tc$ ) and investigated their *in vivo* and *in vitro* activity against breast cancer cells MCF-7 and T47D. However, this conjugation helped to determine their uptake by tumor cells. This study aimed to synthesize radiodiagnosis and/or radiotherapy matched pairs of the novel lysylamide prodrug (Phortress), which passed phase 1 of clinical trials in the UK [74].

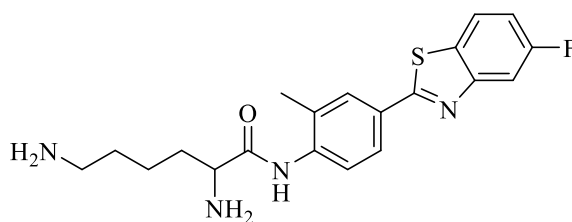


**Figure 2.24.** (*Phortress*) 2,6-diamino-N-[4-(5-fluorobenzothiazol-2-yl)-2-methylphenyl]hexanamide

In 2019 two series of 2-imino-coumarin based hybrids were synthesized by A. Mawkowska et al., one of them 3-(benzothiazol-2-yl)-2H-chromen-2-one derivatives. All the synthesized compounds were designed as potential anticancer and investigated against human cell lines of the urinary bladder, lung, pancreatic, and cervix. Of benzothiazole hybrid containing series compound **26** was reported as the most potent [75].

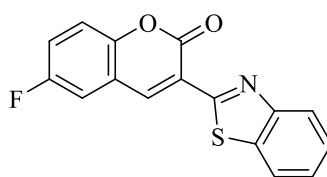


**Figure 2.25.** Compound (26) 3-(benzothiazol-2-yl)-6-fluoro-2H-chromen-2-one

## 2.8. Benzothiazole Derivatives That have Antifungal/ Aromatase Inhibitor Activity

In 2016 Zhao et al. designed and synthesized new derivatives of benzothiazole and amide-imidazole hybrid skeleton. These derivatives were synthesized to overcome the resistance to the commercially available antifungal agents, and their SAR was studied. The most potent compounds were **14o**, **14p**, and **14r** and were compared to fluconazole and itraconazole drugs. The suggested mechanism of antifungal activity for the

synthesized compounds was inhibition of aromatase enzyme (CYP51) of *Candida Albicans*, which was revealed by compound **14p** [76].

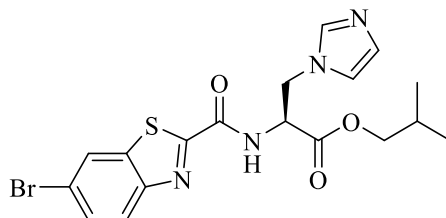


**Figure 2.26.** Compound (14p) *Isobutyl(S)-2-(6-bromobenzothiazole-2-carboxamido)-3-(1H-imidazol-1-yl)propanoate*

In 2018 derivatives of 2-(aryloxymethyl) benzoxazole and benzothiazole were synthesized by Luo et al., all the synthesized compounds were investigated against eight pathogenic species of fungi. The SAR studies and molecular docking studies were conducted for the most active derivatives. Compound **6h** was the most important derivative of benzothiazole containing series [77].

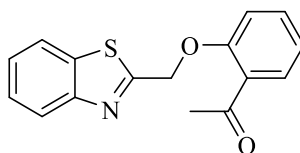


**Figure 2.27.** Compound (6h) *1-[2-(benzothiazol-2-ylmethoxy)phenyl]ethanone*

In 2019 Ballari et al. synthesized eleven derivatives of 2-(benzylsulfonyl)-benzothiazole as antifungal agents and compared them with the commercial drug captan, six fungal species involved in the study, including two resistant species. Of the synthesized compounds, **4f** and **4k** were the most active derivatives [78].

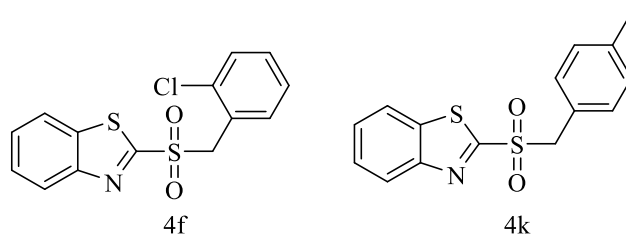


**Figure 2.28.** Compound (4f) 2-[(2-Chlorobenzyl)sulfonyl]benzothiazole, (4k) 2-[(4-Methylbenzyl)sulfonyl]benzothiazole

### 2.9. Thiazolinone and Benzothiazole Hybrid That have Biological Activity

In 2010 Havrylyuk et al. synthesized more than ten derivatives of the 4-thiazolidinone and benzothiazole hybrid ring system. After their structures were elucidated and confirmed by different analytical methods, they were tested for their anticancer activity against multiple cancer cell lines. Compound **6** was reported as the most active derivative against almost all the tested cell lines, including breast, ovarian, and prostate cancer [79].

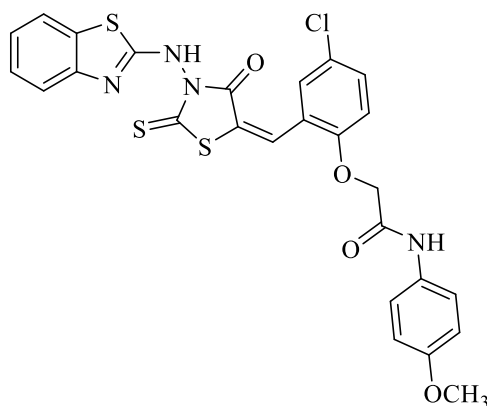


**Figure 2.29.** Compound (6) 2-{2-[3-(Benzothiazol-2-ylamino)-4-oxo-2-thioxothiazolidin-5-ylidene-methyl]-4-chlorophenoxy}-N-(4-methoxyphenyl)-acetamide

In 2012 eight-novel compounds were synthesized by Padmavathi et al. derivatives of 2-[3-(4-oxo-2-substituted phenyl thiazolidin-3-yl)phenyl]benzothiazole-6-carboxylic acid and tested against HeLa the cancer cell line of cervical tissue *in vitro* by mean of (MTT) assay. The compound **PP2** displayed the most significant results when compared to cisplatin [80].

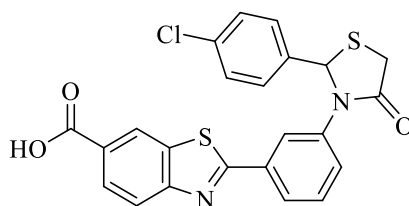


**Figure 2.30.** Compound (PP2) 2-{3-[2-(4-Chlorophenyl)-4-oxothiazolidin-3-yl]phenyl} benzothiazole-6-carboxylic acid

In 2014 Rahul V et al. synthesized new derivatives hybrid of 2-benzothiazolyimino-4-thiazolidinones and piperazine. After their structures were confirmed by analytical methods they were tested for their antifungal and antibacterial activity, the compound **5b** was the most potent derivative with electron-withdrawing substituent [81].

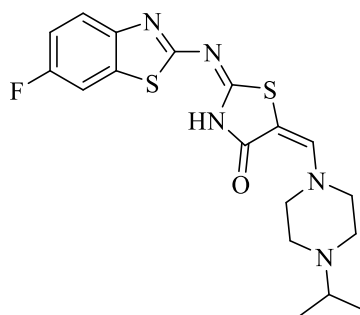


**Figure 2.31.** Compound (5b) 2-[(6-fluorobenzothiazol-2-yl)imino]-5-[(4-isopropylpiperazin-1-yl)methylene]thiazolidin-4-one

### 3. MATERIALS

#### 3.1. Chemicals

2-Bromo acetophenone	: Sigma-Aldrich, Germany
2-Bromo-4`-methyl acetophenone	: Sigma-Aldrich, Germany
2-Bromo-4`-methoxy acetophenone	: Sigma-Aldrich, Germany
2-Bromo-4`-fluoro acetophenone	: Sigma-Aldrich, Germany
2-Bromo-4`-chloro acetophenone	: Sigma-Aldrich, Germany
2-Bromo-4`-cyano acetophenone	: Sigma-Aldrich, Germany
2-Bromo-2`-acetonaphthone	: Sigma-Aldrich, Germany
2-Bromo-2`,4`-dichloro acetophenone	: Sigma-Aldrich, Germany
2-Bromo-3`,4`-dichloro acetophenone	: Sigma-Aldrich, Germany
2-Bromo-(2`-benzofuran)ethanone	: Sigma-Aldrich, Germany
Chloro acetyl chloride	: Sigma-Aldrich, Germany
THF	: Sigma-Aldrich, Germany
TEA	: Sigma-Aldrich, Germany
DMF	: Sigma-Aldrich, Germany
Potassium thiocyanate	: Sigma-Aldrich, Germany
DMSO- <i>d</i> <sub>6</sub>	: Merck, Germany
Ethyl alcohol	: Sigma-Aldrich, Germany
Potassium carbonate	: Sigma-Aldrich, Germany
Methyl alcohol	: Sigma-Aldrich, Germany
Acetonitrile	: Sigma-Aldrich, Germany
Letrozole	: Sigma-Aldrich, Germany
Petroleum ether	: Sigma-Aldrich, Germany
Ethyl acetate	: Sigma-Aldrich, Germany

Chloroform : Merck, Germany  
Aluminum sheet covered with silica gel 60 : Merck, Germany  
F<sub>254</sub> TLC plates  
Acetone : Sigma-Aldrich, Germany

### **3.2. Instruments and Tools**

Electronic balance : Shimadzu, Libror EB-330 HU, Japan  
Melting point detector : Mettler Toledo-MP90 Melting Point System  
Mass spectrometer : Shimadzu, LCMS-IT-TOF, Japan  
Ultraviolet lamp : Camag, Cabinet, Switzerland  
Magnetic based heater stirrer : Heidolph, MR 3003, Germany  
Nuclear magnetic resonance spectrometer : Bruker, UltraShield 400 MHz, USA

## **4. EXPERIMENTAL METHODS**

### **4.1. Chemical Synthesis Methods**

#### **4.1.1. A general method for the synthesis of 2-chloro-N-(5-methylbenzothiazol-2-yl)acetamide (A)**

In a round bottom flask, 5-methylbenzothiazol-2-amine (0.061 mol) was added to anhydrous tetrahydrofuran (THF) and stirred in an ice water bath with a temperature range of 0-5°C, then (0.073 mol) of triethylamine was added and mixed until the solid particles are fully dissolved. (0.085 mol) of chloroacetyl chloride was added dropwise at rate of seven drops per minute over the reaction mixture. After chloroacetyl chloride addition, the reaction mixture was continued to stir at room temperature for three hours. After this period, the reaction was monitored by the mean of TLC method. The tetrahydrofuran was evaporated under reduced pressure, and the residue was washed with cold water, filtered, and left to dry. The solid compound was recrystallized from ethanol [82].

#### **4.1.2. A general method for the synthesis of 2-[(5-methylbenzothiazol-2-yl)amino]thiazol-4(5H)-one (B)**

(0.047 mol) of 2-chloro-N-(5-methylbenzothiazol-2-yl)acetamide was mixed with (0.094 mol) of potassium thiocyanate (KSCN) and refluxed in ethanol for 3-6 hours. TLC results confirmed the completion of the reaction. Then the precipitate was filtered and washed with water and then recrystallized[83, 84].

#### **4.1.3. A general method for the synthesis of 2-[(5-methylbenzothiazol-2-yl)[2-oxo-2-(substituent)ethyl]amino]thiazol-4(5H)-one (C)**

2-[(5-methylbenzothiazol-2-yl)amino]thiazol-4(5H)-one (0.002 mol) was mixed with (0.002 mol) of 2-bromo-1-[4-(substituent)aryl]ethan-1-one and with (0.003mol) of potassium carbonate (K<sub>2</sub>CO<sub>3</sub>) in dimethylformamide (DMF) solution and left overnight at room temperature. TLC was used to determine the end of the reaction. The reaction mixture was poured to salted ice water, and the precipitate was filtered. Then end product was recrystallized by mean of ethanol.

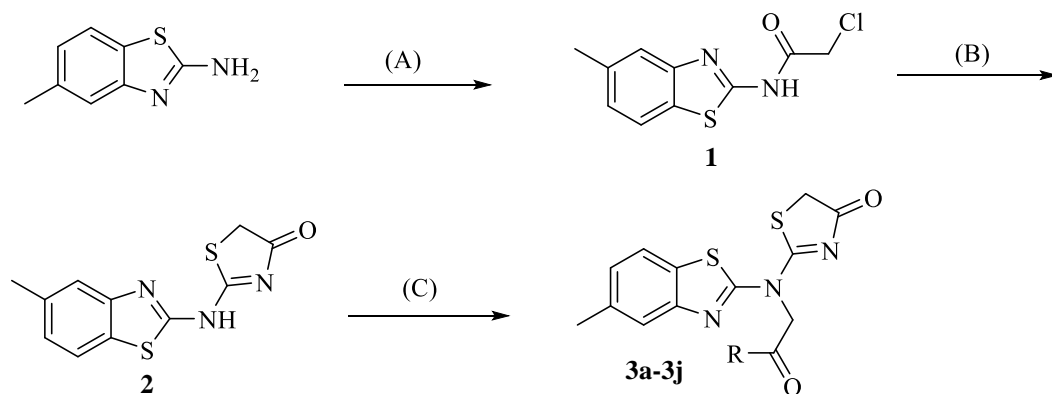


**Figure 4.1.** The general synthesis method of compounds (3a-3j), reaction conditions; (A)  $\text{ClCOCH}_2\text{Cl}$ , THF, TEA,  $0^\circ\text{C}$ , rt, (B) KSCN, EtOH, reflux, (C) DMF,  $\text{K}_2\text{CO}_3$ , 2-bromoacetophenone derivatives

## 4.2. Monitoring the Chemical Reaction

### 4.2.1. Thin-layer chromatography

All the synthesis steps were monitored by the TLC method. This is done by applying the sample from the reaction mixture at a particular time interval. The taken samples were compared with the starting materials dissolved in ethanol. After the sample and starting material were applied to the TLC paper with the assistance of a capillary tube, they were allowed to move upward by the preprepared saturated mixture of suitable solvent called the mobile phase. They are adsorbed to the surface of the aluminum sheet coated with selected silica jell 60 F<sub>254</sub> at different distances returning to its chemical nature and polarity. The resultant spots were detected by ultraviolet light (254 nm-366nm). According to the TLC results, we determine whether the reaction was to be continued or terminated. Depending on the nature of the synthesized product in our thesis, we found the mobile phase (3:1 mixture of petroleum ether and ethyl acetate) is suitable to move the applied sample after trying different mobile phase systems.

### 4.3. Melting Point Determination

Melting point of synthesized compounds were detected using Mettler Toledo-MP90 device. This is done through putting a sample (around 0.5 cm in Height) of the synthesized compound in one side closed capillary tube and located in the chambers of the device. The melting points were detected after watching the video received from the device when the process is finished.

#### **4.4. Chemical Analysis**

##### **4.4.1. Infra-red (IR) spectrometry**

The IR spectra of the synthesized compounds were obtained using the Shimadzu-IR Affinity-IS instrument. The sampling technique was applying the compounds in the form of solid powder to the ATR attachment of the IR spectrophotometry.

##### **4.4.2. High resolution mass spectrometry (HRMS)**

The mass spectra of the newly synthesized molecules were obtained from the sample of their solution in acetonitrile. The sample was injected into LCMS-IT-TOF (Shimadzu, Kyoto, Japan) device and ionized with electron spray ionization (ESI) technique and taken from negative and positive modes.

##### **4.4.3. Proton nuclear magnetic resonance (<sup>1</sup>H-NMR) spectrometry**

<sup>1</sup>H-NMR spectra of the newly synthesized compounds were obtained from their sample solution of DMSO-*d*<sub>6</sub>. Trimethylsilyl was used as an internal standard for calibrating the Bruker 400 MHz NMR device.

##### **4.4.4. Carbon-13 nuclear magnetic resonance (<sup>13</sup>C-NMR) spectrometry**

<sup>13</sup>C-NMR spectra of the newly synthesized compounds were obtained from their sample solution of DMSO-*d*<sub>6</sub>. Trimethylsilyl was used as an internal standard for calibrating the Bruker 400 MHz NMR device.

#### **4.5. Investigation of Aromatase Inhibition Activity (AI)**

The aromatase inhibition activity of the synthesized compounds was determined and compared with letrozole as a positive control. The synthesized compounds were dissolved in dimethyl sulfoxide (DMSO) with concentrations ranging from 10<sup>-3</sup>-10<sup>-9</sup> M and tested according to a commercial fluorometric assay kit (Bio Vision, Aromatase cytochrome P19A enzyme (CYP19A) Inhibitor Screening kit). The recombinant human aromatase stock was reprocessed with 1 mL of aromatase assay buffer. A homogenous solution was obtained by vortex mixing the ingredients completely, and the solution was then poured into a 15ml conical tube for further testing and analysis. The volume was brought to 2450 µl with the aromatase assay buffer, and 50 µl of NADPH production

system (100X) was added for a final total volume of 2.5 ml. The solvent of the control letrozole was prepared by a small amount of the aromatase assay buffer mixed with DMSO, the same solvent used for the tested compounds. Reaction wells containing test compounds and the corresponding no inhibitor controls (which may also serve as a solvent control), as well as a background control (containing no fluorogenic Aromatase Substrate), were prepared.

The incubation of the plate was done for 10 minutes at a temperature of 37°C as a minimum to allow the compounds to interact with the enzyme. The addition of aromatase substrate/NADP<sup>+</sup> mixture (30 µl) to each cell was done after the incubation period had finished. The fluorescence at Ex/Em= 488/527 nm was measured instantly within 1 min [85].

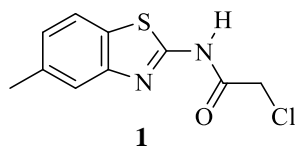
#### **4.6. Molecular Modeling Studies**

Molecular modeling studies were applied by structural based *in silico* procedure, which was done to determine the binding mode of the synthesized compounds to the active binding site of the enzyme, the X-ray crystal structure of aromatase enzyme (3EQM) was retrieved from a protein data bank server ([www.pdb.org](http://www.pdb.org) accessed April 01, 2021). Schrödinger Maestro Schrodinger [86] interface was used to build the structure of the ligands using the LigPrep module [87], then they were presented to the enzyme crystal prepared using the Protein Preparation Wizard protocol of the Schrodinger Suite 2020. Bond orders were assigned, and hydrogen atoms were added to the structures to correctly assign the protonation states as well as the atom types. The grid generation was formed using the Glide module [88], and docking runs were performed in standard precision docking mode (SP).

## 5. RESULTS AND DISCUSSIONS

### 5.1. Synthesis of The Targeted Products

#### 5.1.1. Synthesis of 2-chloro-N-(5-methylbenzothiazol-2-yl)acetamide



Compound **1** was synthesized according to method **A**, 81% yield percent.

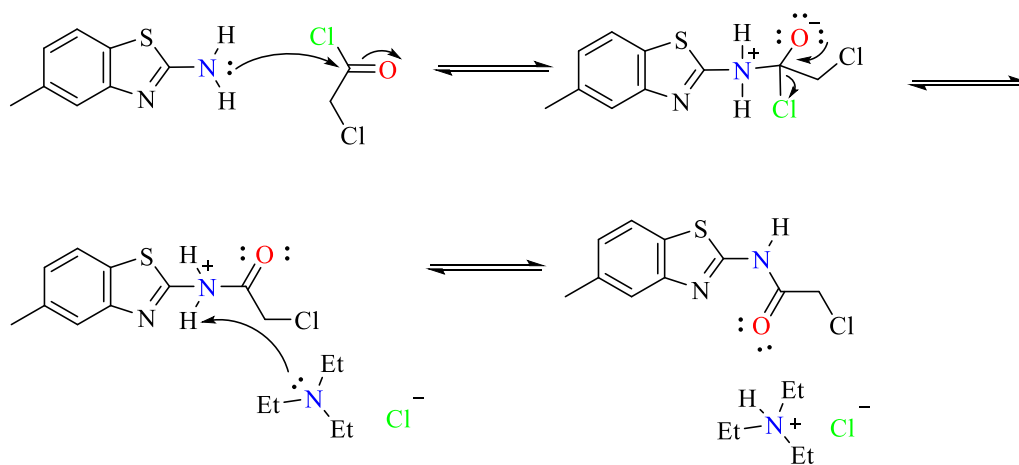
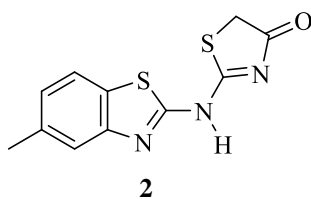


**Figure 5.1.** Mechanism of acetylation reaction of 5-methylbenzothiazol-2-amine

### 5.1.2. Synthesis of 2-[(5-methylbenzothiazol-2-yl)amino]thiazol-4(5H)-one



Compound **2** was synthesized according to method **B**, 69% yield percent. Experimental melting point: 222-223°C.

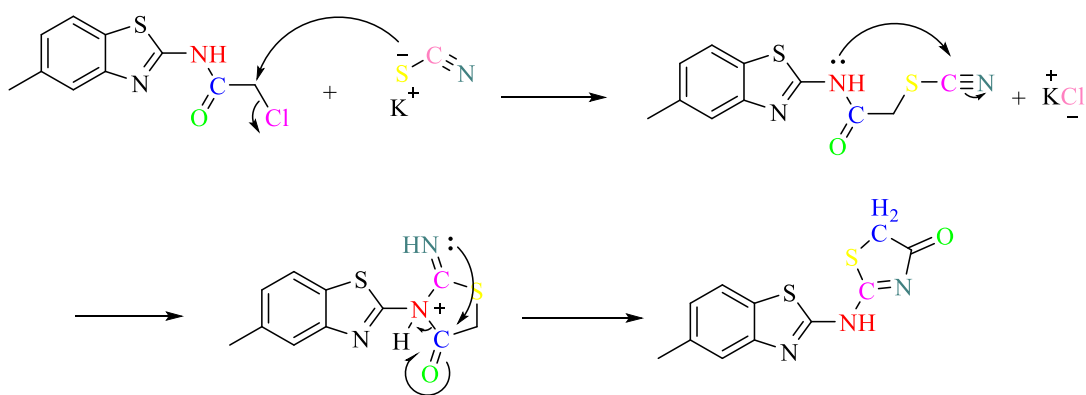


**Figure 5.2.** Mechanism of cyclization of thiazolinone ring [89]

5.1.3. Synthesis of 2-[(5-methylbenzothiazol-2-yl)(2-oxo-2-(substituent)ethyl)amino]thiazol-4(5H)-one

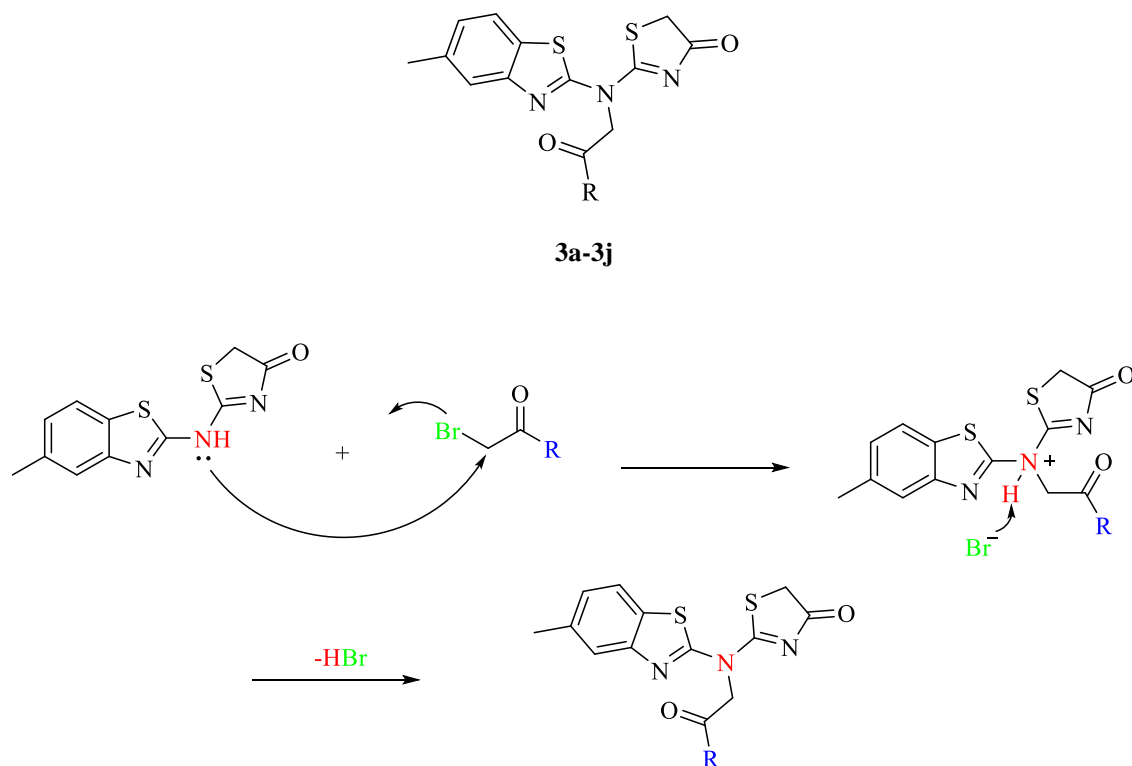
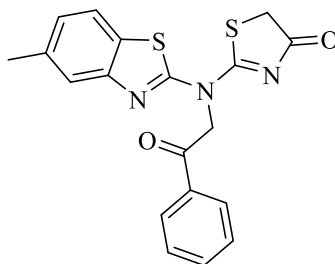


Figure 5.3. Mechanism of reaction for the synthesis of the final derivatives

**5.1.3.1. 2-[(5-ethylbenzothiazol-2-yl)(2-oxo-2-phenylethyl)amino]thiazol-4(5H)-one**



**3a**

Synthesized according to method C, experimental melting point: 221-222°C, 59% yield percent.

**IR (ATR)  $\nu_{\text{max}}(\text{cm}^{-1})$ :** 3061 and 3028 ( aromatic C-H stretching band), 2970 and 2933 ( aliphatic C-H stretching band), 1687 (C=O stretching band), 1494 and 1440 (C=N and C=C stretching band).

**$^1\text{H-NMR}$  (400 MHz, DMSO- $d_6$ ;  $\delta$ , ppm):** 2.43 (3H, s, benzothiazole-CH<sub>3</sub>), 4.05 (2H, s, thiazolinone-CH<sub>2</sub>), 6.17 (2H, s, N-CH<sub>2</sub>), 7.36 (H, s, Ar-H), 7.65-7.78 (4H, m, Ar-H), 7.86 (H, s, Ar-H), 8.15 (2H, s, Ar-H).

**$^{13}\text{C-NMR}$  (100 MHz, DMSO- $d_6$ ;  $\delta$ , ppm)** 21.24 (benzothiazole-CH<sub>3</sub>), 31.25 (thiazolinone-CH<sub>2</sub>), 36.25 (N-CH<sub>2</sub>-C=O), 116.26, 123.55, 128.90, 129.51, 134.90, 154.96, 162.78, 172.38, 176.70 (thiazolinone-C=O), 188.25 (N-CH<sub>2</sub>-C=O).

**HRMS (-m/z): [M+H]<sup>+</sup>:** For C<sub>19</sub>H<sub>15</sub>N<sub>3</sub>O<sub>2</sub>S<sub>2</sub> calculated molecular weight: 382.0678, found: 382.0674.

# DOPNALAB

Item	Value
Acquired Date&Time	10.06.2022 09:56:25
Acquired by	System Administrator
Filename	C:\Users\dopnalab\Desktop\MASAÜSTÜ\LEYLA YURTDAŞ\AF-TA\AF-TA-C-11.ispd
Spectrum name	AF-TA-C-11
Sample name	AF-TA-C-1
Sample ID	
Option	
Comment	
No. of Scans	15
Resolution	4 [cm-1]
Apodization	Happ-Genzel

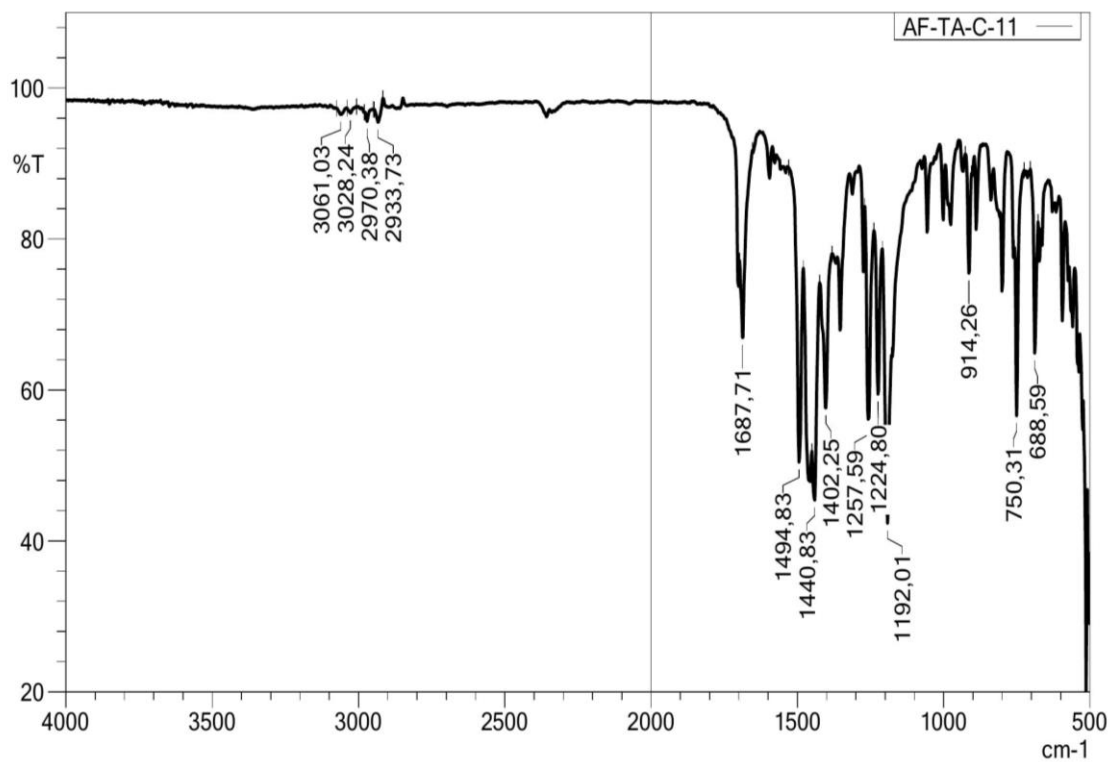
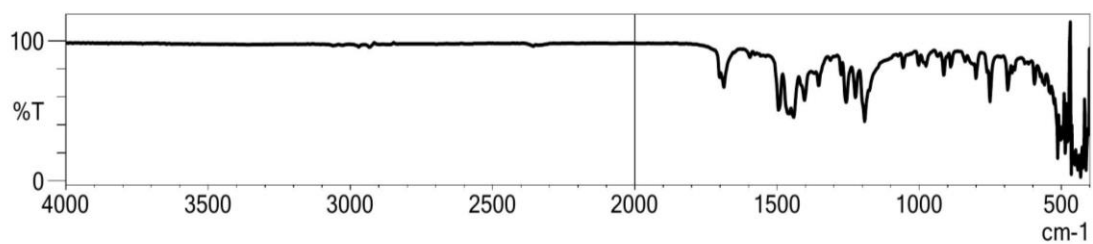


Figure 5.4. IR spectrum of the compound 3a

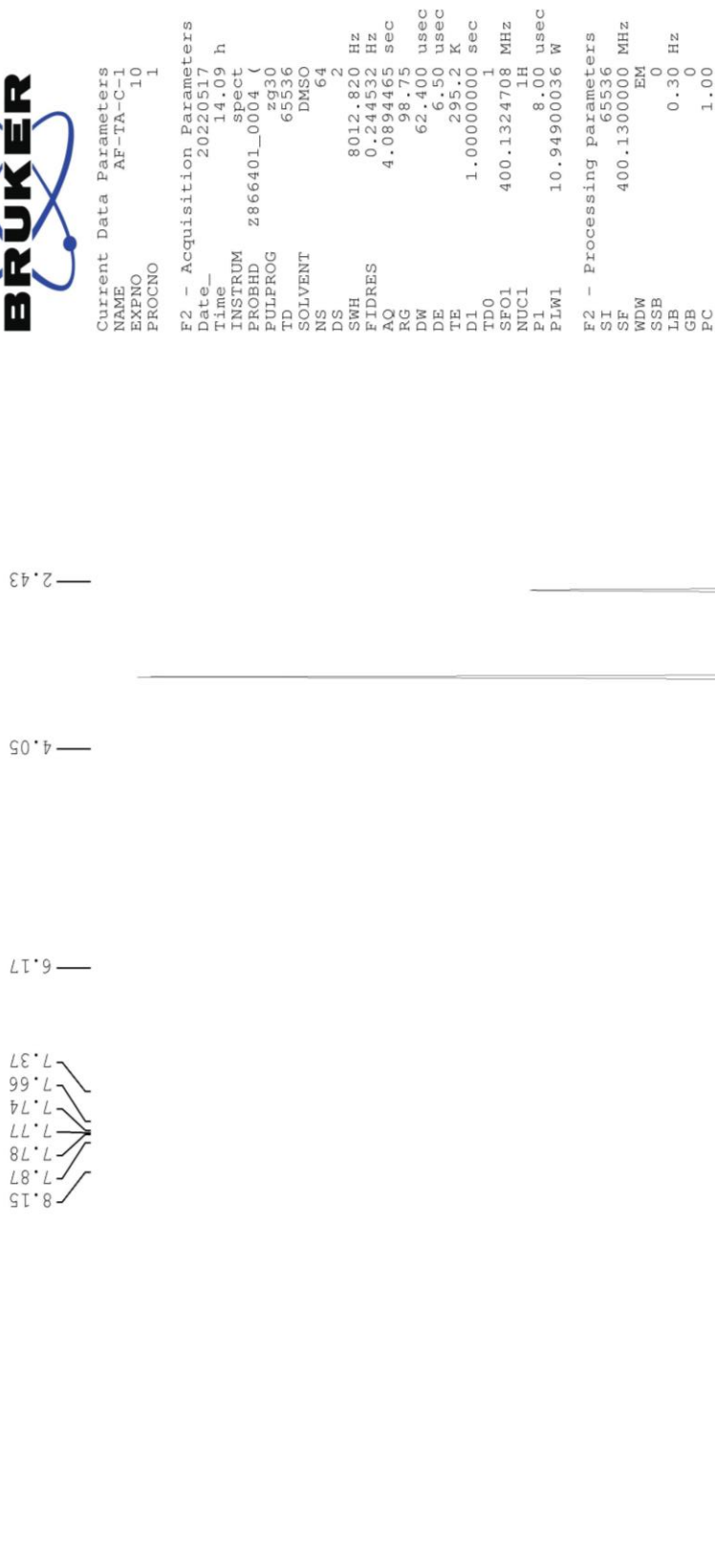


Figure 5.5.  $^1\text{H}$ -NMR spectrum of the compound **3a**



Current Data Parameters  
NAME AF-TA-C1  
EXPNO 11  
PROCNO 1

F2 - Acquisition Parameters  
Date\_ 20220621  
Time 7.59 h  
INSTRUM spect  
PROBHD zgpg30  
PULPROG zgpg30  
TD 65536  
SOLVENT DMSO  
NS 4096  
DS 4  
SWH 24038.461 Hz  
FIDRES 0.732596 Hz  
AQ 1.3631486 sec  
RG 42.75  
DM 20.800 usec  
DE 6.50 usec  
TE 295.8 K  
D1 2.00000000 sec  
D11 0.03000000 sec  
TD0 1  
SFO1 100.6228296 MHz  
NUC1 13C  
F1 15.00 usec  
PLW1 90.29693707 W  
SFO2 400.1316005 MHz  
NUC2 1H  
CFPRG2 waltz16  
PCPD2 90.00 usec  
PLW2 10.94900036 W  
PLW12 0.08651100 W  
PLW13 0.04351400 W

F2 - Processing Parameters  
SI 32768  
SF 100.6127690 MHz  
WDW EM  
SSB 0  
LB 1.00 Hz  
GB 0  
PC 1.40

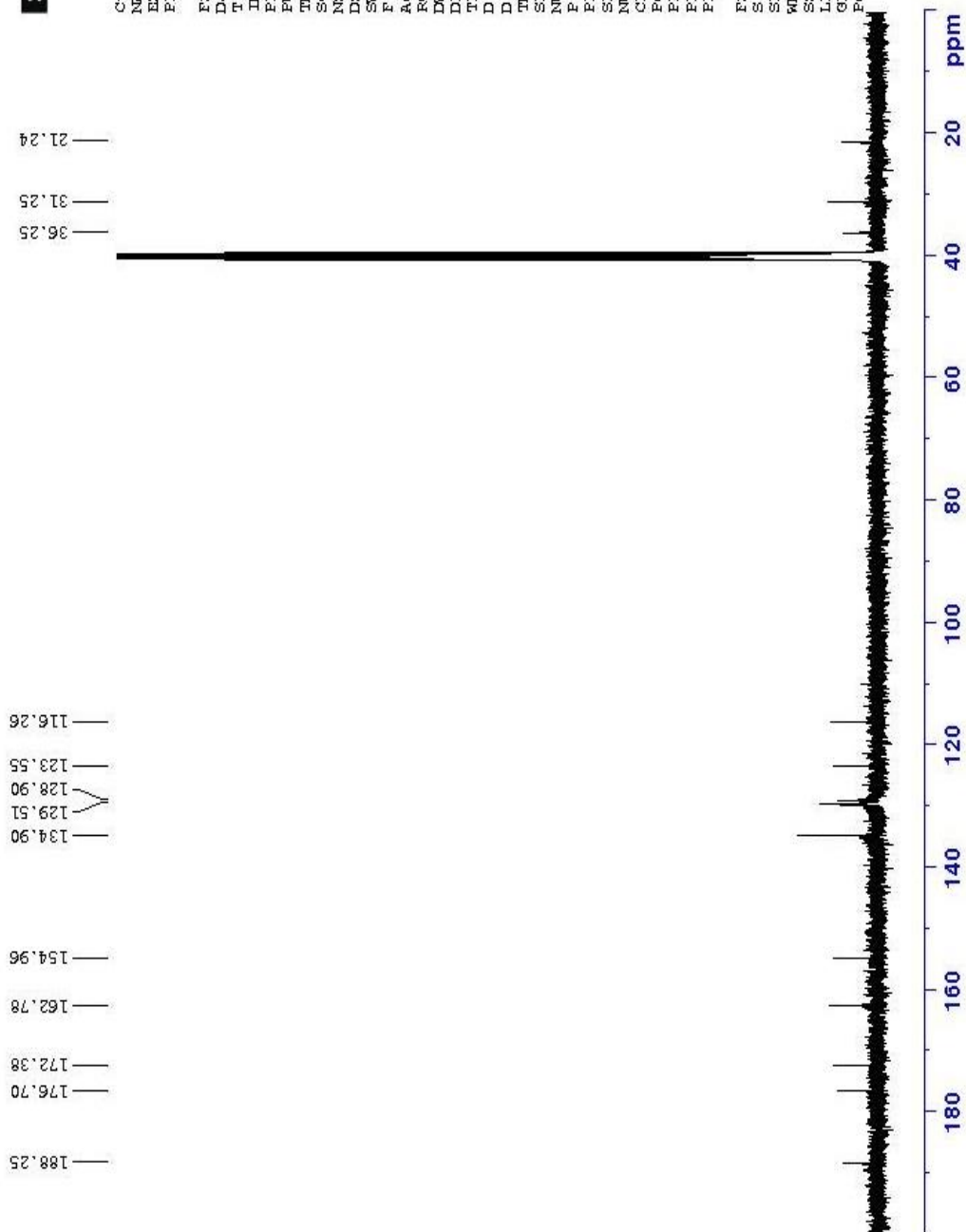


Figure 5.6.  $^{13}\text{C}$ -NMR spectrum of the compound 3a

Data File: C:\LabSolutions\Data\Analiz\Asaf\AFTA-C-1\_57.lcd

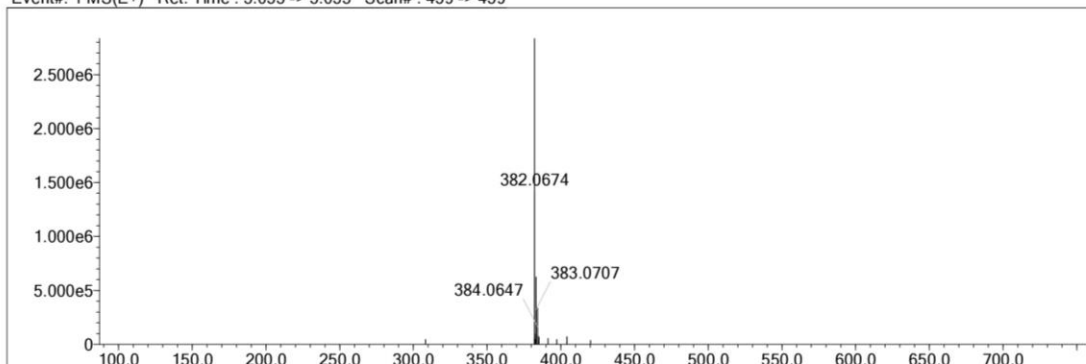
Elmt	Val.	Min	Max	Elmt	Val.	Min	Max	Elmt	Val.	Min	Max	Elmt	Val.	Min	Max	Use Adduct
H	1	9	35	O	2	0	3	S	2	0	2	Ru	2	0	0	H
C	4	7	35	F	1	0	0	Cl	1	0	0	Pd	2	0	0	
N	3	0	5	P	3	0	0	Br	1	0	0	I	3	0	0	

Error Margin (ppm): 5  
 HC Ratio: unlimited  
 Max Isotopes: 3  
 MSn Iso RI (%): 10.00

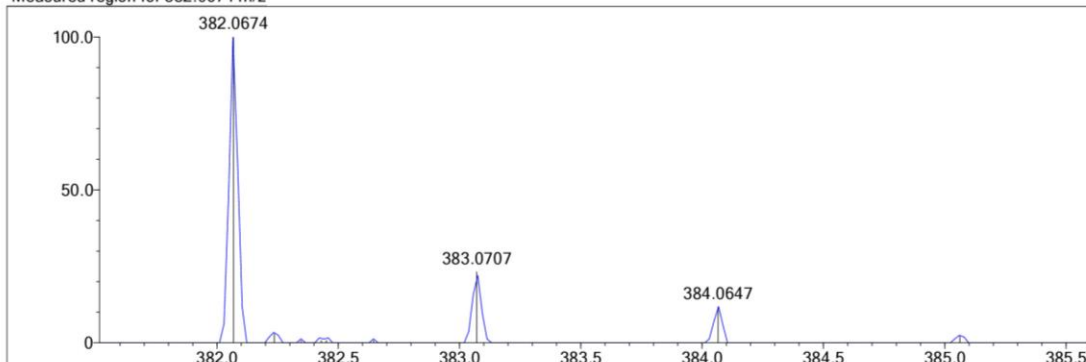
DBE Range: 5.0 - 25.0  
 Apply N Rule: yes  
 Isotope RI (%): 1.00  
 MSn Logic Mode: AND

Electron Ions: both  
 Use MSn Info: yes  
 Isotope Res: 9000  
 Max Results: 50

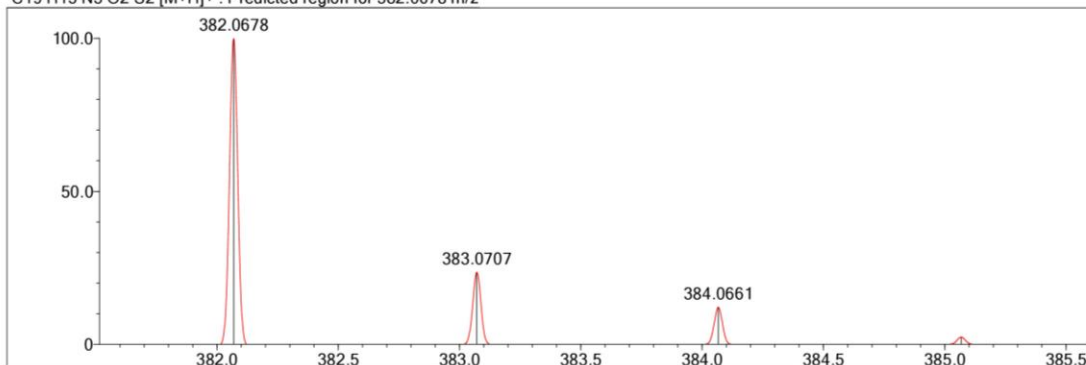
Event#: 1 MS(E+) Ret. Time : 3.053 -> 3.053 Scan# : 459 -> 459



Measured region for 382.0674 m/z



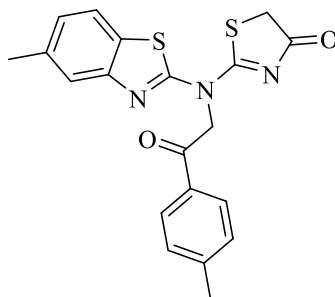
C19 H15 N3 O2 S2 [M+H]+ : Predicted region for 382.0678 m/z



Rank	Score	Formula (M)	Ion	Meas. m/z	Pred. m/z	Df. (mDa)	Df. (ppm)	Iso	DBE
1	83.28	C19 H15 N3 O2 S2	[M+H]+	382.0674	382.0678	-0.4	-1.05	83.39	14.0

Figure 5.7. Mass spectrum of the compound 3a

5.1.3.2. 2-*{(5-methylbenzothiazol-2-yl)[2-oxo-2-(p-tolyl)ethyl]amino}thiazol-4(5H)-one*



**3b**

Synthesized according to method **C**, experimental melting point: 234-235°C, 61% yield present.

**IR (ATR)  $\nu_{\max}(\text{cm}^{-1})$ :** 2927 and 2916 ( aromatic C-H stretching band), 2848 ( aliphatic C-H stretching band), 1693 (C=O stretching band), 1444 and 1406 (C=N and C=C stretching band), 812 (1,3 di-substituted benzene out of plane bending band).

**$^1\text{H-NMR}$  (400 MHz, DMSO- $d_6$ ;  $\delta$ , ppm):** 2.43(3H, s, benzothiazole-CH<sub>3</sub>), 2.45(3H, s, ph-CH<sub>3</sub>), 4.05 (2H, s, thiazolinone-CH<sub>2</sub>), 6.13 (2H, s, N-CH<sub>2</sub>), 7.34-7.46(2H, m, Ar-H), 7.64 (H, d,  $J=8$  Hz, Ar-H), 7.86 (H, s, Ar-H), 7.96 (H, s, Ar-H), 8.05 (2H, d,  $J=8$ , Ar-H).

**$^{13}\text{C-NMR}$  (100 MHz, DMSO- $d_6$ ;  $\delta$ , ppm)** 21.26 (benzothiazole-CH<sub>3</sub>), 21.79 (phenyl-CH<sub>3</sub>), 31.24 (thiazolinone-CH<sub>2</sub>), 36.25 (N-CH<sub>2</sub>-C=O), 129.09, 129.28, 130.06, 131.60, 133.27, 139.47, 145.70, 151.82, 158.95, 162.78, 170.36 (thiazolinone-C=O), 188.93 ( N-CH<sub>2</sub>-C=O).

**HRMS (-m/z): [M+H]<sup>+</sup>:** For C<sub>20</sub>H<sub>17</sub>N<sub>3</sub>O<sub>2</sub>S<sub>2</sub> calculated molecular weight: 396.0835, found: 396.0827.

# DOPNALAB

Item	Value
Acquired Date&Time	10.06.2022 10:03:09
Acquired by	System Administrator
Filename	C:\Users\dopnalab\Desktop\MASAÜSTÜLEYLA YURTDAŞ\AF-TA\AF-TA-C-21.ispd
Spectrum name	AF-TA-C-21
Sample name	AF-TA-C-2
Sample ID	
Option	
Comment	
No. of Scans	15
Resolution	4 [cm <sup>-1</sup> ]
Apodization	Happ-Genzel

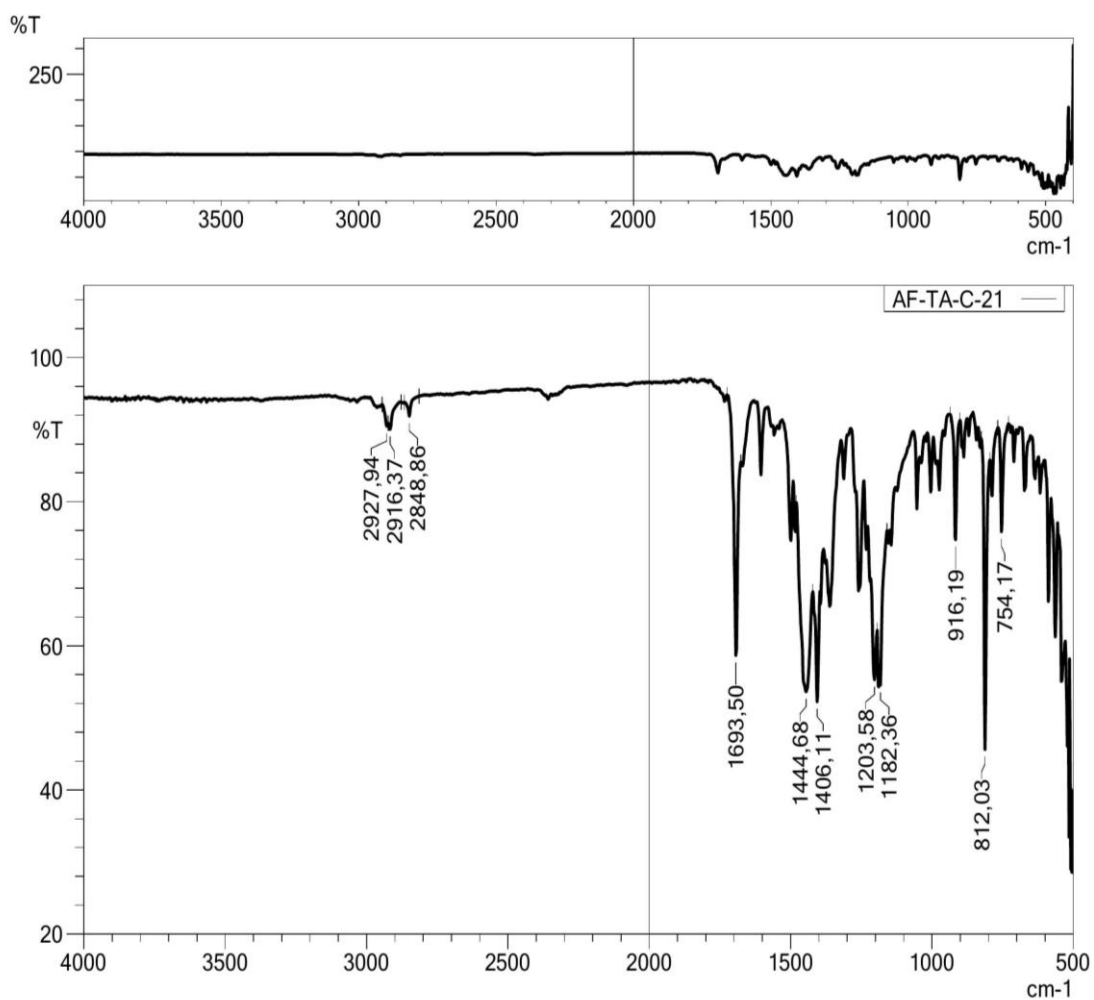


Figure 5.8. IR spectrum of the compound 3b



Current Data Parameters  
NAME AF-TA-C-2  
EXNO 10  
PROCNO 1

F2 - Acquisition Parameters  
Date\_ 20220425  
Time 14.59 h  
INSTRUM spect  
PROBHD Z866401\_0004 (  
PULPROG zg30  
TD 65536  
SOLVENT DMSO  
NS 128  
DS 2  
SWH 8012.820 Hz  
FIDRES 0.244532 Hz  
AQ 4.0894465 sec  
RG 111.15  
DW 62.400 usec  
DE 6.50 usec  
TE 295.6 K  
D1 1.00000000 sec  
TDO 1  
SFO1 400.1324708 MHz  
NUC1 1H  
P1 8.00 usec  
PLW1 10.94900036 W

F2 - Processing parameters  
SI 65536  
SF 400.1300000 MHz  
WDW EM  
SSB 0  
LB 0.30 Hz  
GB 0  
PC 1.00

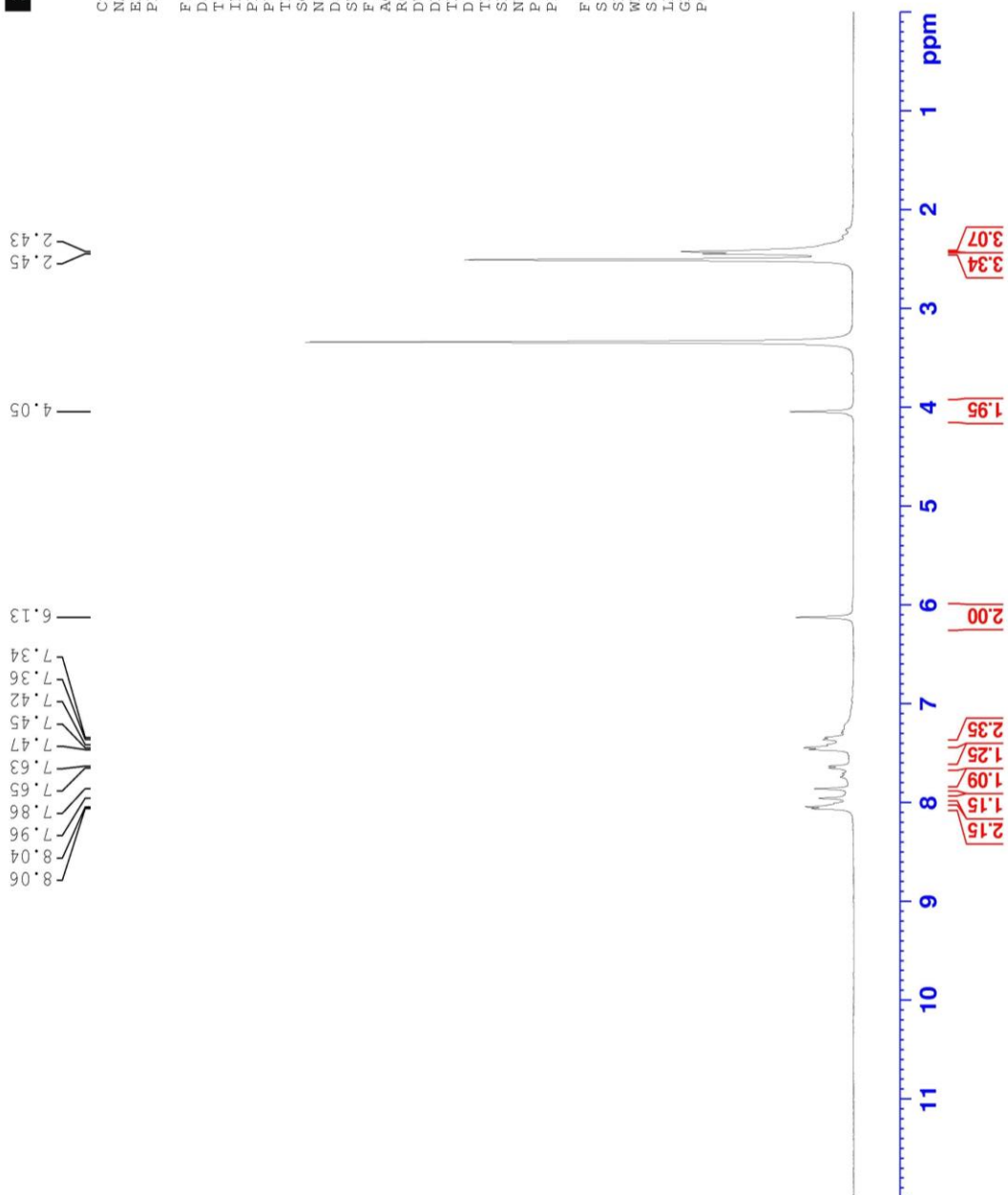


Figure 5.9. <sup>1</sup>H-NMR spectrum of the compound 3b

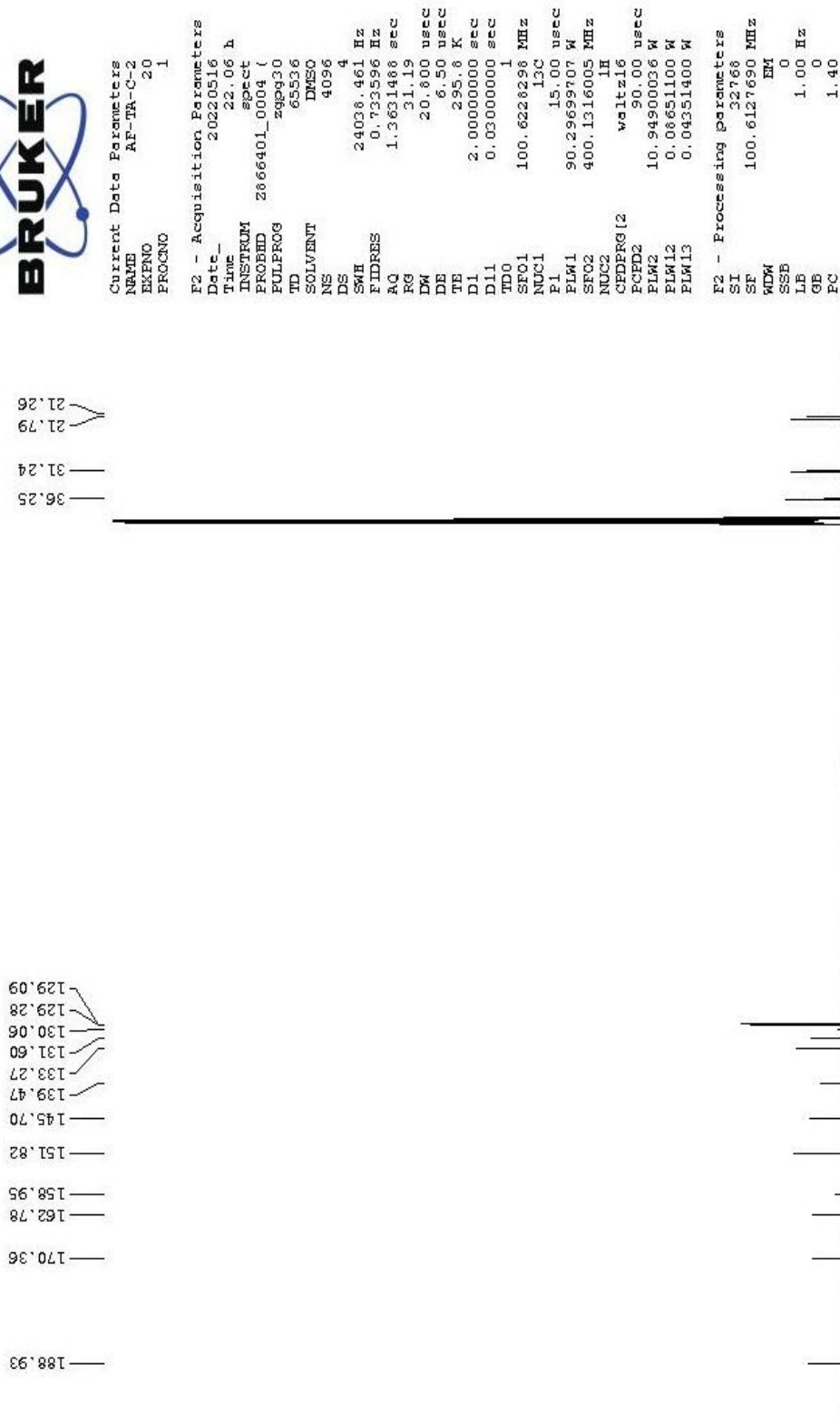


Figure 5.10.  $^{13}\text{C}$ -NMR spectrum of the compound **3b**

Data File: C:\LabSolutions\Data\Analiz\Asaf\AFTA-C-2\_58.lcd

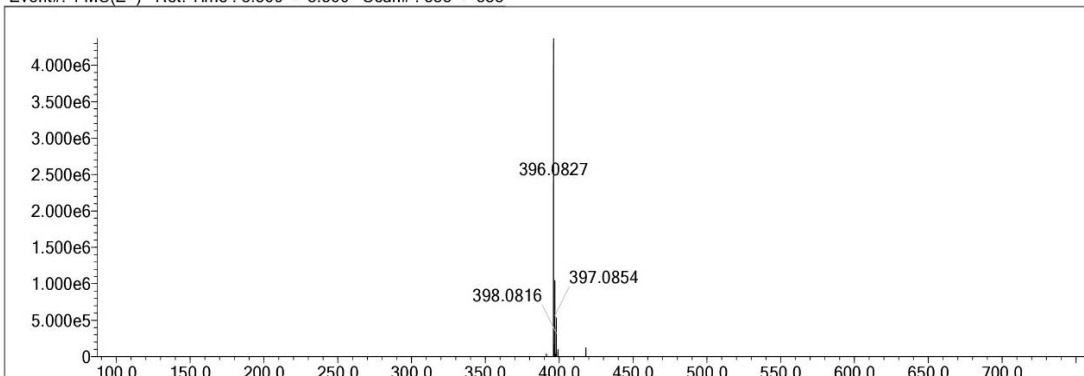
Elmt	Val.	Min	Max	Elmt	Val.	Min	Max	Elmt	Val.	Min	Max	Elmt	Val.	Min	Max	Use Adduct
H	1	9	35	O	2	0	3	S	2	0	2	Ru	2	0	0	H
C	4	7	35	F	1	0	0	Cl	1	0	0	Pd	2	0	0	
N	3	0	5	P	3	0	0	Br	1	0	0	I	3	0	0	

Error Margin (ppm): 5  
 HC Ratio: unlimited  
 Max Isotopes: 3  
 MSn Iso RI (%): 10.00

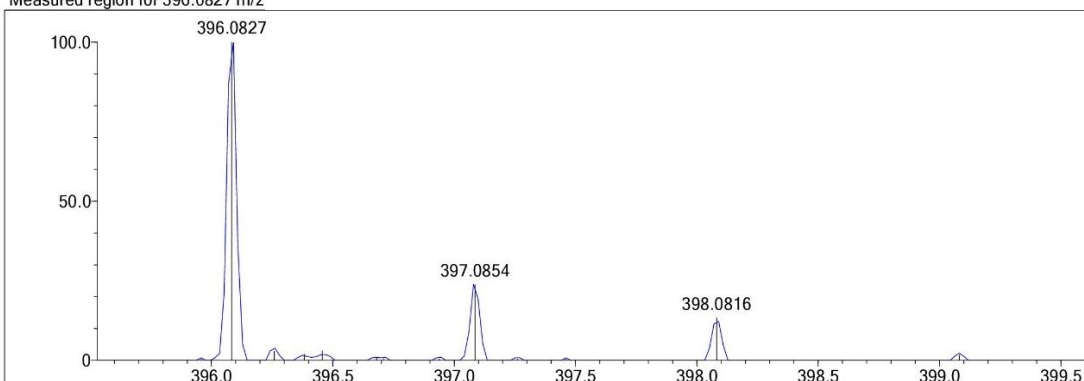
DBE Range: 5.0 - 25.0  
 Apply N Rule: yes  
 Isotope RI (%): 1.00  
 MSn Logic Mode: AND

Electron Ions: both  
 Use MSn Info: yes  
 Isotope Res: 9000  
 Max Results: 50

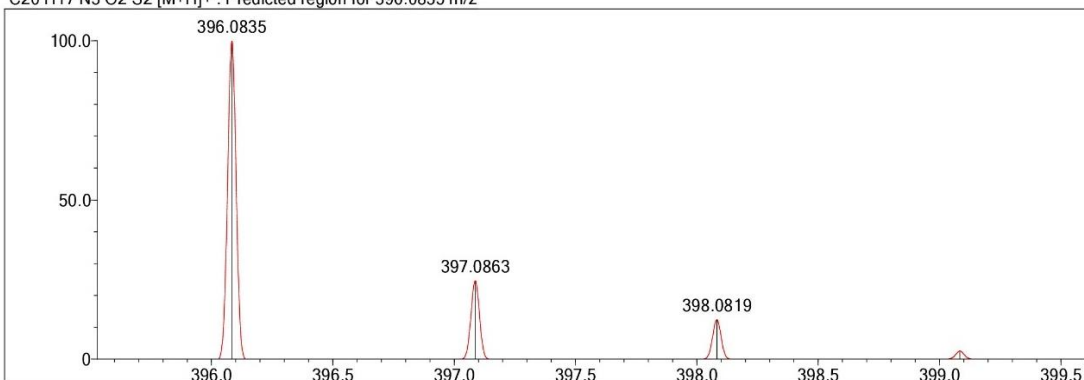
Event#: 1 MS(E+) Ret. Time : 3.560 -> 3.560 Scan# : 535 -> 535



Measured region for 396.0827 m/z



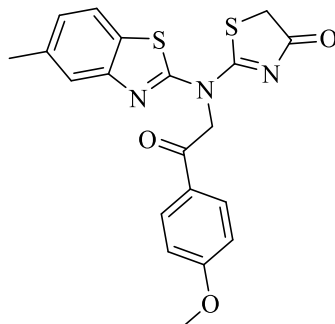
C20 H17 N3 O2 S2 [M+H]<sup>+</sup> : Predicted region for 396.0835 m/z



Rank	Score	Formula (M)	Ion	Meas. m/z	Pred. m/z	Df. (mDa)	Df. (ppm)	Iso	DBE
1	93.94	C20 H17 N3 O2 S2	[M+H] <sup>+</sup>	396.0827	396.0835	-0.8	-2.02	96.40	14.0

Figure 5.11. Mass spectrum of the compound 3b

5.1.3.3. 2-[[2-(4-methoxyphenyl)-2-oxoethyl](5-methylbenzothiazol-2-yl)amino]thiazol-4(5H)-one



3c

Synthesized according to method C, experimental melting point: 233-234°C, 52% yield percent.

**IR (ATR)  $\nu_{\text{max}}(\text{cm}^{-1})$ :** 2964 ( aromatic C-H stretching band), 2929 ( aliphatic C-H stretching band), 1685 (C=O stretching band), 1595 and 1408 (C=N and C=C stretching band), 1168 (C-O stretching band), 827 (1,3 di-substituted benzene out of plane bending band).

**$^1\text{H-NMR}$  (400 MHz, DMSO- $d_6$ ;  $\delta$ , ppm):** 2.42 (3H, s, benzothiazole-CH<sub>3</sub>), 3.91 (3H, s, O-CH<sub>3</sub>), 4.05 (2H, s, thiazolinone-CH<sub>2</sub>), 6.11 (2H, s, N-CH<sub>2</sub>), 7.16 (2H, d,  $J=8$  Hz, Ar-H), 7.35 (H, d,  $J=8$  Hz, Ar-H), 7.62 (H, d,  $J=8$  Hz, Ar-H), 7.86 (H, s, Ar-H), 7.96 (H, s, Ar-H), 8.13 (H, d,  $J=8$  Hz, Ar-H).

**$^{13}\text{C-NMR}$  (100 MHz, DMSO- $d_6$ ;  $\delta$ , ppm)** 21.29 (benzothiazole-CH<sub>3</sub>), 31.24 (thiazolinone-CH<sub>2</sub>), 36.25 (N-CH<sub>2</sub>-C=O), 56.27 (phenyl-O-CH<sub>3</sub>), 114.76, 120.87, 123.55, 125.34, 131.33, 134.57, 161.94, 162.78, 164.64, 176.48, 178.87, (thiazolinone-C=O) 190.23 ( N-CH<sub>2</sub>-C=O).

**HRMS (-m/z): [M+H]<sup>+</sup>:** For C<sub>20</sub>H<sub>17</sub>N<sub>3</sub>O<sub>3</sub>S<sub>2</sub>, calculated molecular weight: 412.0784, found: 412.0783.

# DOPNALAB

Item	Value
Acquired Date&Time	10.06.2022 10:09:07
Acquired by	System Administrator
Filename	C:\Users\dopnalab\Desktop\MASAÜSTÜ\LEYLA YURTDAŞ\AF-TA\AF-TA-C-31.ispd
Spectrum name	AF-TA-C-31
Sample name	AF-TA-C-3
Sample ID	
Option	
Comment	
No. of Scans	15
Resolution	4 [cm <sup>-1</sup> ]
Apodization	Happ-Genzel

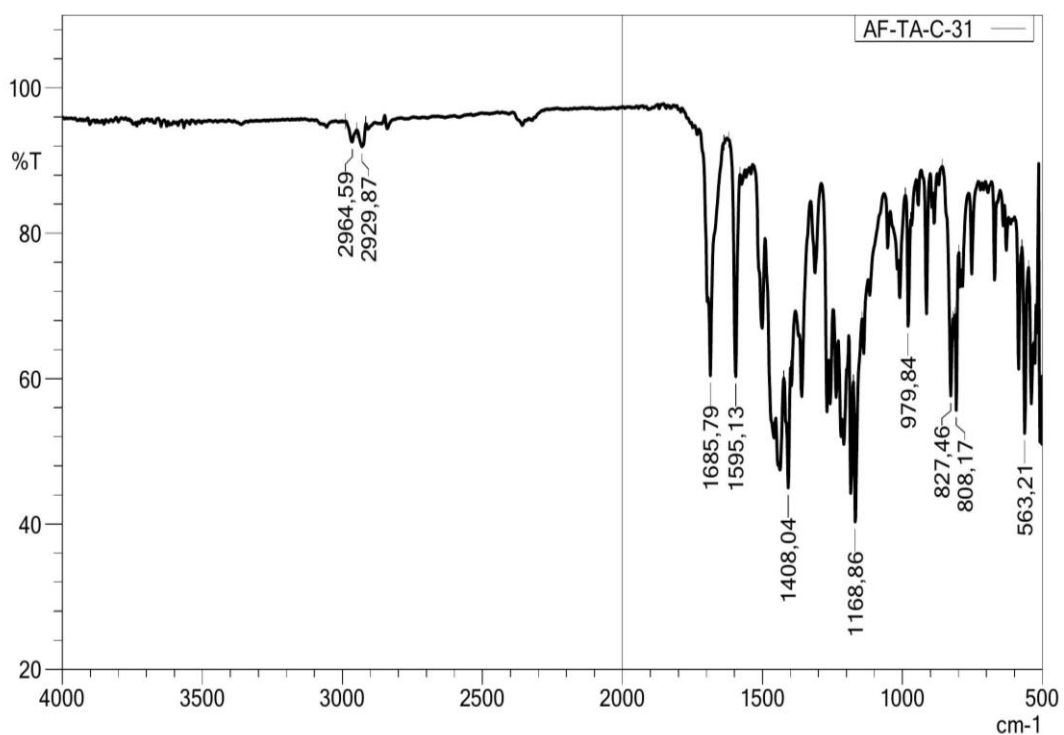
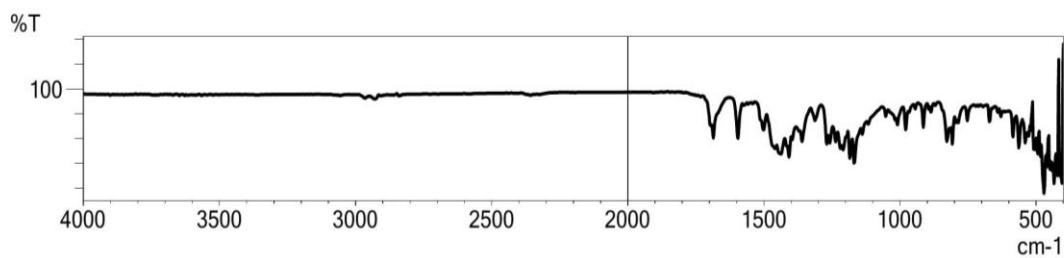


**Figure 5.12.** IR spectrum of the compound **3c**



Current Data Parameters  
NAME AF-TA-C-3  
EXPNO 10  
PROCNO 1

F2 - Acquisition Parameters  
Date\_ 20220517  
Time 13.20 h  
INSTRUM spect  
PROBHD zg30  
PULPROG zg30  
TD 65536  
SOLVENT DMSO  
NS 64  
DS 2  
SWH 8012.820 Hz  
FIDRES 0.244532 Hz  
AQ 4.0894465 sec  
RG 111.15  
DW 62.400 usec  
DE 6.50 usec  
TE 295.2 K  
D1 1.00000000 sec  
TD0 1  
SFO1 400.1324708 MHz  
NUC1 1H  
PI 8.00 usec  
PLW1 10.94900036 W

F2 - Processing parameters  
SI 65536  
SF 400.1300000 MHz  
WDW EM  
SSB 0  
LB 0.30 Hz  
GB 0  
PC 1.00

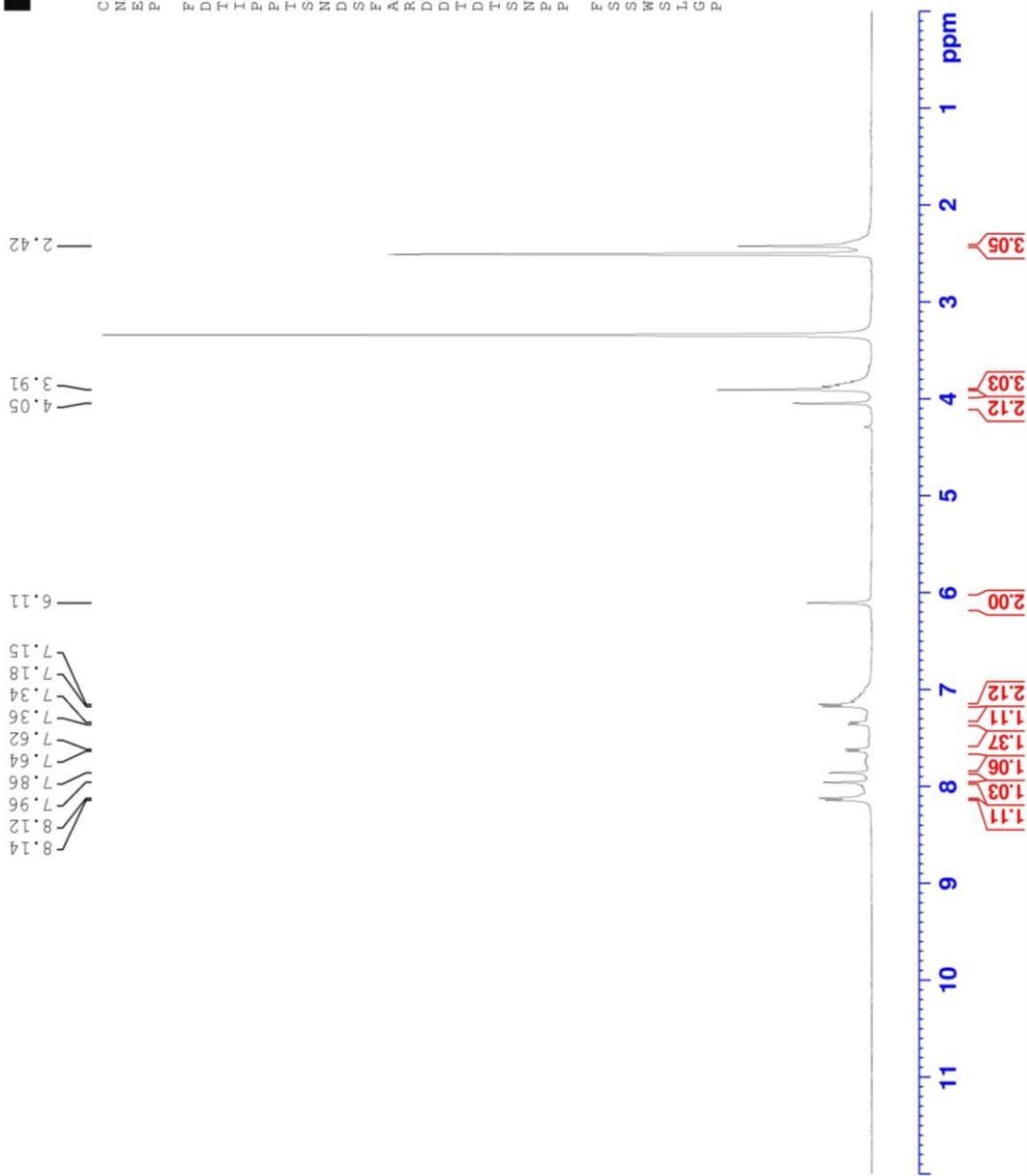


Figure 5.13.  $^1\text{H-NMR}$  spectrum of the compound **3c**



Current Data Parameters  
NAME AF-TA-C3  
EXPNO 11  
PROCNO 1

F2 - Acquisition Parameters  
Date\_ 20220621  
Time 11.56 h  
INSTRUM spect  
PROBHD zgpg30  
PULPROG zgpg30  
TD 65536  
SOLVENT DMSO  
NS 4096  
DS 4  
SWH 24028.461 Hz  
FIDRES 0.733556 Hz  
AQ 1.3631488 sec  
RG 31.19  
DM 20.800 use  
DE 6.50 use  
TE 296.0 K  
D1 2.00000000 sec  
D11 0.03000000 sec  
TD0 1  
SFO1 100.6228296 MHz  
NUC1 13C  
P1 15.00 use  
PLW1 90.29699707 W  
SFO2 400.1316005 MHz  
NUC2 1H  
CDEPRG12 waltz16  
PCPD2 90.00 use  
PLW2 10.94900036 W  
PLW12 0.08651100 W  
PLW13 0.04251400 W

F2 - Processing Parameters  
SI 32768  
SF 100.6127630 MHz  
WDW EM  
SSB 0  
LB 1.00 Hz  
GB 0  
PC 1.40

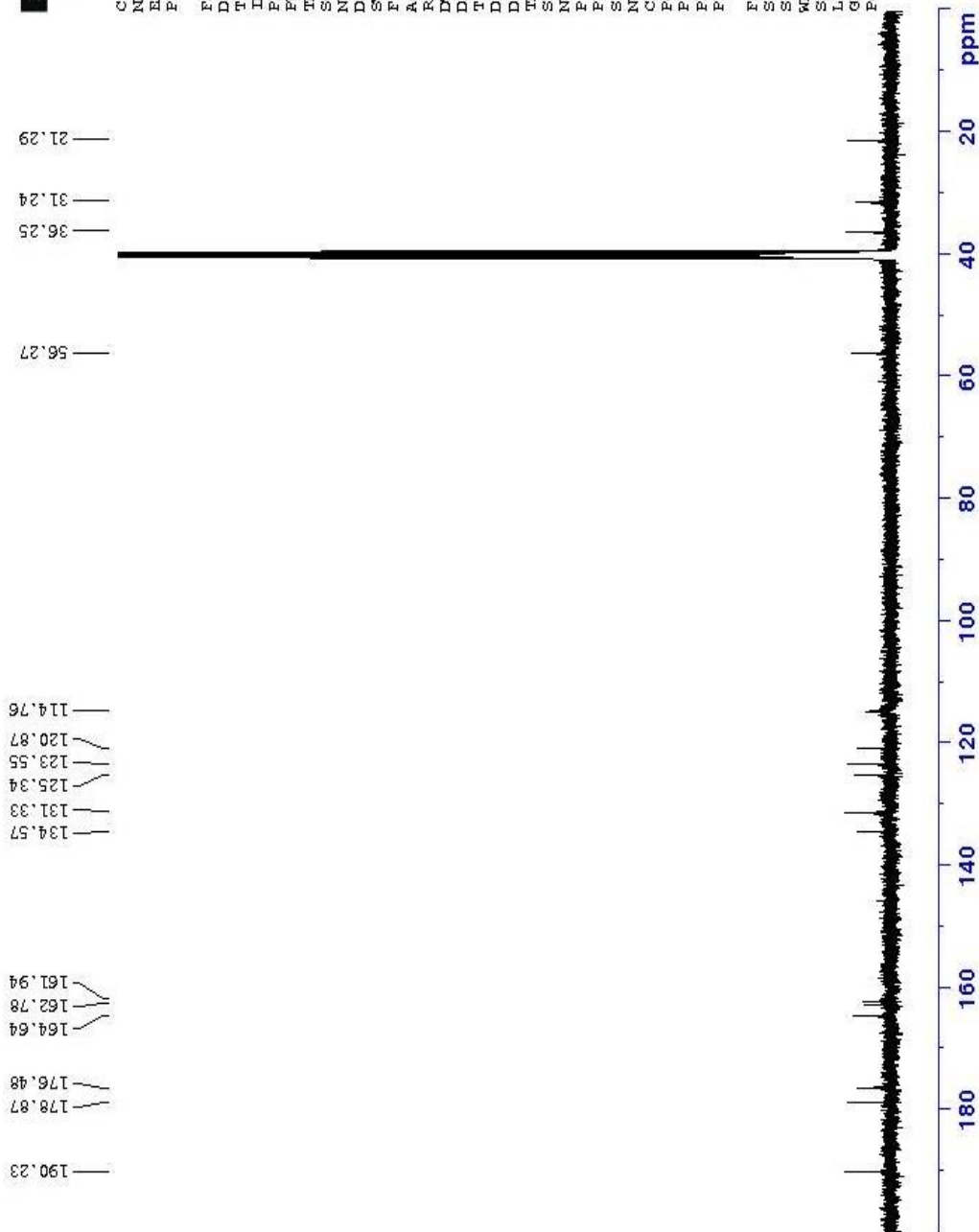


Figure 5.14.  $^{13}\text{C}$ -NMR spectrum of the compound 3c

Data File: C:\LabSolutions\Data\Analiz\Asaf\AFTA-C-3\_59.lcd

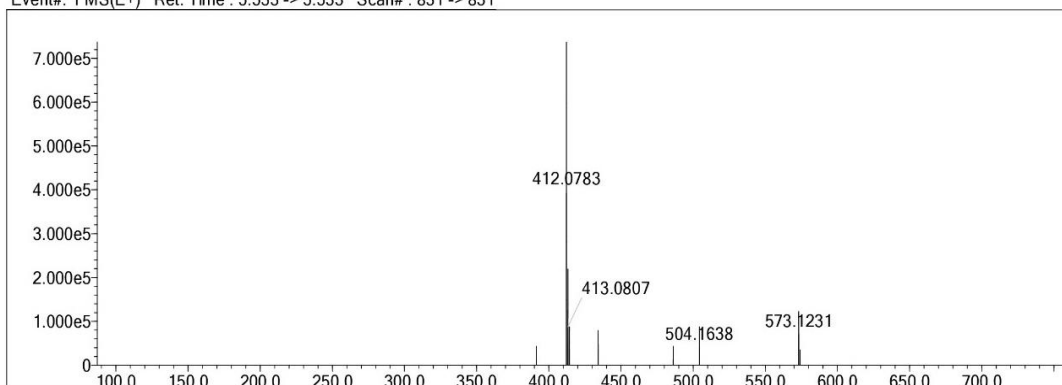
Elmt	Val.	Min	Max	Elmt	Val.	Min	Max	Elmt	Val.	Min	Max	Elmt	Val.	Min	Max	Use Adduct
H	1	9	35	O	2	0	3	S	2	0	2	Ru	2	0	0	H
C	4	7	35	F	1	0	0	Cl	1	0	0	Pd	2	0	0	
N	3	0	5	P	3	0	0	Br	1	0	0	I	3	0	0	

Error Margin (ppm): 5  
 HC Ratio: unlimited  
 Max Isotopes: 3  
 MSn Iso RI (%): 10.00

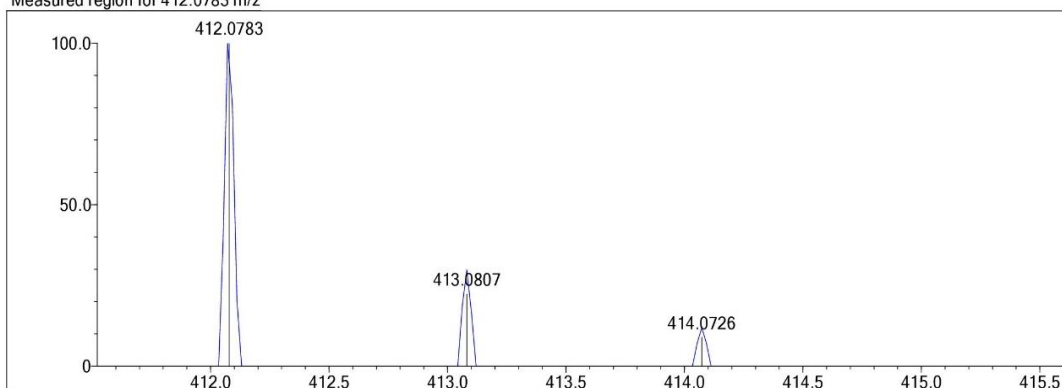
DBE Range: 5.0 - 25.0  
 Apply N Rule: yes  
 Isotope RI (%): 1.00  
 MSn Logic Mode: AND

Electron Ions: both  
 Use MSn Info: yes  
 Isotope Res: 9000  
 Max Results: 50

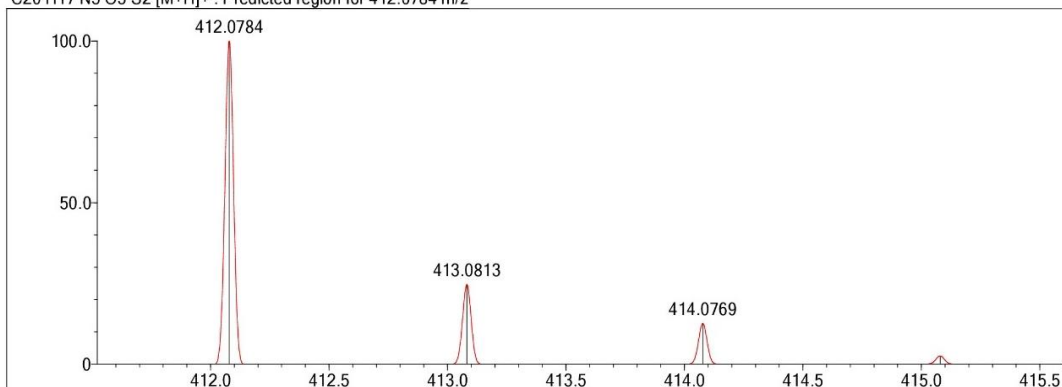
Event#: 1 MS(E+) Ret. Time: 5.533 -> 5.533 Scan#: 831 -> 831



Measured region for 412.0783 m/z



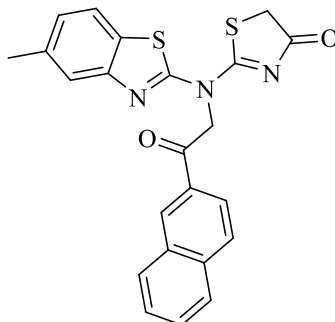
C20 H17 N3 O3 S2 [M+H]<sup>+</sup> : Predicted region for 412.0784 m/z



Rank	Score	Formula (M)	Ion	Meas. m/z	Pred. m/z	Df. (mDa)	Df. (ppm)	Iso	DBE
1	71.31	C20 H17 N3 O3 S2	[M+H] <sup>+</sup>	412.0783	412.0784	-0.1	-0.24	71.31	14.0

Figure 5.15. Mass spectrum of the compound 3c

**5.1.3.4. 2-[(5-methylbenzothiazol-2-yl)[2-(naphthalen-2-yl)-2-oxoethyl]amino]thiazol-4(5H)-one**



**3d**

Synthesized according to method **C**, experimental melting point 180-181 °C, 65% yield percent.

**IR (ATR)  $\nu_{\text{max}}(\text{cm}^{-1})$ :** 3059 ( aromatic C-H stretching band), 2929 ( aliphatic C-H stretching band), 1687 (C=O stretching band), 1446 (C=N and C=C stretching band).

**$^1\text{H-NMR}$  (400 MHz, DMSO- $d_6$ ;  $\delta$ , ppm):** 2.43 (3H, s, benzothiazole-CH<sub>3</sub>), 4.04 (2H, s, thiazolinone-CH<sub>2</sub>), 6.32 (2H, s, N-CH<sub>2</sub>), 7.36 (H, d,  $J=8$  Hz, Ar-H), 7.69 -7.76 (3H, m, Ar-H), 7.88 (H, s, Ar-H), 8.06 -8.12 (3H, m, Ar-H), 8.22 (H, d,  $J=8$  Hz, Ar-H), 8.99 (H, s, Ar-H).

**$^{13}\text{C-NMR}$  (100 MHz, DMSO- $d_6$ ;  $\delta$ , ppm)** 21.24 (benzothiazole-CH<sub>3</sub>), 36.32 (thiazolinone-CH<sub>2</sub>), 52.57 (N-CH<sub>2</sub>-C=O), 113.57, 123.59, 123.83, 126.55, 127.79, 128.34, 129.14, 129.75, 130.21, 131.47, 131.89, 132.56, 135.14, 135.75, 136.02, 166.51, 188.26, 188.74 (thiazolinone-C=O), 191.91 (N-CH<sub>2</sub>-C=O).

**HRMS (- $m/z$ ):  $[\text{M}+\text{H}]^+$ :** For C<sub>23</sub>H<sub>17</sub>N<sub>3</sub>O<sub>2</sub>S<sub>2</sub>, calculated molecular weight: 432.0835, found: 432.0848.

# DOPNALAB

Item	Value
Acquired Date&Time	10.06.2022 10:17:57
Acquired by	System Administrator
Filename	C:\Users\dopnalab\Desktop\MASAÜSTÜLEYLE YURTDAŞIAF-TA\AF-TA-C-41.ispd
Spectrum name	AF-TA-C-41
Sample name	AF-TA-C-4
Sample ID	
Option	
Comment	
No. of Scans	15
Resolution	4 [cm-1]
Apodization	Happ-Genzel

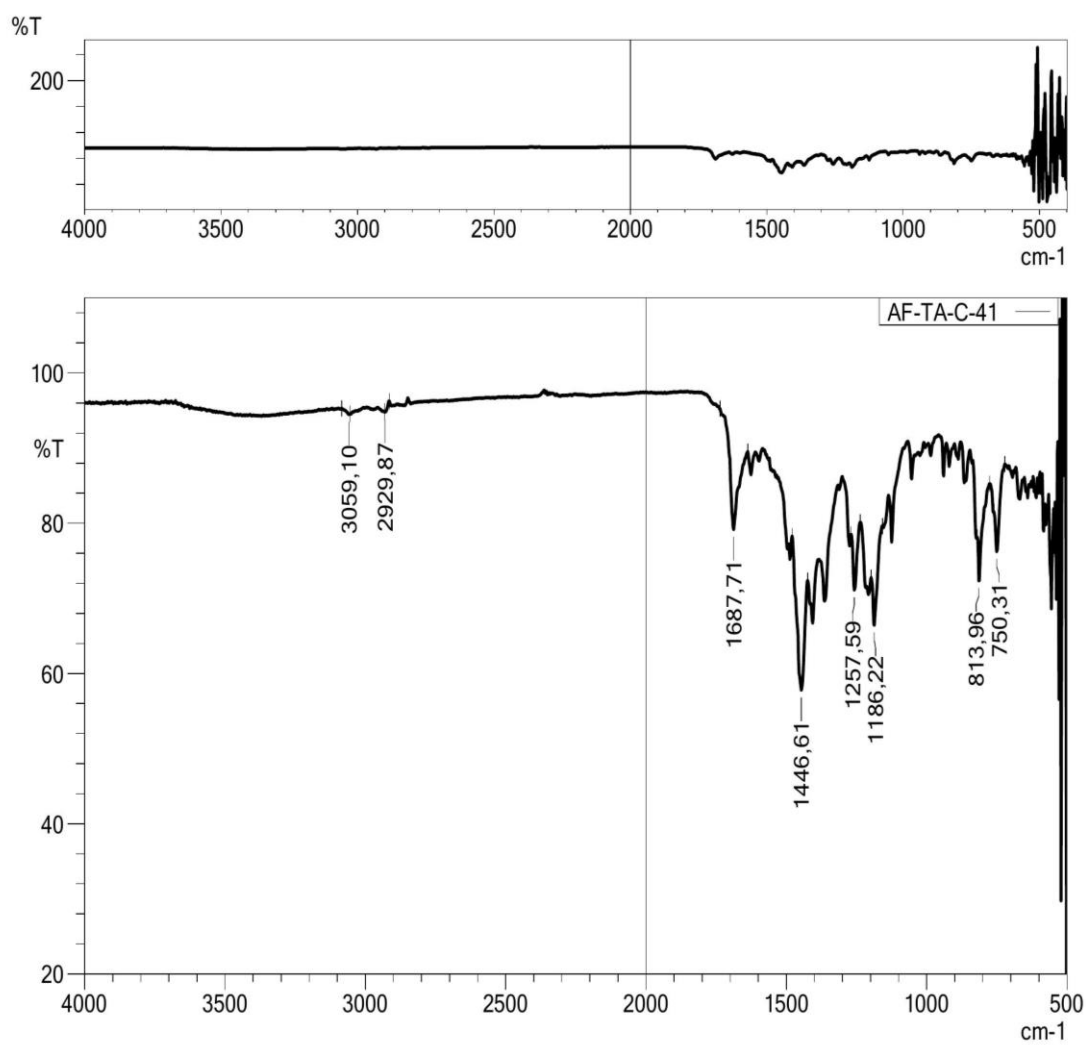


Figure 5.16. IR spectrum of the compound 3d

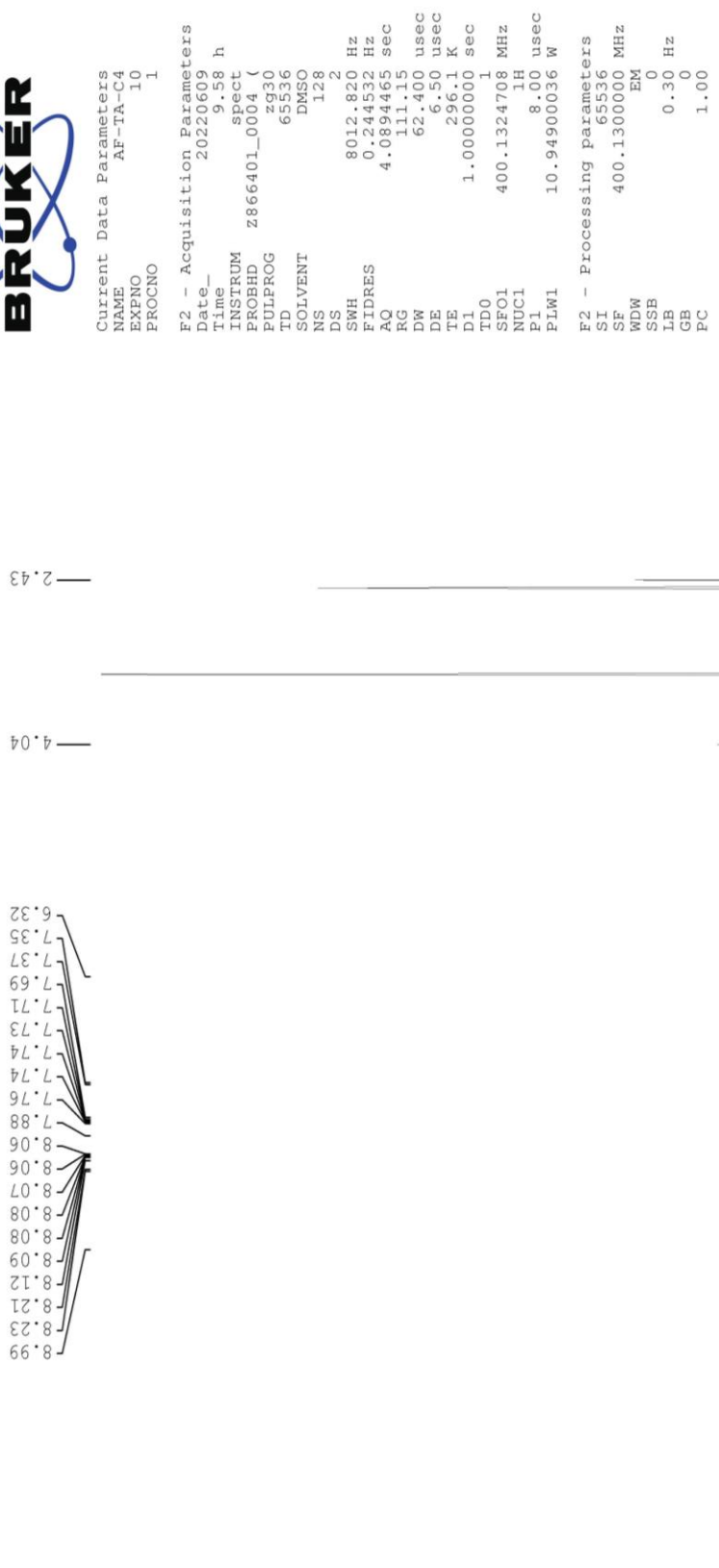


Figure 5.17. <sup>1</sup>H-NMR spectrum of the compound 3d



Current Data Parameters  
 NAME AF-TR-C4  
 EKFN0 12  
 FROCN0 1

F2 - Acquisition Parameters  
 Date\_ 20220622  
 Time\_ 7.41 h  
 INSTRUM spect  
 PROBD 2666401\_0004 ( )  
 FULPRG zqzq30  
 TD 65536  
 SOLVENT DMSO  
 NS 4096  
 DS 4  
 SWH 24038.461 Hz  
 FIDRES 0.733596 Hz  
 AQ 1.3631466 sec  
 RG 31.19  
 DW 20.800 usec  
 DE 6.50 usec  
 TE 295.7 K  
 D1 2.00000000 sec  
 D11 0.03000000 sec  
 TDO 1  
 SFO1 100.6228298 MHz  
 NUC1 13C  
 P1 15.00 usec  
 PLW1 90.29699707 W  
 SFO2 400.1316005 MHz  
 NUC2 1H  
 CPDPRG12 waltz16  
 FCPD2 90.00 usec  
 PLW2 10.94900036 W  
 PLW12 0.08651100 W  
 PLW13 0.04351400 W

F2 - Processing parameters  
 SI 32768  
 SF 100.6127690 MHz  
 WDW EM  
 SSB 0  
 LB 1.00 Hz  
 GB 0  
 PC 1.40

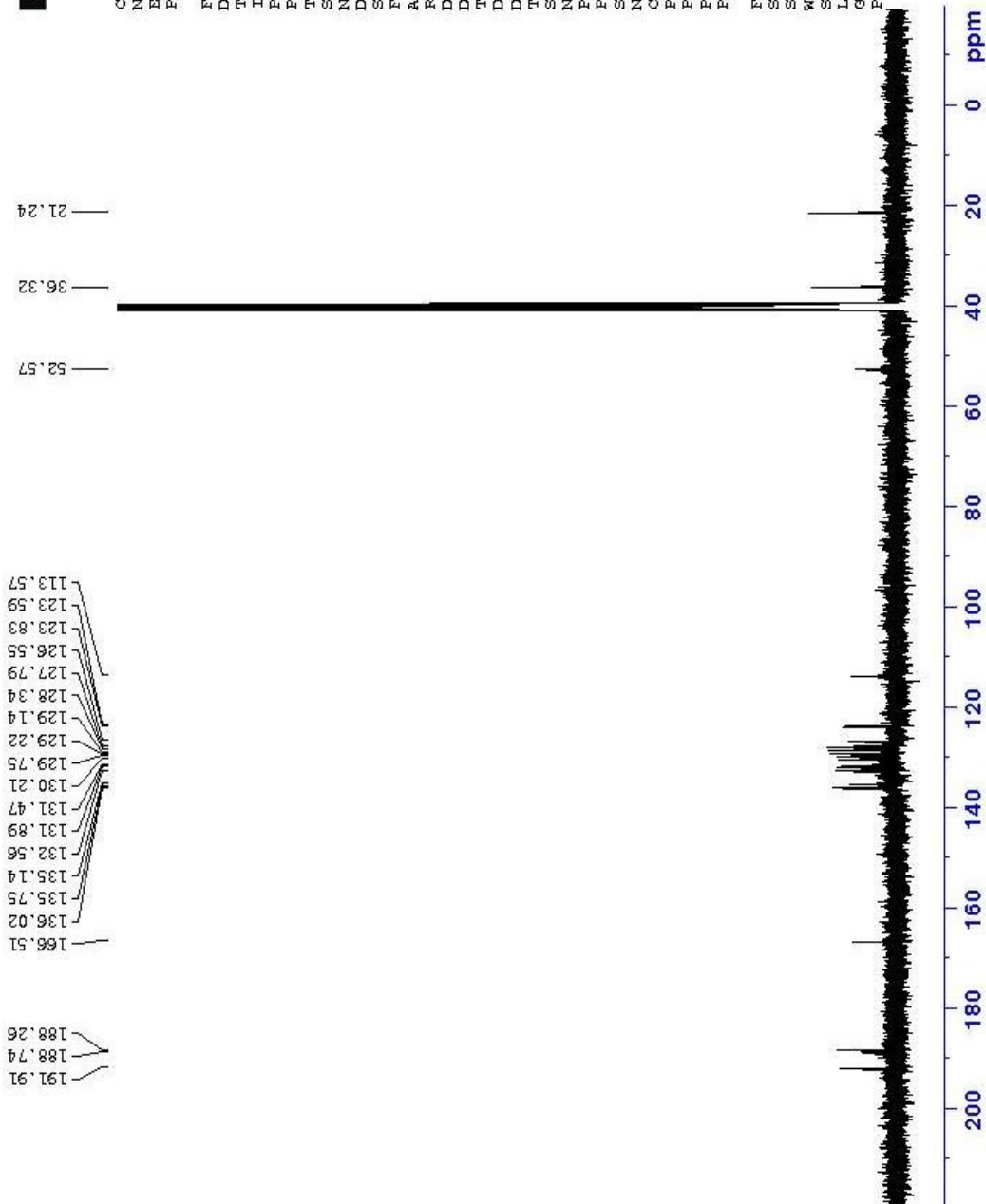


Figure 5.18. <sup>13</sup>C-NMR spectrum of the compound 3d

Data File: C:\LabSolutions\Data\Analiz\Asaf\AF-TA-C-4\_240.lcd

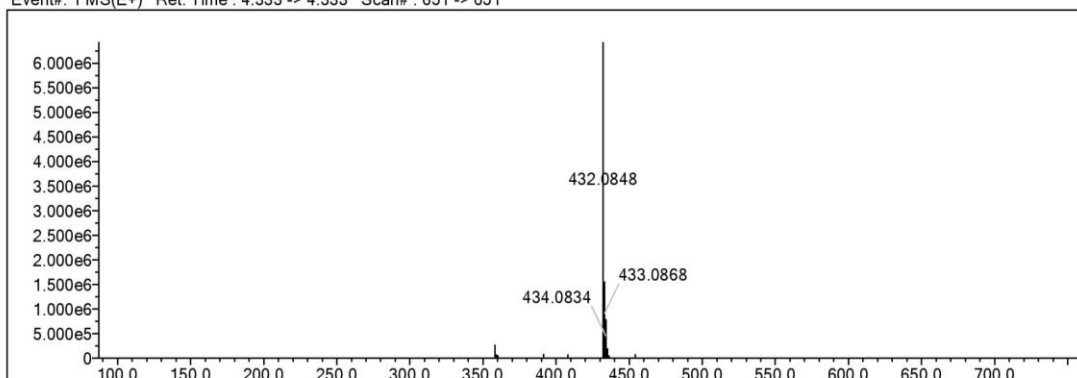
Elmt	Val.	Min	Max	Elmt	Val.	Min	Max	Elmt	Val.	Min	Max	Elmt	Val.	Min	Max	Use Adduct
H	1	9	26	O	2	0	4	Cl	1	0	2	I	3	0	0	H
B	3	0	0	F	1	0	0	Br	1	0	0					
C	4	7	37	P	3	0	0	Ru	2	0	0					
N	3	2	6	S	2	0	2	Pd	2	0	0					

Error Margin (ppm): 5  
 HC Ratio: unlimited  
 Max Isotopes: 3  
 MSn Iso RI (%): 10.00

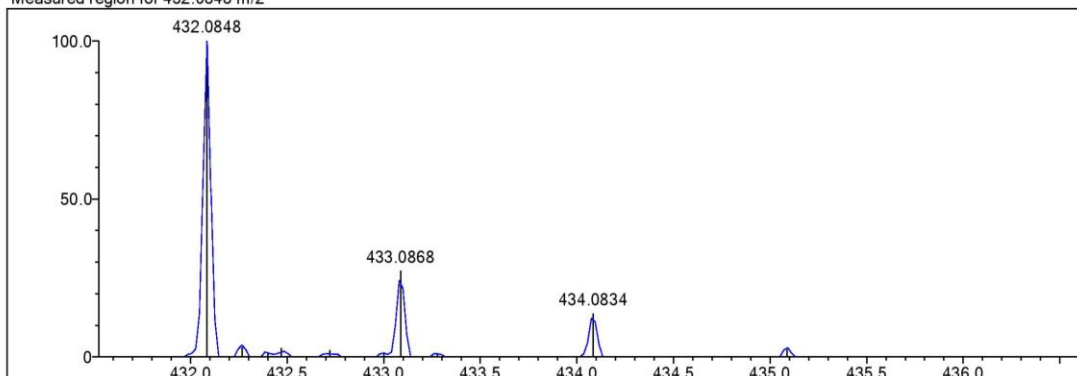
DBE Range: 5.0 - 20.0  
 Apply N Rule: yes  
 Isotope RI (%): 1.00  
 MSn Logic Mode: AND

Electron Ions: both  
 Use MSn Info: yes  
 Isotope Res: 9000  
 Max Results: 50

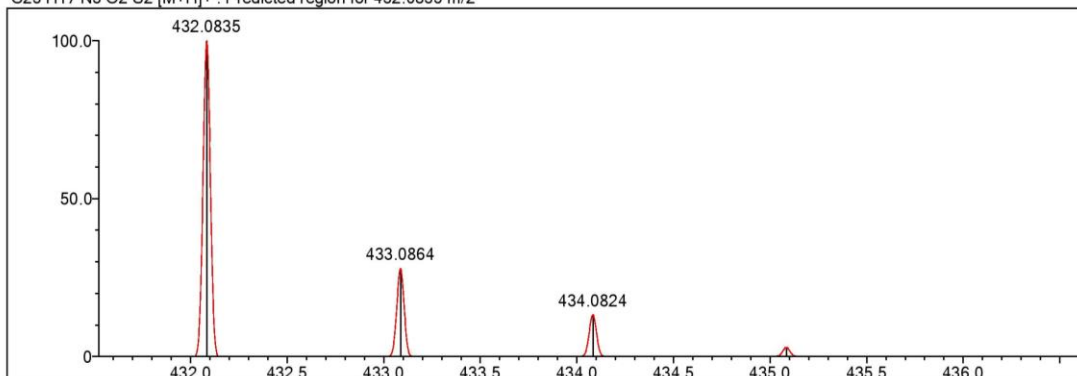
Event#: 1 MS(E+) Ret. Time : 4.333 -> 4.333 Scan# : 651 -> 651



Measured region for 432.0848 m/z



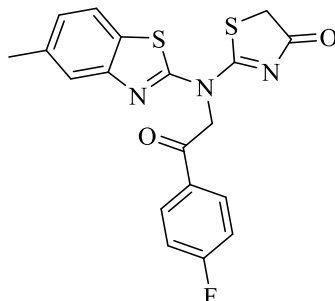
C23 H17 N3 O2 S2 [M+H]+ : Predicted region for 432.0835 m/z



Rank	Score	Formula (M)	Ion	Meas. m/z	Pred. m/z	Df. (mDa)	Df. (ppm)	Iso	DBE
1	81.88	C23 H17 N3 O2 S2	[M+H]+	432.0848	432.0835	1.3	3.01	86.21	17.0

Figure 5.19. Mass spectrum of the compound 3d

5.1.3.5. 2-[[2-(4-fluorophenyl)-2-oxoethyl](5-methylbenzothiazol-2-yl)amino]thiazol-4(5H)-one



3e

Synthesized according to method C, experimental melting point: 214-215°C, 63% yield percent.

**IR (ATR)  $\nu_{\max}(\text{cm}^{-1})$ :** 2972 ( aromatic C-H stretching band), 2935 ( aliphatic C-H stretching band), 1689 (C=O stretching band), 1490 and 1456 (C=N and C=C stretching band), 800 (1,3 di-substituted benzene out of plane bending band).

**$^1\text{H-NMR}$  (400 MHz, DMSO- $d_6$ ;  $\delta$ , ppm):** 2.42 (3H, s, benzothiazole-CH<sub>3</sub>), 4.05 (2H, s, thiazolinone-CH<sub>2</sub>), 6.16 (2H, s, N-CH<sub>2</sub>), 7.35 (H, d,  $J=8$  Hz, Ar-H), 7.49 (2H, t,  $J=8$  Hz, Ar-H), 7.66 (H, d,  $J=8$  Hz, Ar-H), 7.86 (H, s, Ar-H), 8.23-8.27 (2H, m, Ar-H).

**$^{13}\text{C-NMR}$  (100 MHz, DMSO- $d_6$ ;  $\delta$ , ppm)** 21.23 (benzothiazole-CH<sub>3</sub>), 35.58 (thiazolinone-CH<sub>2</sub>), 52.45 (N-CH<sub>2</sub>-C=O), 113.51, 116.51, 116.73, 123.58, 126.50, 129.18, 131.39, 132.03, 132.13, 135.12, 135.66, 164.92, 166.47, 167.44, 188.24, 188.73 (thiazolinone-C=O), 190.69 (N-CH<sub>2</sub>-C=O).

**HRMS (-m/z): [M+H]<sup>+</sup>:** For C<sub>19</sub>H<sub>14</sub>FN<sub>3</sub>O<sub>2</sub>S<sub>2</sub>, calculated molecular weight: 400.0584, found: 400.0580.

# DOPNALAB

Item	Value
Acquired Date&Time	10.06.2022 10:33:05
Acquired by	System Administrator
Filename	C:\Users\dopnalab\Desktop\MASAÜSTÜ\LEYLA YURTDAS\AF-TA\AF-TA-C-61.ispd
Spectrum name	AF-TA-C-61
Sample name	AF-TA-C-6
Sample ID	
Option	
Comment	
No. of Scans	15
Resolution	4 [cm-1]
Apodization	Happ-Genzel

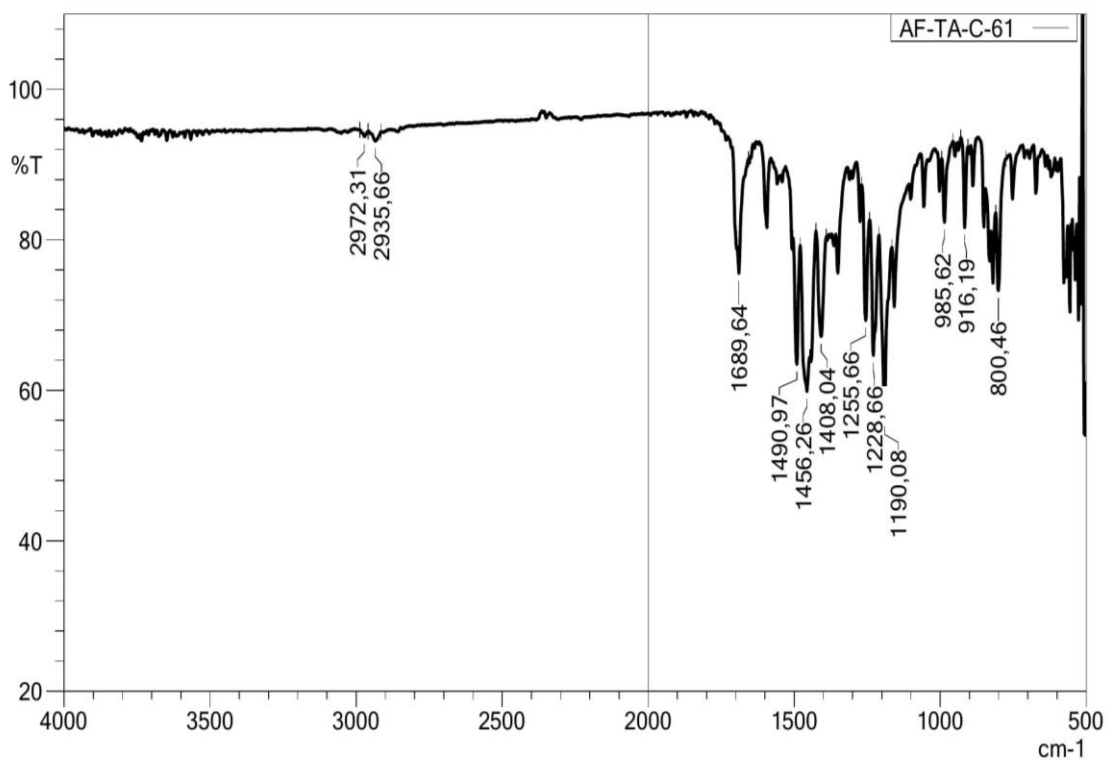
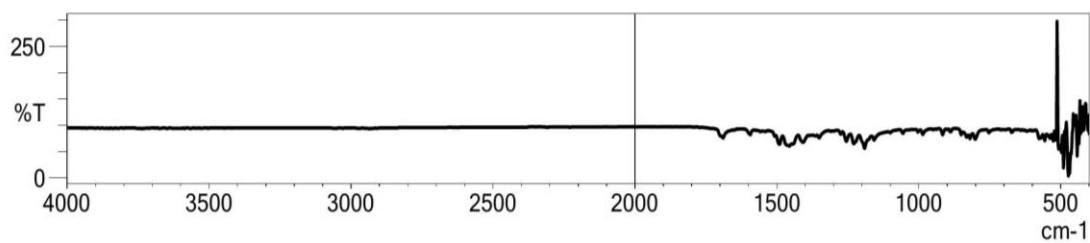


Figure 5.20. IR spectrum of the compound *3e*



Current Data Parameters  
NAME AF-TA-C-6  
EXPNO 10  
PROCNO 1

F2 - Acquisition Parameters  
Date\_ 20220517  
Time 14.17 h  
INSTRUM spect  
PROBHD Z866401\_0004 (   
PULPROG zg30  
TD 65536  
SOLVENT DMSO  
NS 64  
DS 2  
SWH 8012.820 Hz  
FIDRES 0.244532 Hz  
AQ 4.0894465 sec  
RG 143.29  
DW 62.400 usec  
DE 6.50 usec  
TE 295.2 K  
D1 1.00000000 sec  
TD0 1  
SFO1 400.1324708 MHz  
NUC1 1H  
P1 8.00 usec  
PLW1 10.94900036 W

F2 - Processing parameters  
SI 65536  
SF 400.1300000 MHz  
WDW EM  
SSB 0  
LB 0.30 Hz  
GB 0  
PC 1.00

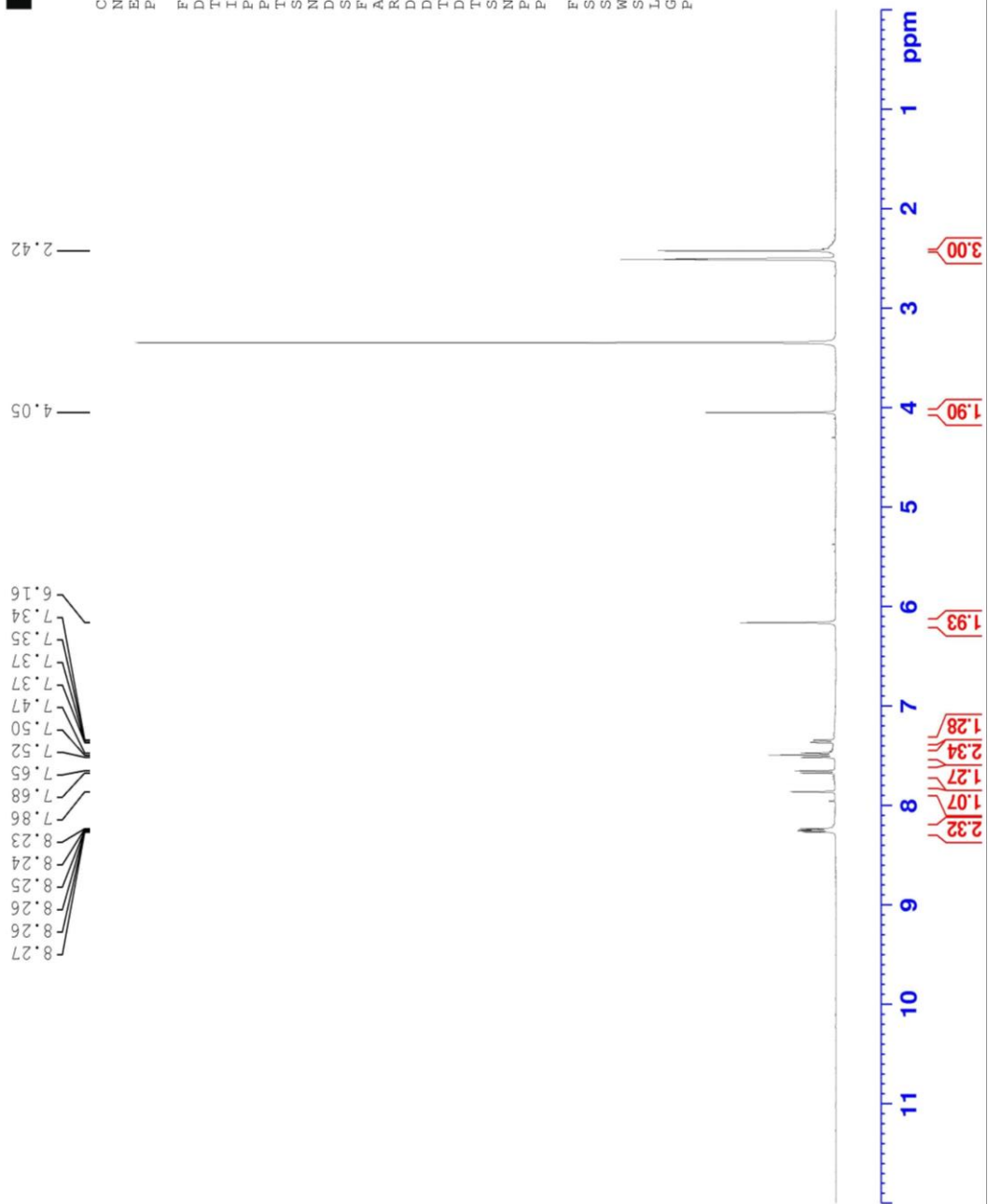


Figure 5.21.  $^1\text{H}$ -NMR spectrum of the compound **3e**

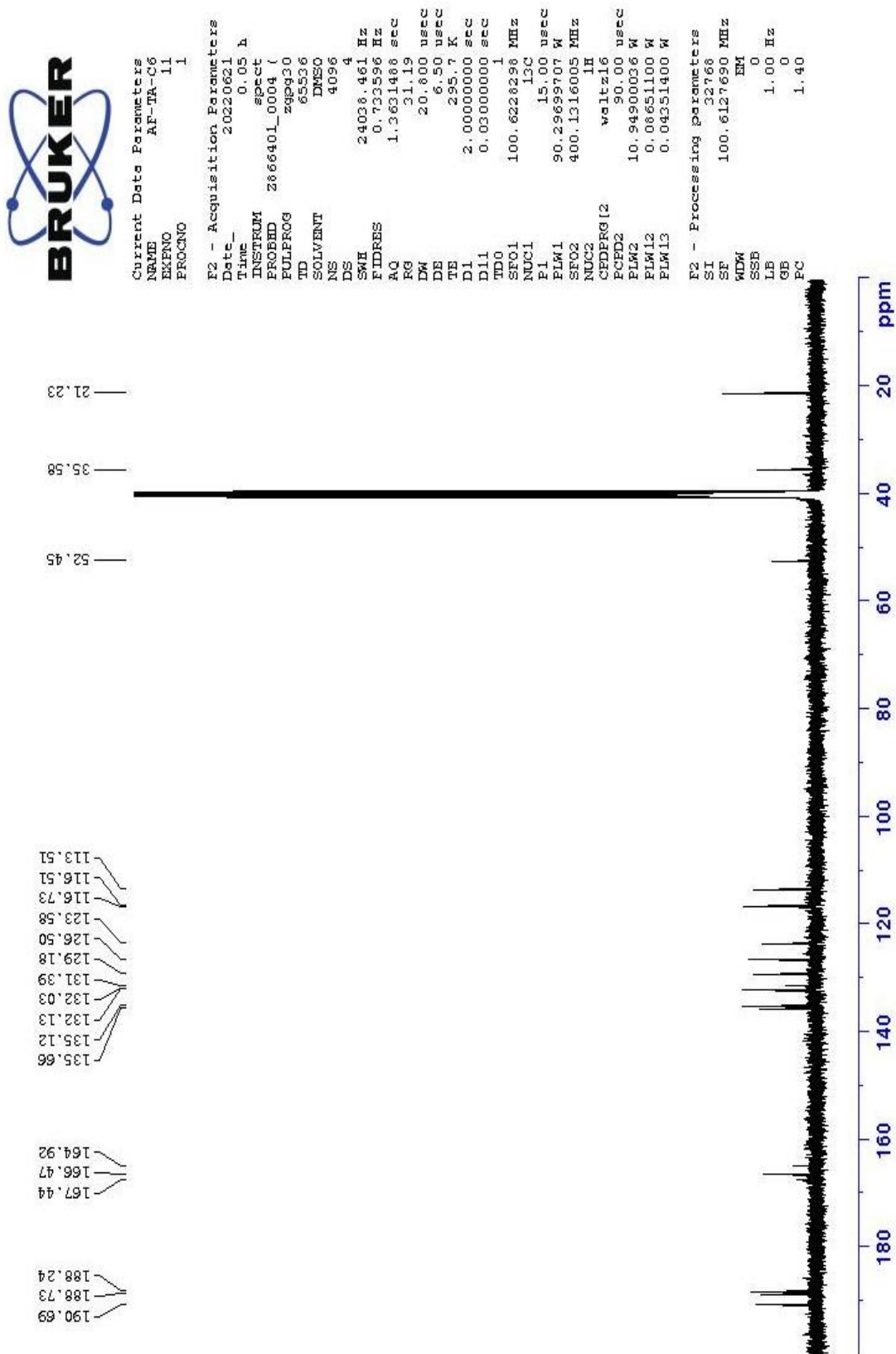


Figure 5.22.  $^{13}\text{C}$ -NMR spectrum of the compound **3e**

Data File: C:\LabSolutions\Data\Analyze\Asaf\AFTA-C-6\_61.lcd

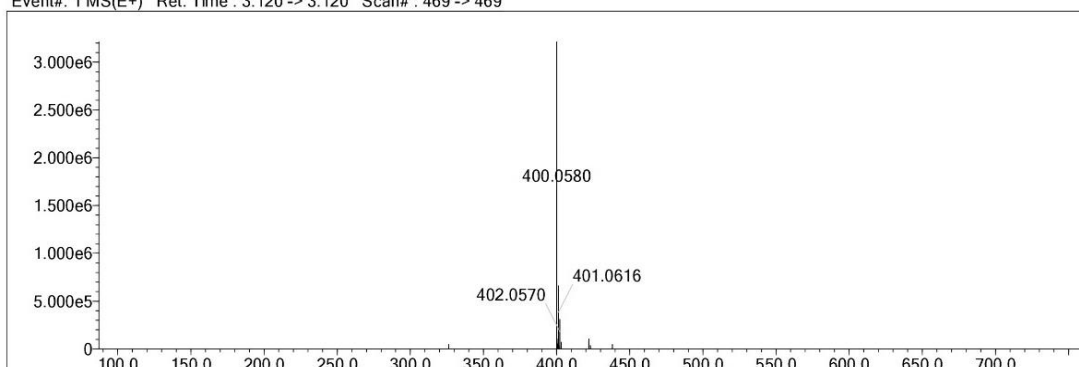
Elmt	Val.	Min	Max	Elmt	Val.	Min	Max	Elmt	Val.	Min	Max	Elmt	Val.	Min	Max	Use Adduct
H	1	9	35	O	2	0	3	S	2	0	2	Ru	2	0	0	H
C	4	7	35	F	1	0	1	Cl	1	0	0	Pd	2	0	0	
N	3	0	5	P	3	0	0	Br	1	0	0	I	3	0	0	

Error Margin (ppm): 5  
 HC Ratio: unlimited  
 Max Isotopes: 3  
 MSn Iso RI (%): 10.00

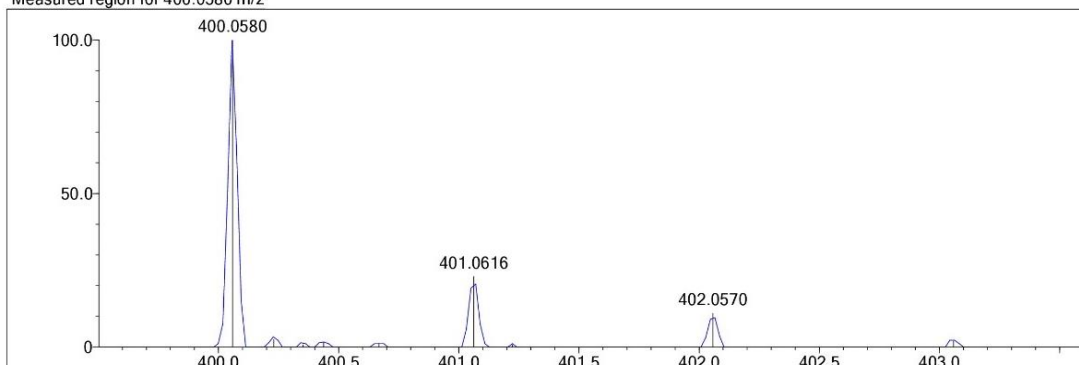
DBE Range: 5.0 - 25.0  
 Apply N Rule: yes  
 Isotope RI (%): 1.00  
 MSn Logic Mode: AND

Electron Ions: both  
 Use MSn Info: yes  
 Isotope Res: 9000  
 Max Results: 50

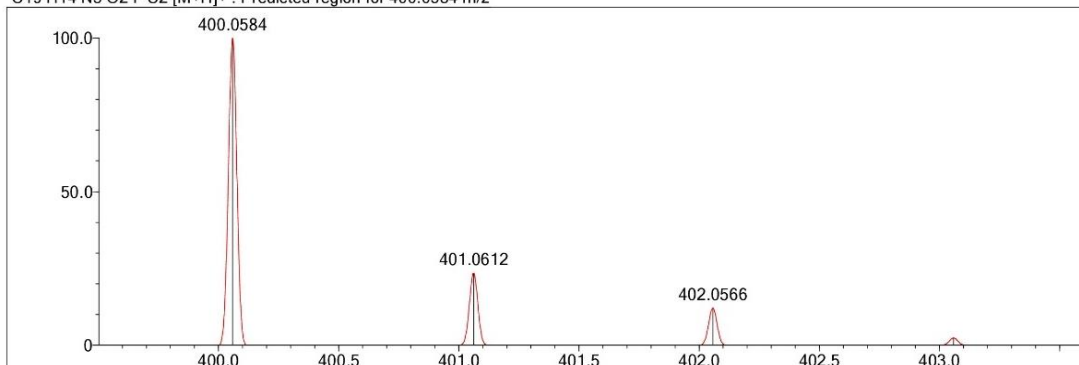
Event#: 1 MS(E+) Ret. Time : 3.120 -> 3.120 Scan#: 469 -> 469



Measured region for 400.0580 m/z



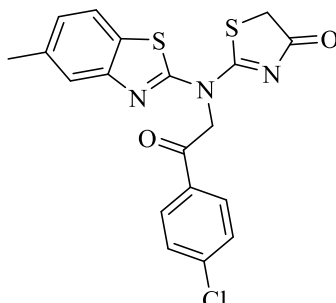
C19 H14 N3 O2 F S2 [M+H]<sup>+</sup> : Predicted region for 400.0584 m/z



Rank	Score	Formula (M)	Ion	Meas. m/z	Pred. m/z	Df. (mDa)	Df. (ppm)	Iso	DBE
1	89.58	C19 H14 N3 O2 F S2	[M+H] <sup>+</sup>	400.0580	400.0584	-0.4	-1.00	89.58	14.0

Figure 5.23. Mass spectrum of the compound 3e

5.1.3.6. 2-[[2-(4-chlorophenyl)-2-oxoethyl](5-methylbenzothiazol-2-yl)amino]thiazol-4(5H)-one



3f

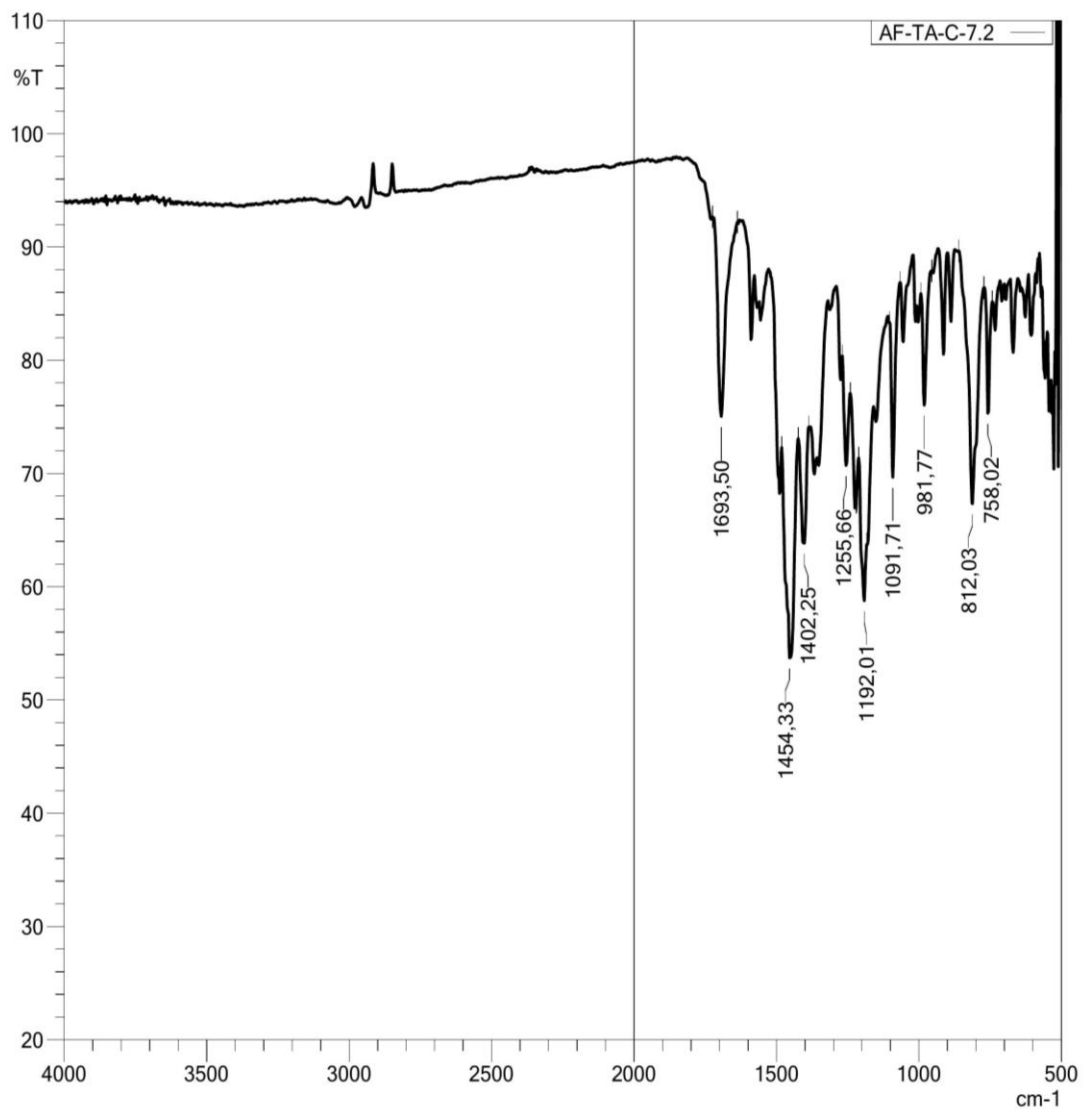
Synthesized according to method C, experimental melting point: 216-217°C, 58% yield percent.

**IR (ATR)  $\nu_{\text{max}}(\text{cm}^{-1})$ :** 1693 (C=O stretching band), 1454 and 1402 (C=N and C=C stretching band), 812 (1,3 di-substituted benzene out of plane bending band).

**$^1\text{H-NMR}$  (400 MHz, DMSO- $d_6$ ;  $\delta$ , ppm):** 2.42 (3H, s, benzothiazole-CH<sub>3</sub>), 4.05 (2H, s, thiazolinone-CH<sub>2</sub>), 6.16 (2H, s, N-CH<sub>2</sub>), 7.35 (H, d,  $J=8$  Hz, Ar-H), 7.65-7.74 (3H, m, Ar-H), 7.86 (H, s, Ar-H), 8.17 (2H, d,  $J=8$  Hz, Ar-H).

**$^{13}\text{C-NMR}$  (100 MHz, DMSO- $d_6$ ;  $\delta$ , ppm)** 21.23 (benzothiazole-CH<sub>3</sub>), 36.17 (thiazolinone-CH<sub>2</sub>), 52.50 (N-CH<sub>2</sub>-C=O), 113.51, 123.59, 126.50, 129.18, 129.64, 130.66, 130.84, 133.29, 135.14, 135.63, 139.83, 166.44, 188.25 (thiazolinone-C=O), 191.23 (N-CH<sub>2</sub>-C=O).

**HRMS (-m/z):  $[\text{M}+\text{H}]^+$ :** For C<sub>19</sub>H<sub>14</sub>ClN<sub>3</sub>O<sub>2</sub>S<sub>2</sub>, calculated molecular weight: 416.0289, found: 416.0297.



C:\Users\dopnalab\Desktop\MASA7ST7\LEYLELA YURTDA\AF-TA\AF-TA-C-7.2.ispd

	Item	Value
2	Sample name	AF-TA-C-7
3	Sample ID	
4	Option	
5	Intensity Mode	% Transmittance
6	Apodization	Happ-Genzel
9	No. of Scans	15

Figure 5.24. IR spectrum of the compound 3f



Current Data Parameters  
NAME AF-TA-C-7  
EXPNO 10  
PROCNO 1

F2 - Acquisition Parameters  
Date\_ 20220517  
Time 14.01 h  
INSTRUM spect  
PROBHD z866401\_0004 ( )  
PULPROG zg30  
TD 65536  
SOLVENT DMSO  
NS 64  
DS 2  
SWH 8012.820 Hz  
FIDRES 0.244532 Hz  
AQ 4.0894465 sec  
RG 128.58  
DW 62.400 usec  
DE 6.50 usec  
TE 295.1 K  
D1 1.00000000 sec  
ID0 1  
SFO1 400.1324708 MHz  
NUC1 1H  
P1 8.00 usec  
PLW1 10.94900036 W

F2 - Processing parameters  
SI 65536  
SF 400.1300000 MHz  
WDW EM  
SSB 0  
LB 0.30 Hz  
GB 0  
PC 1.00

6.1579

7.3470  
7.3668  
7.6576  
7.6789  
7.6837  
7.7054  
7.7236  
7.7447  
7.8616  
8.1829  
8.1615

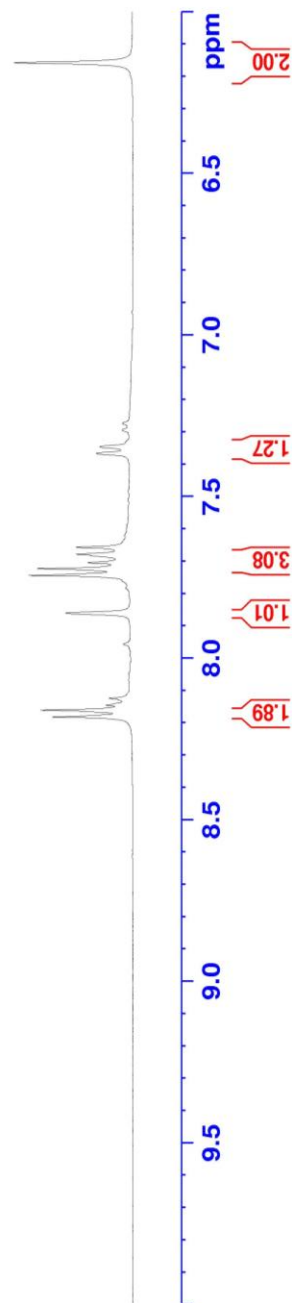


Figure 5.25.  $^1\text{H}$ -NMR spectrum of the compound 3f



```

Current Data Parameters
NAME      AF-TA-C7
EXPNO    11
PROCNO   1

F2 - Acquisition Parameters
Date_    20220620
Time     20.08 h
INSTRUM  spect
PROBHD   zgpg30
PULPROG  zgpg30
TD        65536
SOLVENT  DMSO
NS        4096
DS        4
SWH       24036.461 Hz
FIDRES   0.733596 Hz
AQ        1.3631488 sec
RG        31.19
DM        20.800 usec
DE        6.50 usec
TE        295.6 K
D1        2.00000000 sec
D11       0.03000000 sec
TD0       1
SFO1      100.6228298 MHz
NUC1      13C
F1         15.00 usec
PLW1      90.29699707 W
SFO2      400.1316005 MHz
NUC2      1H
PCPD2     waltz16
PLW2      90.00 usec
PLW12     10.94900036 W
PLW13     0.06651100 W
PLW14     0.04251400 W

F2 - Processing parameters
SI         32768
SF         100.6127690 MHz
WDW        EM
SSB        0
LB         1.00 Hz
GB         0
PC         1.40
  
```

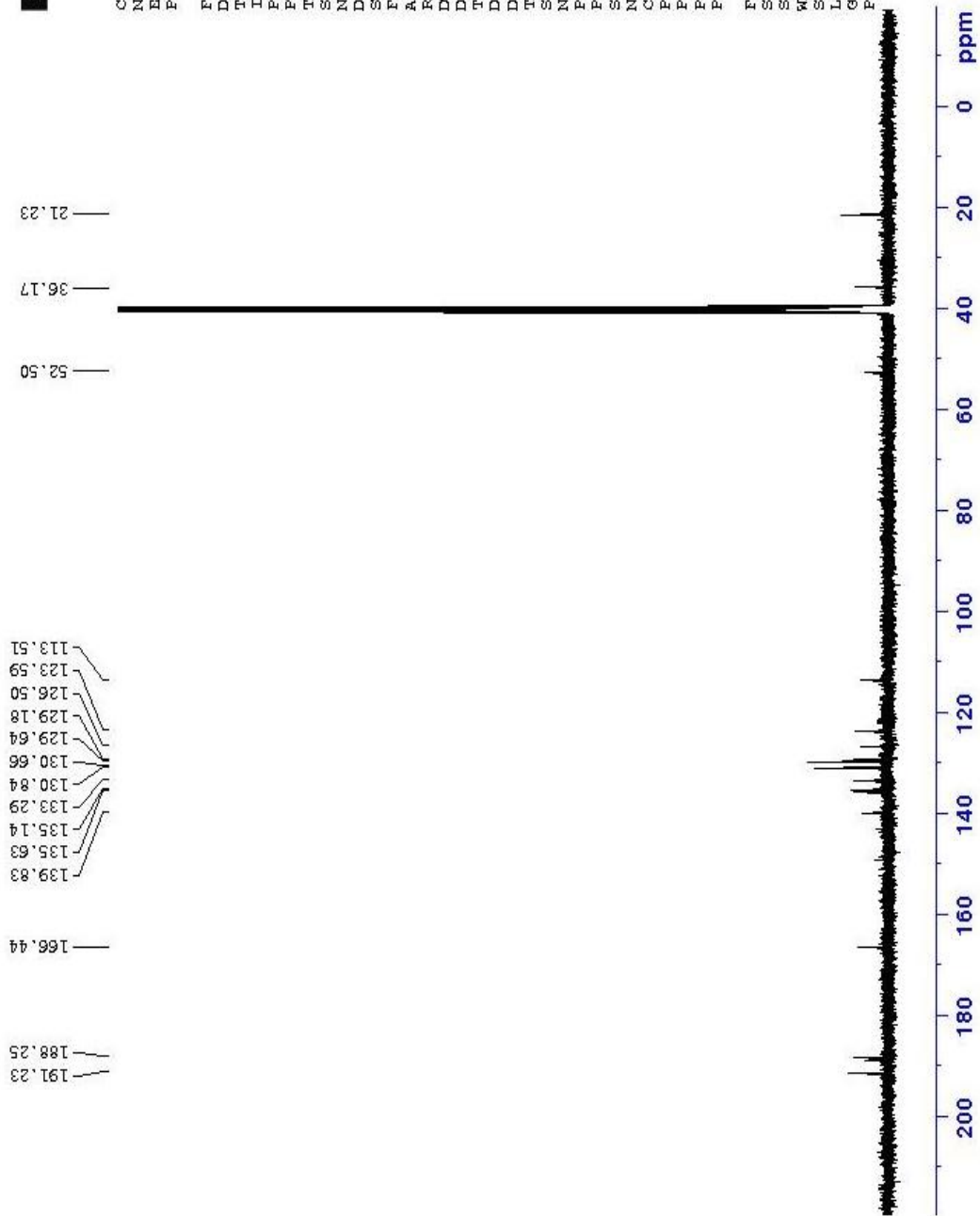


Figure 5.26. <sup>13</sup>C-NMR spectrum of the compound 3f

Data File: C:\LabSolutions\Data\Analiz\Asaf\AFTA-C-8\_63.lcd

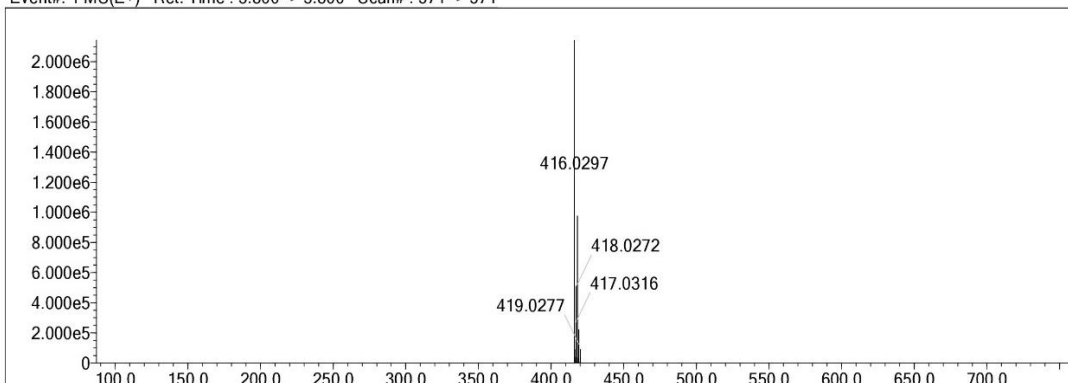
Elmt	Val.	Min	Max	Elmt	Val.	Min	Max	Elmt	Val.	Min	Max	Elmt	Val.	Min	Max	Use Adduct
H	1	9	35	O	2	0	3	S	2	0	2	Ru	2	0	0	H
C	4	7	35	F	1	0	0	Cl	1	0	1	Pd	2	0	0	
N	3	0	5	P	3	0	0	Br	1	0	0	I	3	0	0	

Error Margin (ppm): 5  
 HC Ratio: unlimited  
 Max Isotopes: 3  
 MSn Iso RI (%): 10.00

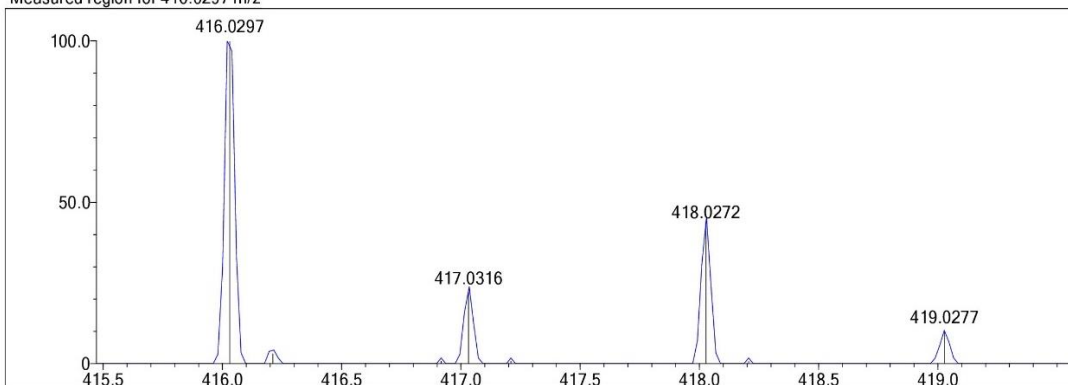
DBE Range: 5.0 - 25.0  
 Apply N Rule: yes  
 Isotope RI (%): 1.00  
 MSn Logic Mode: AND

Electron Ions: both  
 Use MSn Info: yes  
 Isotope Res: 9000  
 Max Results: 50

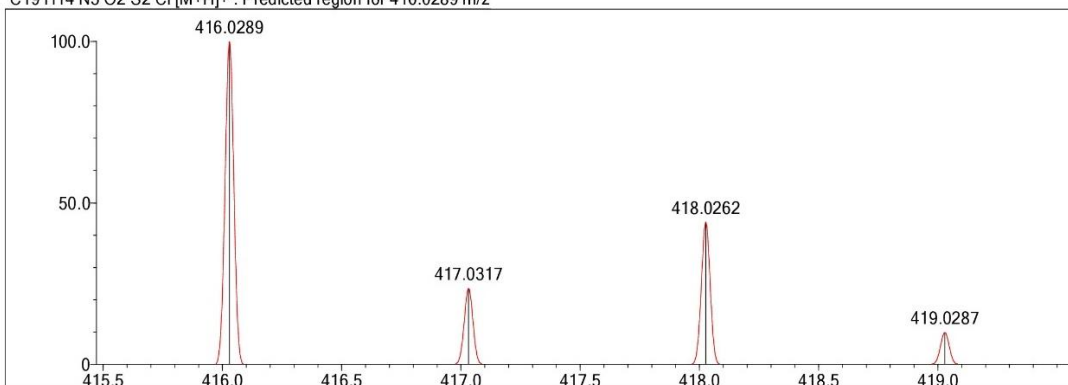
Event#: 1 MS(E+) Ret. Time : 3.800 -> 3.800 Scan# : 571 -> 571



Measured region for 416.0297 m/z



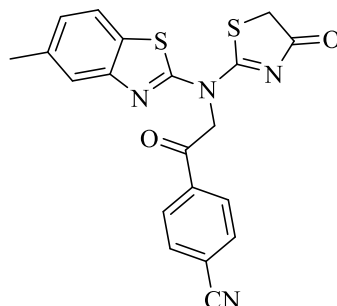
C19 H14 N3 O2 S2 Cl [M+H]<sup>+</sup> : Predicted region for 416.0289 m/z



Rank	Score	Formula (M)	Ion	Meas. m/z	Pred. m/z	Df. (mDa)	Df. (ppm)	Iso	DBE
1	97.70	C19 H14 N3 O2 S2 Cl	[M+H] <sup>+</sup>	416.0297	416.0289	0.8	1.92	100.00	14.0

Figure 5.27. Mass spectrum of the compound 3f

5.1.3.7. 4-[N-(5-methylbenzothiazol-2-yl)-N-(4-oxo-4,5-dihydrothiazol-2-yl)glycyl]benzonitrile



3g

Synthesized according to method C, experimental melting point 185-186°C, 55% yield percent.

**IR (ATR)  $\nu_{\max}(\text{cm}^{-1})$ :** 2927 ( aromatic C-H stretching band), 2858 ( aliphatic C-H stretching band), 2229 (  $\text{C}\equiv\text{N}$  stretching band), 1703 and 1666 (C=O stretching band), 1487 and 1446 (C=N and C=C stretching band), 815 (1,3 di-substituted benzene out of plane bending band).

**$^1\text{H-NMR}$  (400 MHz,  $\text{DMSO-}d_6$ ;  $\delta$ , ppm):** 2.42 (3H, s, benzothiazole- $\text{CH}_3$ ), 4.05 (2H, s, thiazolinone- $\text{CH}_2$ ), 6.21 (2H, s, N- $\text{CH}_2$ ), 7.36 (H, d,  $J=8$  Hz, Ar-H), 7.69 (H, d,  $J=8$  Hz, Ar-H), 7.87 (H, s, Ar-H), 8.15 (2H, d,  $J=8$  Hz, Ar-H) 8.31 (2H, d,  $J=8$  Hz, Ar-H).

**$^{13}\text{C-NMR}$  (100 MHz,  $\text{DMSO-}d_6$ ;  $\delta$ , ppm)** 21.46 (benzothiazole- $\text{CH}_3$ ), 31.24 (thiazolinone- $\text{CH}_2$ ), 36.25 (N- $\text{CH}_2$ -C=O), 117.87, 121.27, 121.94, 126.87, 127.39, 127.97, 128.22, 128.72, 130.37, 131.69, 132.84, 132.91, 133.06, 162.78 (thiazolinone- $\text{C}=\text{O}$ ), 166.12 (N- $\text{CH}_2$ - $\text{C}=\text{O}$ ).

**HRMS ( $-\text{m/z}$ ):  $[\text{M}+\text{H}]^+$ :** For  $\text{C}_{20}\text{H}_{14}\text{N}_4\text{O}_2\text{S}_2$ , calculated molecular weight: 407.0631, found: 407.0628.

# DOPNALAB

Item	Value
Acquired Date&Time	10.06.2022 10:23:37
Acquired by	System Administrator
Filename	C:\Users\dopnalab\Desktop\MASAÜSTÜ\LEYLA YURTDAŞ\AF-TA\AF-TA-C-51.ispd
Spectrum name	AF-TA-C-51
Sample name	AF-TA-C-5
Sample ID	
Option	
Comment	
No. of Scans	15
Resolution	4 [cm-1]
Apodization	Happ-Genzel

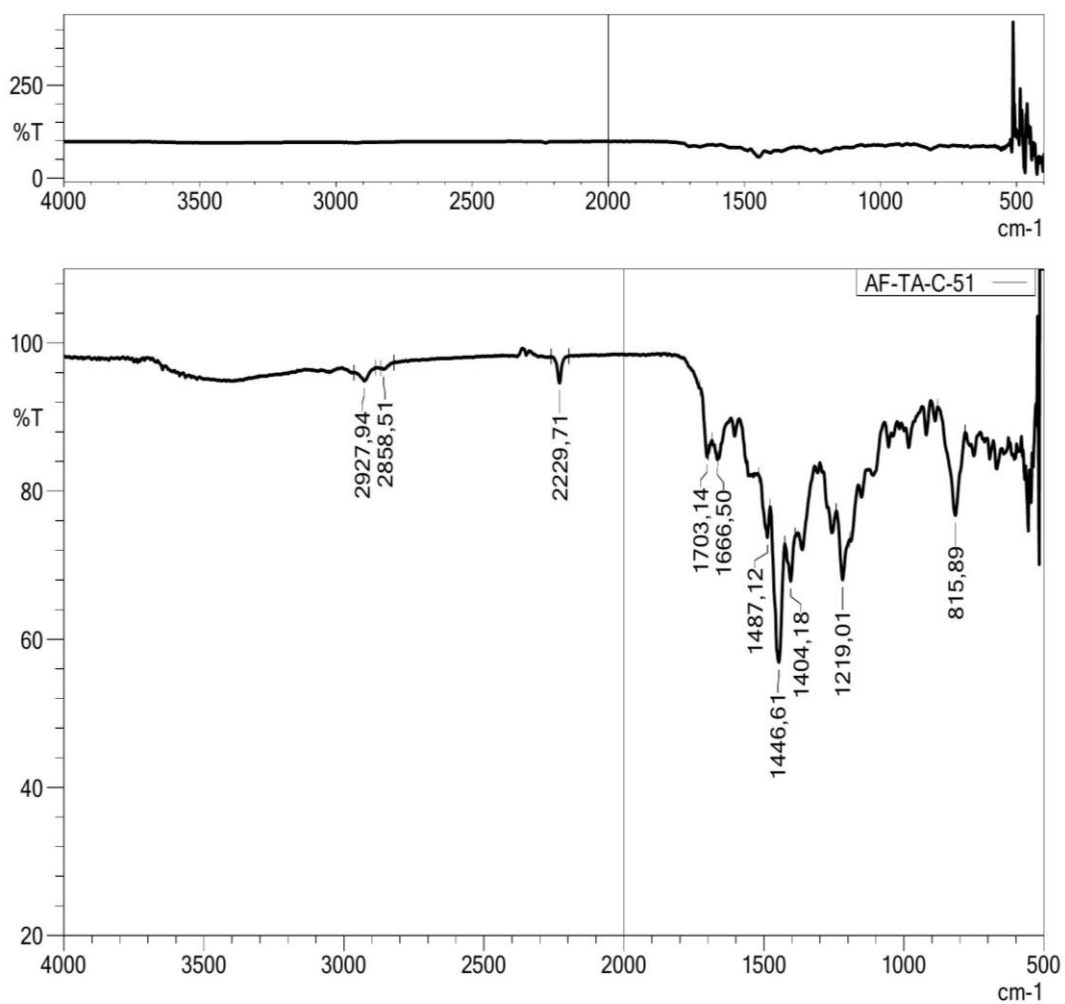


Figure 5.28. IR spectrum of the compound 3g

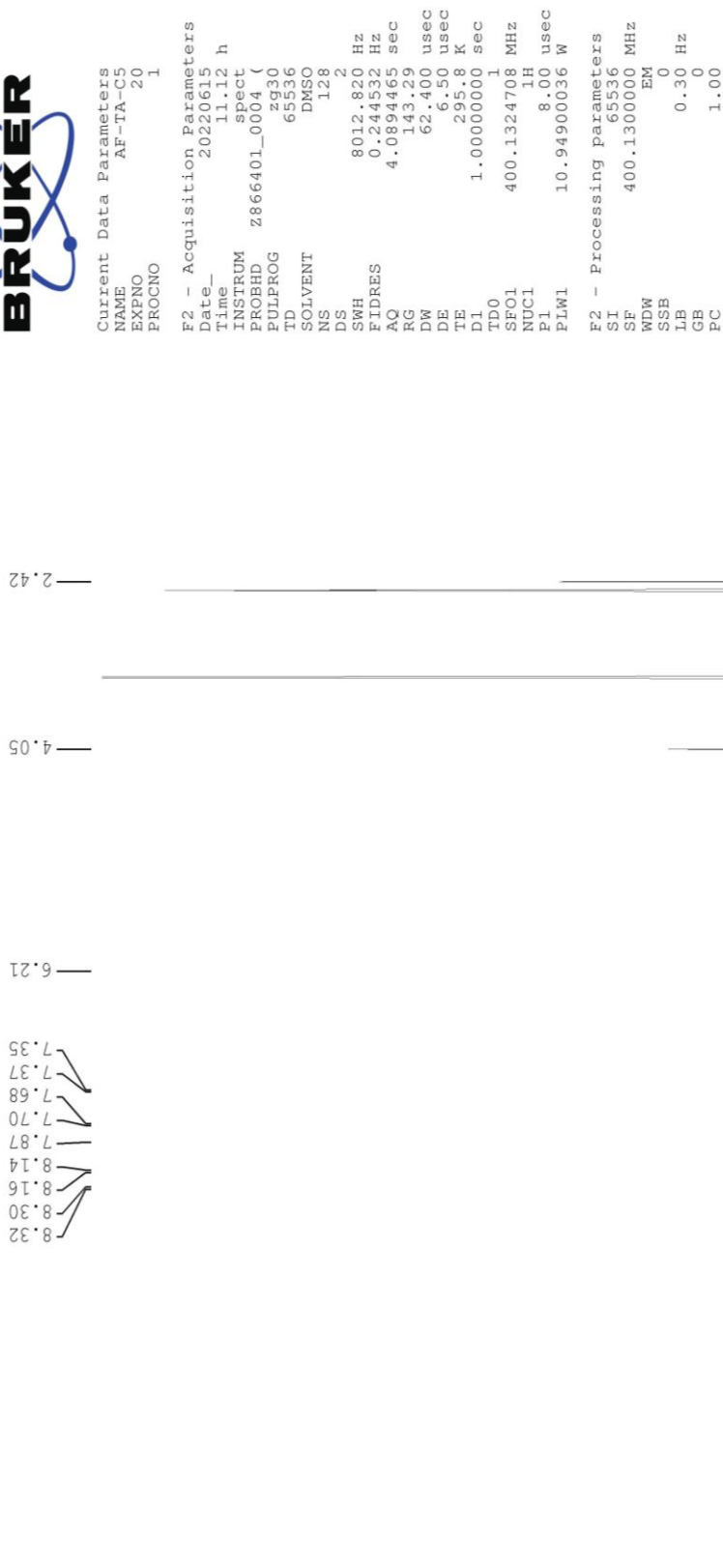


Figure 5.29.  $^1\text{H-NMR}$  spectrum of the compound **3g**



Current Data Parameters  
NAME AF-TA-CS  
EXNO 12  
PROGNO 1

F2 - Acquisition Parameters  
Date\_ 20220621  
Time 23.47 h  
INSTRUM spect  
PROBHD zgpg30  
PULPROG zgpg30  
TD 65536  
SOLVENT DMSO  
NS 4096  
DS 4  
SWH 24038.461 Hz  
FIDRES 0.733596 Hz  
AQ 1.3631488 sec  
RG 31.19  
DM 20.800 usec  
DE 6.50 usec  
TE 295.7 K  
D1 2.00000000 sec  
D11 0.03000000 sec  
TD0 1  
SFO1 100.6228298 MHz  
NUC1 13C  
P1 15.00 usec  
PLW1 90.29699707 W  
SFO2 400.1316005 MHz  
NUC2 1H  
PCPD2 waltz16  
PLW2 90.00 usec  
PLW12 10.94900036 W  
PLW13 0.08651100 W  
PLW14 0.04351400 W

F2 - Processing Parameters  
SI 32768  
SF 100.6127690 MHz  
WDW EM  
SSB 0  
LB 1.00 Hz  
GB 0  
PC 1.40

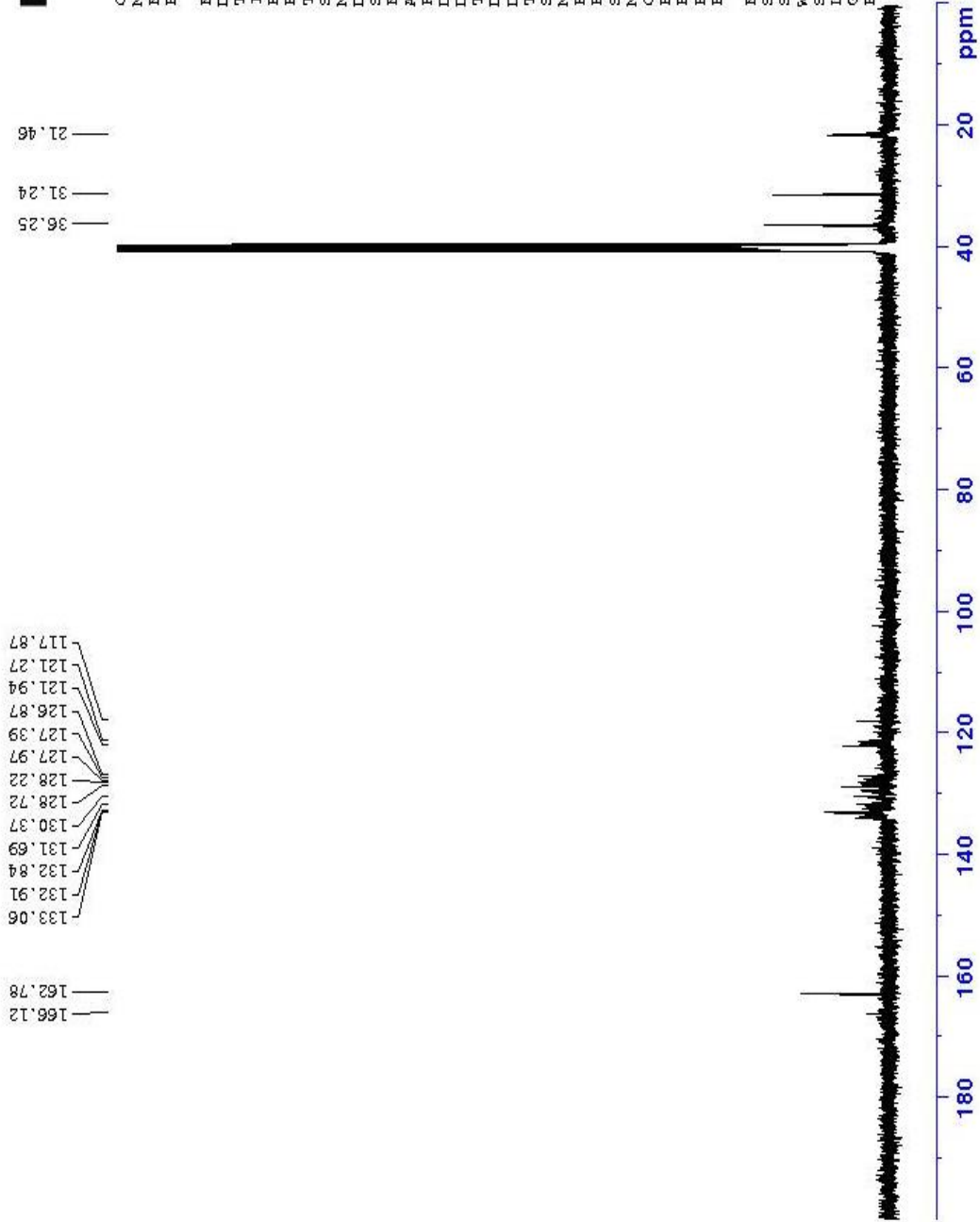


Figure 5.30.  $^{13}\text{C}$ -NMR spectrum of the compound 3g

Data File: C:\LabSolutions\Data\Analiz\Asaf\AFTA-C-5\_60.lcd

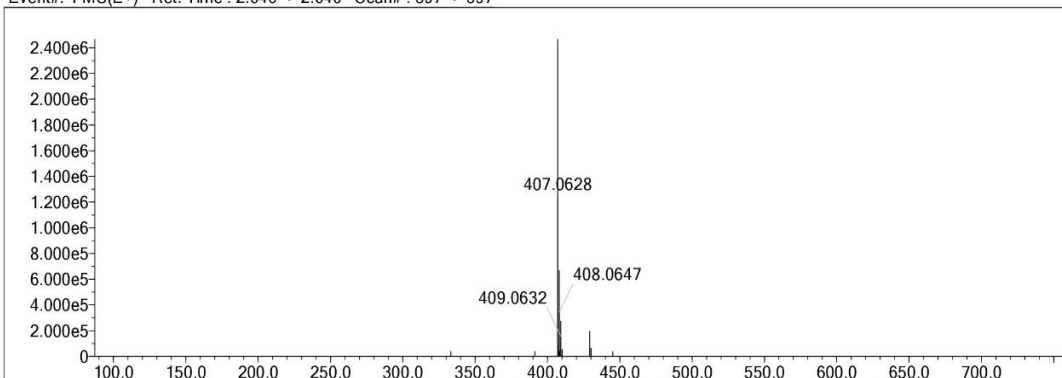
Elmt	Val.	Min	Max	Elmt	Val.	Min	Max	Elmt	Val.	Min	Max	Elmt	Val.	Min	Max	Use Adduct
H	1	9	35	O	2	0	3	S	2	0	2	Ru	2	0	0	H
C	4	7	35	F	1	0	0	Cl	1	0	0	Pd	2	0	0	
N	3	0	5	P	3	0	0	Br	1	0	0	I	3	0	0	

Error Margin (ppm): 5  
 HC Ratio: unlimited  
 Max Isotopes: 3  
 MSn Iso RI (%): 10.00

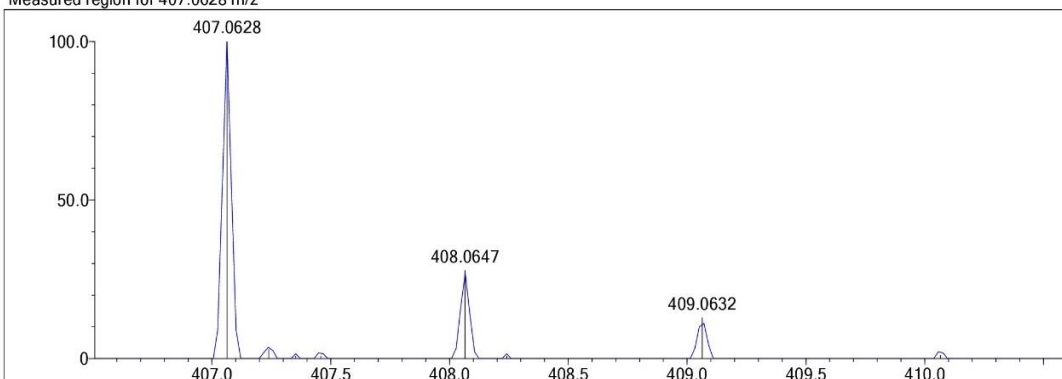
DBE Range: 5.0 - 25.0  
 Apply N Rule: yes  
 Isotope RI (%): 1.00  
 MSn Logic Mode: AND

Electron Ions: both  
 Use MSn Info: yes  
 Isotope Res: 9000  
 Max Results: 50

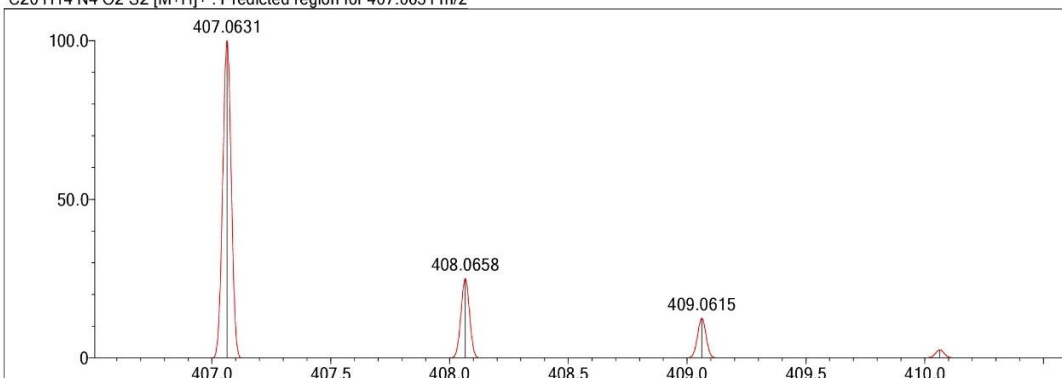
Event#: 1 MS(E+) Ret. Time : 2.640 -> 2.640 Scan# : 397 -> 397



Measured region for 407.0628 m/z



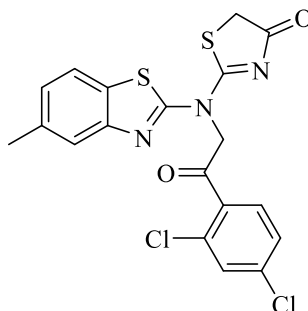
C20 H14 N4 O2 S2 [M+H]<sup>+</sup> : Predicted region for 407.0631 m/z



Rank	Score	Formula (M)	Ion	Meas. m/z	Pred. m/z	Df. (mDa)	Df. (ppm)	Iso	DBE
1	100.00	C20 H14 N4 O2 S2	[M+H] <sup>+</sup>	407.0628	407.0631	-0.3	-0.74	100.00	16.0

Figure 5.31. Mass spectrum of the compound 3g

5.1.3.8. 2-[[2-(2,4-dichlorophenyl)-2-oxoethyl](5-methylbenzothiazol-2-yl)amino]thiazol-4(5H)-one



**3h**

Synthesized according to method C, experimental melting point 259-260°C, 58% yield percent.

**IR (ATR)  $\nu_{\text{max}}(\text{cm}^{-1})$ :** 1703 and 1660 (C=O stretching band), 1454 (C=N and C=C stretching band).

**$^1\text{H-NMR}$  (400 MHz, DMSO- $d_6$ ;  $\delta$ , ppm):** 2.42 (3H, s, bty-CH<sub>3</sub>), 4.05 (2H, s, thiazolinone CH<sub>2</sub>), 6.19 (2H, s, N-CH<sub>2</sub>), 7.35 (H, d,  $J=8$  Hz, Ar-H), 7.66 (H, d,  $J=8$  Hz, Ar-H), 7.85 (H, s, Ar-H), 7.91-7.96 (H, m, Ar-H), 8.07 (H, d,  $J=12$  Hz, Ar-H), 8.42 (H, s, Ar-H).

**$^{13}\text{C-NMR}$  (100 MHz, DMSO- $d_6$ ;  $\delta$ , ppm)** 21.23 (benzothiazole-CH<sub>3</sub>), 31.24 (thiazolinone-CH<sub>2</sub>), 36.25 (N-CH<sub>2</sub>-C=O), 113.47, 126.49, 128.80, 129.19, 131.05, 131.82, 132.57, 134.65, 135.17, 135.52, 137.73, 162.78, 166.45, 188.24 (thiazolinone-C=O), 190.66 (N-CH<sub>2</sub>-C=O).

**HRMS (-m/z):  $[\text{M}+\text{H}]^+$ :** For  $\text{C}_{19}\text{H}_{13}\text{Cl}_2\text{N}_3\text{O}_2\text{S}_2$ , calculated molecular weight: 499.9899, found: 499.9897.

# DOPNALAB

Item	Value
Acquired Date&Time	10.06.2022 10:53:10
Acquired by	System Administrator
Filename	C:\Users\dopnalab\Desktop\MASAÜSTÜ\LEYLA YURTDAŞ\AF-TA\AF-TA-C-9.1.ispd
Spectrum name	AF-TA-C-9.1
Sample name	AF-TA-C-9
Sample ID	
Option	
Comment	
No. of Scans	15
Resolution	4 [cm-1]
Apodization	Happ-Genzel

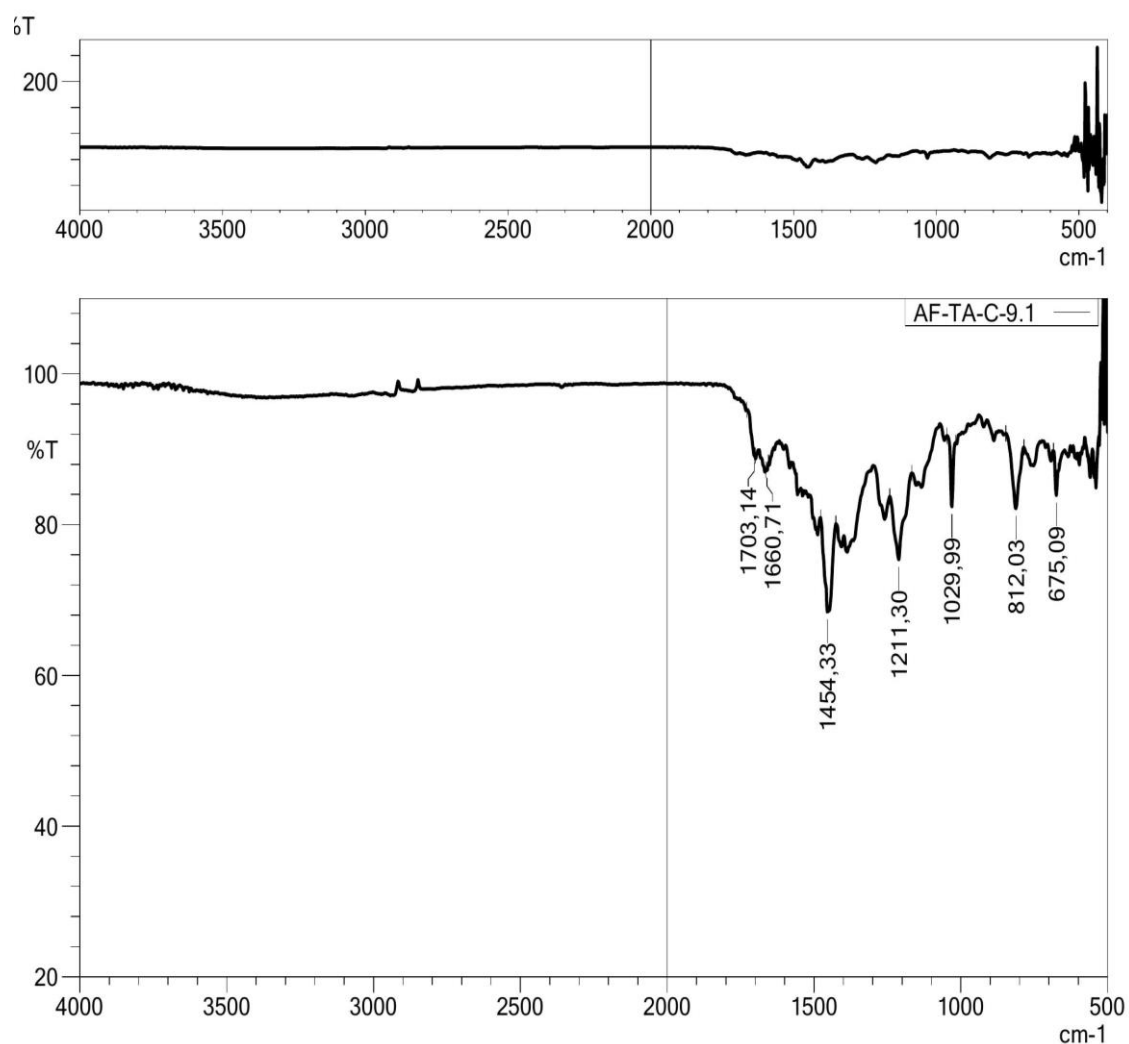


**Figure 5.32.** IR spectrum of the compound **3h**



Current Data Parameters  
NAME AF-TA-C9  
EXPNO 10  
PROCNO 1

F2 - Acquisition Parameters  
Date\_ 20220606  
Time 15.05 h  
INSTRUM spect  
PROBHD zg30  
PULPROG zg30  
TD 65536  
SOLVENT DMSO  
NS 128  
DS 2  
SWH 8012.820 Hz  
FIDRES 0.244532 Hz  
AQ 4.0894465 sec  
RG 111.15  
DW 62.400 usec  
DE 6.50 usec  
TE 296.5 K  
D1 1.00000000 sec  
TDO 1  
SF01 400.1324708 MHz  
NUC1 1H  
P1 8.00 usec  
PLWI 10.94900036 W

F2 - Processing Parameters  
SI 65536  
SF 400.1300000 MHz  
WDW EM  
SSB 0  
LB 0.30 Hz  
GB 0  
PC 1.00

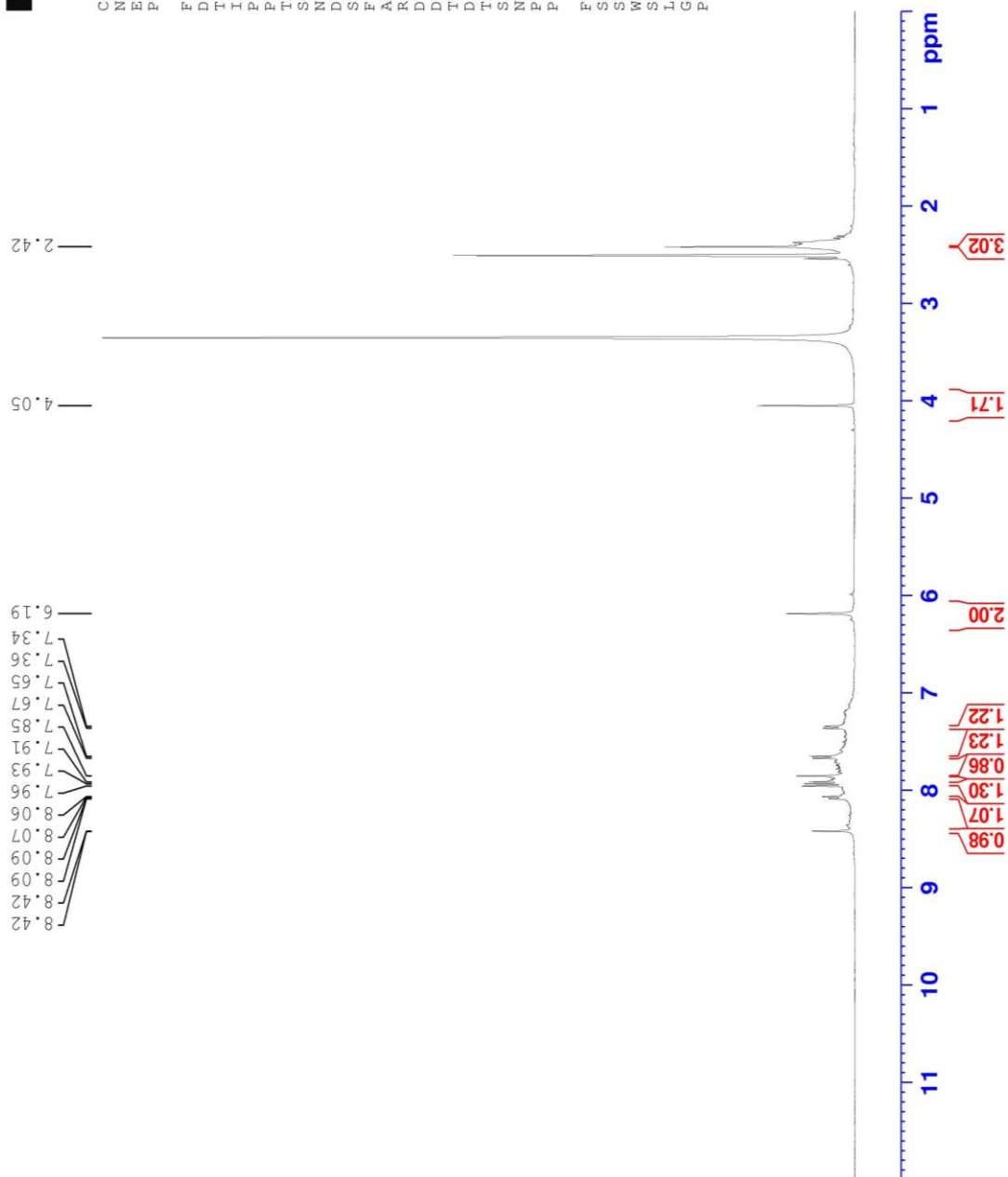


Figure 5.33.  $^1\text{H}$ -NMR spectrum of the compound **3h**



Current Data Parameters  
NAME AF-TA-C9  
EXFNO 12  
PROCNO 1

F2 - Acquisition Parameters  
Date\_ 20220622  
Time 3.44 h  
INSTRUM spect  
PROBHD Z866401\_0004 ( Z866401 )  
PULPROG zgpg30  
TD 65536  
SOLVENT DMSO  
NS 4096  
DS 4  
SWH 24038.461 Hz  
FIDRES 0.733596 Hz  
AQ 1.3631488 sec  
RG 31.19  
DM 20.800 usec  
DB 6.50 usec  
TE 296.0 K  
D1 2.00000000 sec  
D11 0.03000000 sec  
TD0 1  
SFO1 100.6228296 MHz  
NUC1 13C  
P1 15.00 usec  
PLW1 90.29699707 W  
SFO2 400.1316005 MHz  
NUC2 1H  
CPDPRG2 waltz16  
PCPD2 90.00 usec  
PLW2 10.94900036 W  
PLW12 0.08651100 W  
PLW13 0.04351400 W

F2 - Processing Parameters  
SI 32766  
SF 100.6127690 MHz  
WDW EM  
SSB 0  
LB 1.00 Hz  
GB 0  
PC 1.40

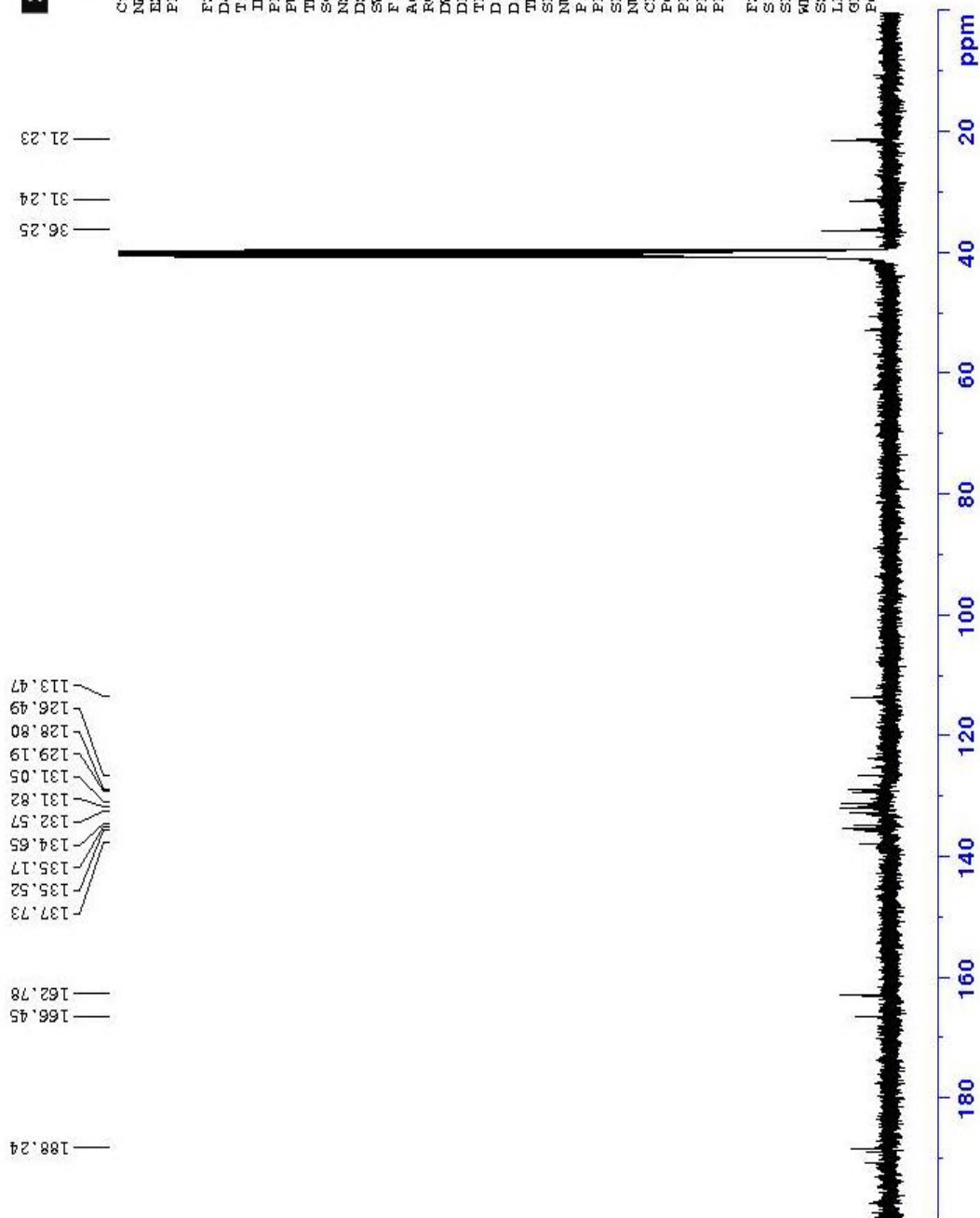


Figure 5.34.  $^{13}\text{C}$ -NMR spectrum of the compound **3h**

Data File: C:\LabSolutions\Data\Analiz\Asaf\AF-TA-C-9\_239.lcd

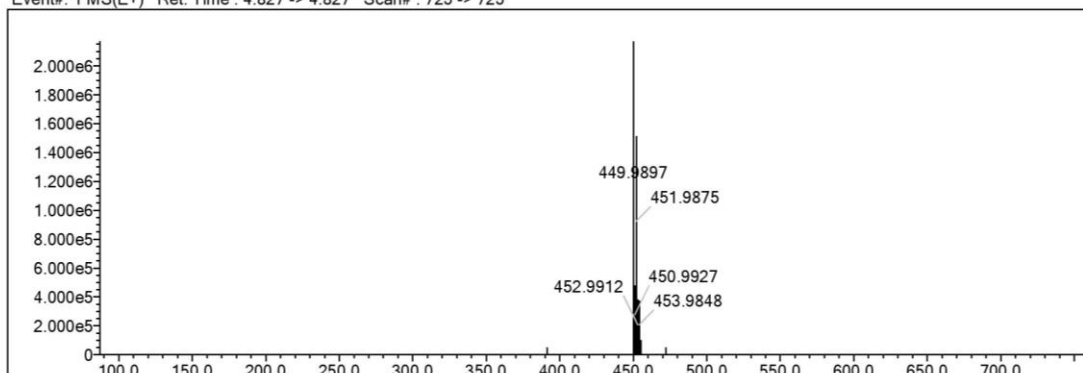
Elmt	Val.	Min	Max	Elmt	Val.	Min	Max	Elmt	Val.	Min	Max	Elmt	Val.	Min	Max	Use Adduct
H	1	9	26	O	2	0	4	Cl	1	0	2	I	3	0	0	H
B	3	0	0	F	1	0	0	Br	1	0	0					
C	4	7	37	P	3	0	0	Ru	2	0	0					
N	3	2	6	S	2	0	2	Pd	2	0	0					

Error Margin (ppm): 5  
 HC Ratio: unlimited  
 Max Isotopes: 3  
 MSn Iso RI (%): 10.00

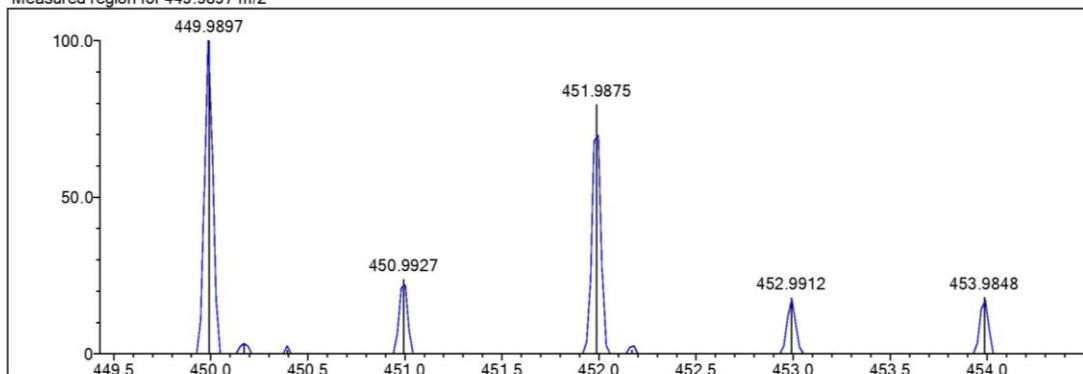
DBE Range: 5.0 - 20.0  
 Apply N Rule: yes  
 Isotope RI (%): 1.00  
 MSn Logic Mode: AND

Electron Ions: both  
 Use MSn Info: yes  
 Isotope Res: 9000  
 Max Results: 50

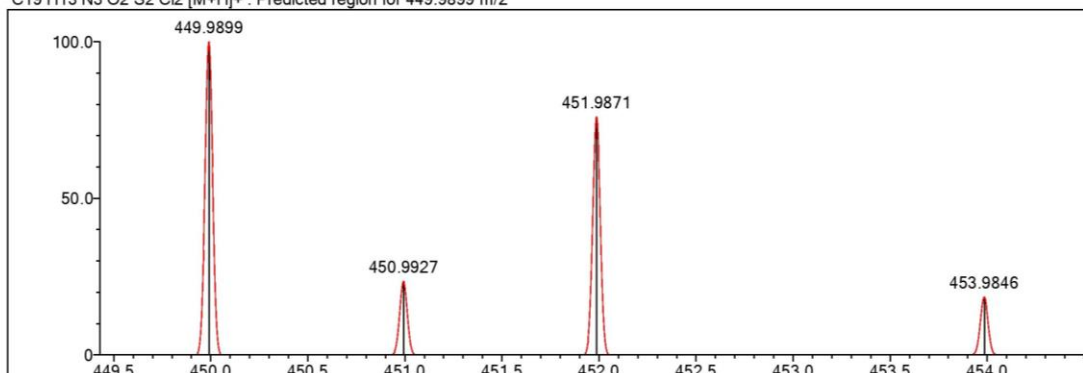
Event#: 1 MS(E+) Ret. Time : 4.827 -> 4.827 Scan# : 725 -> 725



Measured region for 449.9897 m/z



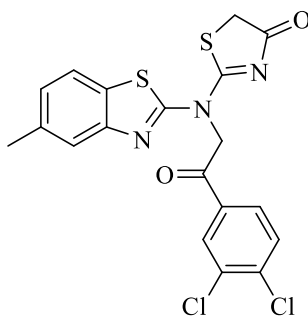
C19 H13 N3 O2 S2 Cl2 [M+H]<sup>+</sup> : Predicted region for 449.9899 m/z



Rank	Score	Formula (M)	Ion	Meas. m/z	Pred. m/z	Df. (mDa)	Df. (ppm)	Iso	DBE
1	82.33	C19 H13 N3 O2 S2 Cl2	[M+H] <sup>+</sup>	449.9897	449.9899	-0.2	-0.44	82.33	14.0

Figure 5.35. Mass spectrum of the compound 3h

5.1.3.9. 2-[[2-(3,4-dichlorophenyl)-2-oxoethyl](5-methylbenzothiazol-2-yl)amino]thiazol-4(5H)-one



3i

Synthesized according to method C, experimental melting point 269-270°C, 46% yield percent.

**IR (ATR)  $\nu_{\max}(\text{cm}^{-1})$ :** 2926 ( aromatic C-H stretching band), 2854 ( aliphatic C-H stretching band), 1699 (C=O stretching band), 1446 (C=N and C=C stretching band).

**$^1\text{H-NMR}$  (400 MHz, DMSO- $d_6$ ;  $\delta$ , ppm):** 2.42 (3H, s, bty-CH<sub>3</sub>), 4.05 (2H, s, thiazolinone CH<sub>2</sub>), 6.19 (2H, s, N-CH<sub>2</sub>), 7.35 (H, d,  $J=8$  Hz, Ar-H), 7.66 (H, d,  $J=8$  Hz, Ar-H), 7.85 (H, s, Ar-H), 7.92 (H, d,  $J=12$  Hz, Ar-H), 8.08 (H, d,  $J=8$  Hz, Ar-H), 8.42 (H, s, Ar-H).

**$^{13}\text{C-NMR}$  (100 MHz, DMSO- $d_6$ ;  $\delta$ , ppm)** 21.23 (benzothiazole-CH<sub>3</sub>), 36.51 (thiazolinone-CH<sub>2</sub>), 52.59 (N-CH<sub>2</sub>-C=O), 113.46, 123.60, 126.49, 128.89, 129.19, 131.05, 131.83, 132.57, 134.66, 135.17, 135.51, 137.73, 166.45, 188.25. 188.77 (thiazolinone-C=O), 190.64 (N-CH<sub>2</sub>-C=O).

**HRMS (-m/z):  $[\text{M}+\text{H}]^+$ :** For  $\text{C}_{19}\text{H}_{13}\text{Cl}_2\text{N}_3\text{O}_2\text{S}_2$ , calculated molecular weight: 449.9899, found: 449.9893.

# DOPNALAB

Item	Value
Acquired Date&Time	10.06.2022 11:04:23
Acquired by	System Administrator
Filename	C:\Users\dopnalab\Desktop\MASAÜSTÜLEYLA YURTDAŞ\AF-TA\AF-TA-C-10.1.ispd
Spectrum name	AF-TA-C-10.1
Sample name	AF-TA-C-10
Sample ID	
Option	
Comment	
No. of Scans	15
Resolution	4 [cm-1]
Apodization	Happ-Genzel

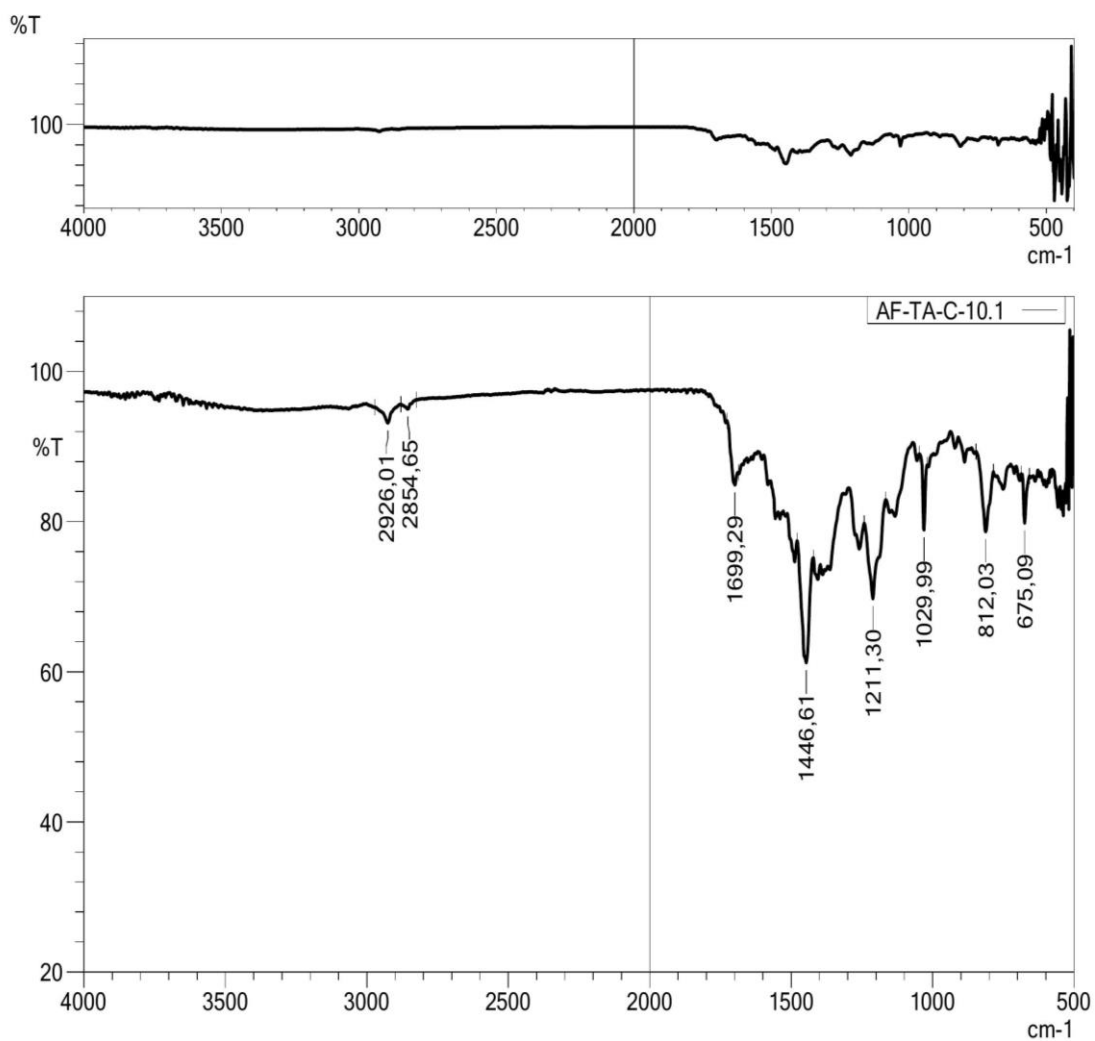


Figure 5.36. IR spectrum of the compound *3i*



Figure 5.37.  $^1\text{H-NMR}$  spectrum of the compound **3i**



```

Current Data Parameters
NAME      SF-TH-C10
EXPNO    12
PROCNO   1

F2 - Acquisition Parameters
Date_    20220621
Time     19.30 h
SYSTEM  spect
PROBHD   zgpg30
PULPROG zgpg30
TD       65536
SOLVENT  DMSO
NS       4096
DS       4
SWH      24035.461 Hz
FIDRES   0.723596 Hz
AQ       1.3621988 sec
RG       31.19
RW       20.800 usec
DE       6.30 usec
TE       296.2 K
D1       2.00000000 sec
D11      0.03000000 sec
TD0      1
SFO1     100.628295 MHz
NUC1     13C
P1       15.00 usec
FIDW1    50.29699707 W
SFO2     400.1316005 MHz
NUC2     1H
CFPRG12 waltz16
PCPD2    90.00 usec
P1W2     10.94900036 W
FIDW2    0.08651100 W
P1W13    0.04351900 W

F2 - Processing Parameters
SI       32768
SF       100.6127690 MHz
WDW      EM
SSB      0
LB       1.00 Hz
GB       0
PC       1.90
  
```

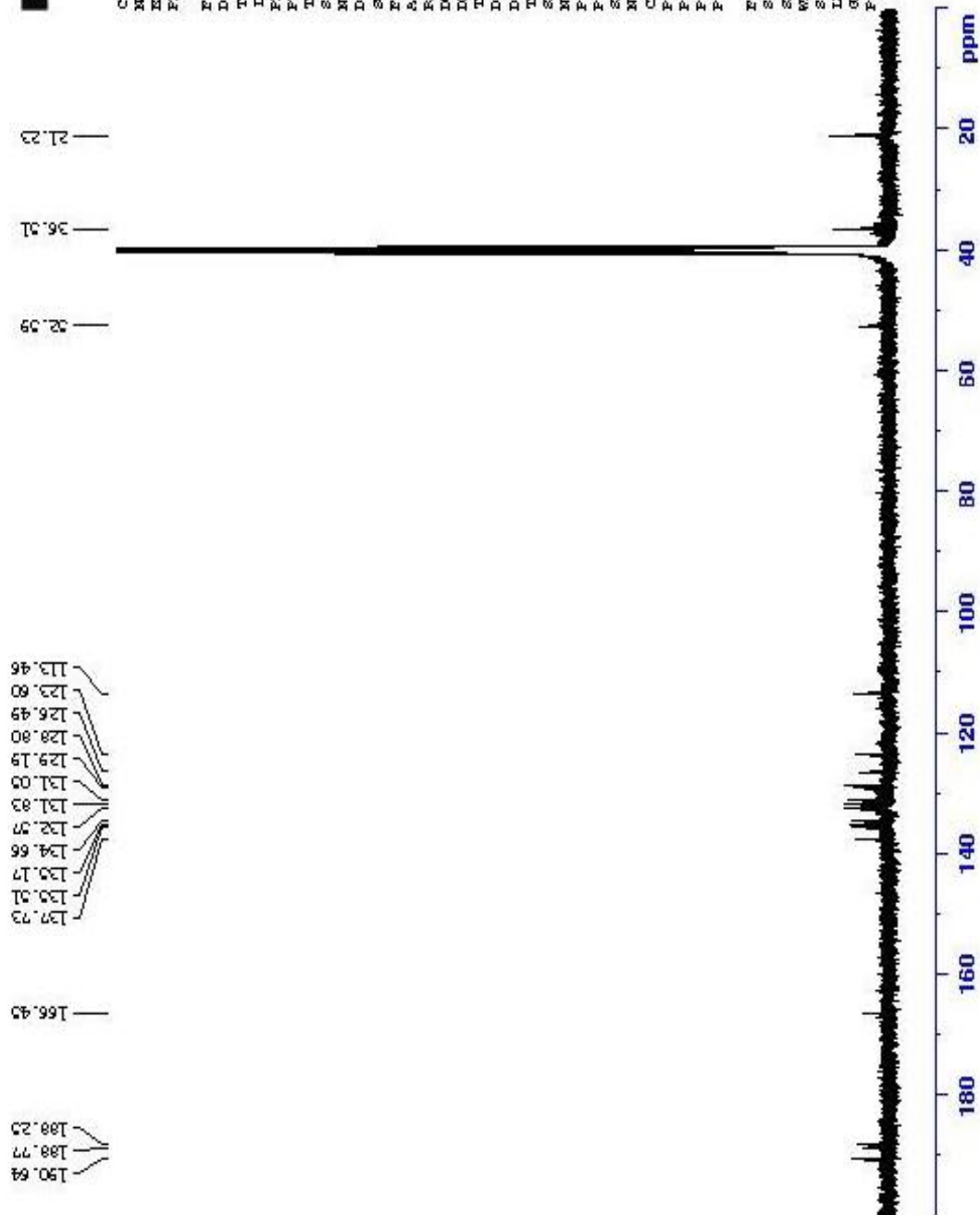


Figure 5.38.  $^{13}\text{C}$ -NMR spectrum of the compound *3i*

Data File: C:\LabSolutions\Data\Analiz\Asaf\AF-TA-C-10\_240.lcd

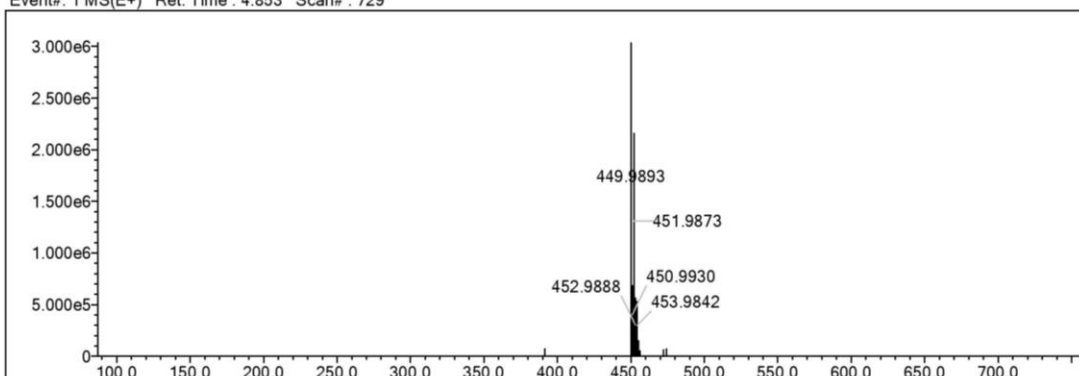
Elmt	Val.	Min	Max	Elmt	Val.	Min	Max	Elmt	Val.	Min	Max	Elmt	Val.	Min	Max	Use Adduct
H	1	9	26	O	2	0	4	Cl	1	0	2	I	3	0	0	H
B	3	0	0	F	1	0	0	Br	1	0	0					
C	4	7	37	P	3	0	0	Ru	2	0	0					
N	3	2	6	S	2	0	2	Pd	2	0	0					

Error Margin (ppm): 5  
 HC Ratio: unlimited  
 Max Isotopes: 3  
 MSn Iso RI (%): 10.00

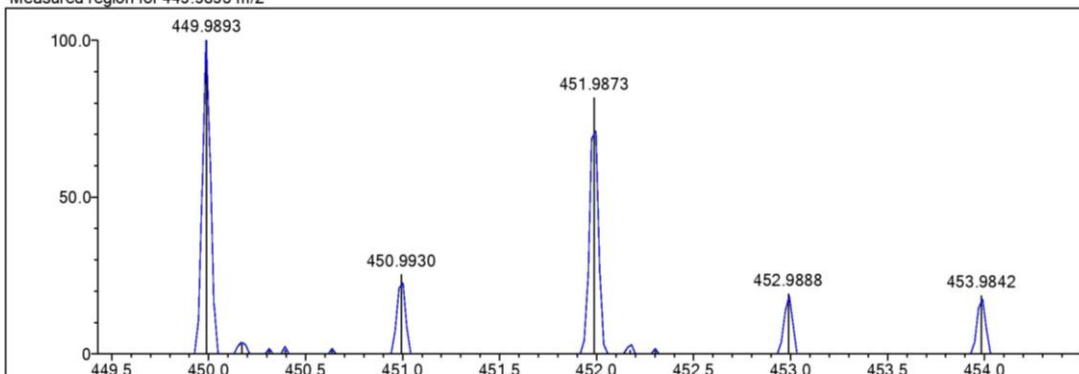
DBE Range: 5.0 - 20.0  
 Apply N Rule: yes  
 Isotope RI (%): 1.00  
 MSn Logic Mode: AND

Electron Ions: both  
 Use MSn Info: yes  
 Isotope Res: 9000  
 Max Results: 50

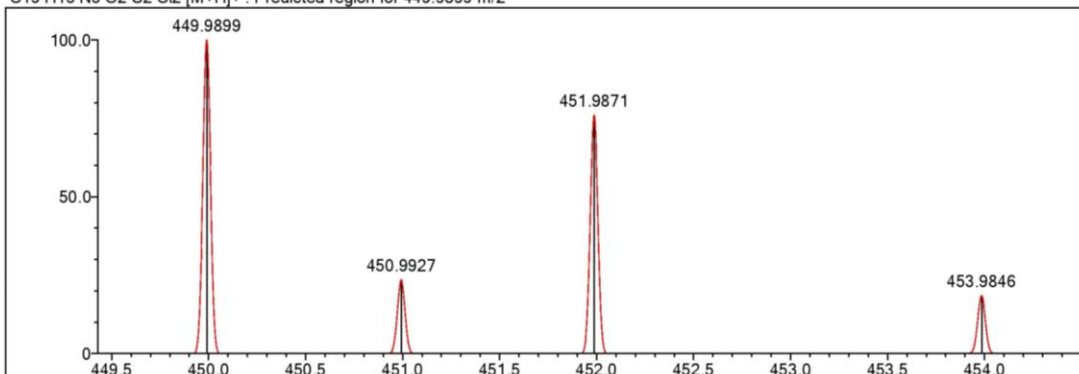
Event#: 1 MS(E+) Ret. Time : 4.853 Scan# : 729



Measured region for 449.9893 m/z



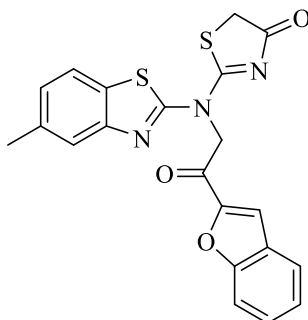
C19 H13 N3 O2 S2 Cl2 [M+H]<sup>+</sup> : Predicted region for 449.9899 m/z



Rank	Score	Formula (M)	Ion	Meas. m/z	Pred. m/z	Df. (mDa)	Df. (ppm)	Iso	DBE
1	84.16	C19 H13 N3 O2 S2 Cl2	[M+H] <sup>+</sup>	449.9893	449.9899	-0.6	-1.33	84.86	14.0

Figure 5.39. Mass spectrum of the compound 3i

5.1.3.10. 2-[[2-(benzofuran-2-yl)-2-oxoethyl](5-methylbenzothiazol-2-yl)amino]thiazol-4(5H)-one



3j

Synthesized according to method C, experimental melting point 182-183°C, 47% yield percent.

**IR (ATR)  $\nu_{\text{max}}(\text{cm}^{-1})$ :** 2918 ( aromatic C-H stretching band), 2848 ( aliphatic C-H stretching band), 1699 (C=O stretching band), 1552 and 1489 (C=N and C=C stretching band), 1213 (C-O stretching band).

**$^1\text{H-NMR}$  (400 MHz, DMSO- $d_6$ ;  $\delta$ , ppm):** 2.43 (3H, s, bty- $\text{CH}_3$ ), 4.05 (2H, s, thiazolinone  $\text{CH}_2$ ), 6.09 (2H, s, N- $\text{CH}_2$ ), 7.33-7.47 (2H, m, Ar-H), 7.58-7.65 (3H, m, Ar-H), 7.70-7.96 (2H, m, Ar-H), 8.26 (H, s, Ar-H).

**$^{13}\text{C-NMR}$  (100 MHz, DMSO- $d_6$ ;  $\delta$ , ppm)** 21.46 (benzothiazole- $\text{CH}_3$ ), 36.32 (thiazolinone- $\text{CH}_2$ ), 46.30 (N- $\text{CH}_2$ -C=O), 106.12, 112.84, 124.12, 124.51, 127.08, 128.02, 128.92, 129.66, 133.67, 154.44, 155.71, 168.51, 176.48 (thiazolinone- $\text{C}=\text{O}$ ), 181.46 (N- $\text{CH}_2$ - $\text{C}=\text{O}$ ).

**HRMS (-m/z):  $[\text{M}+\text{H}]^+$ :** For:  $\text{C}_{21}\text{H}_{15}\text{N}_3\text{O}_3\text{S}_2$ , calculated molecular weight: 422.0628, found: 422.0622.

# DOPNALAB

Item	Value
Acquired Date&Time	10.06.2022 11:09:04
Acquired by	System Administrator
Filename	C:\Users\dopnalab\Desktop\MASAÜSTÜLEYLA YURTDAŞ\AF-TA\AF-TA-C-11.1.ispd
Spectrum name	AF-TA-C-11.1
Sample name	AF-TA-C-11
Sample ID	
Option	
Comment	
No. of Scans	15
Resolution	4 [cm-1]
Apodization	Happ-Genzel

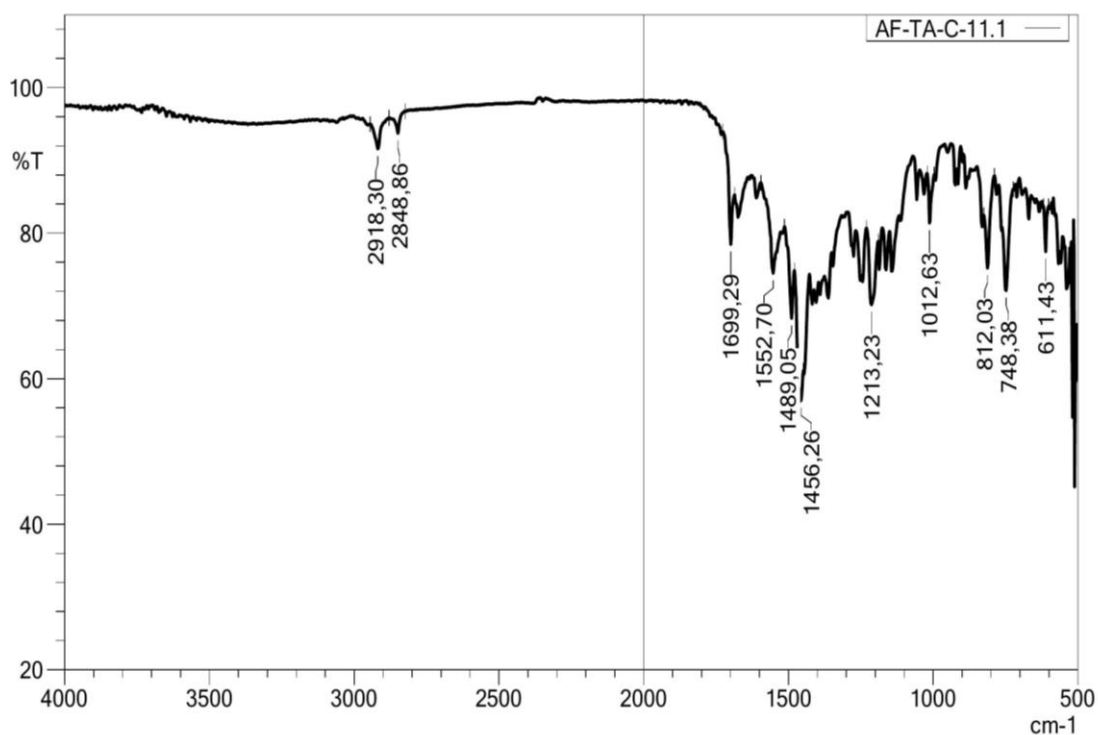
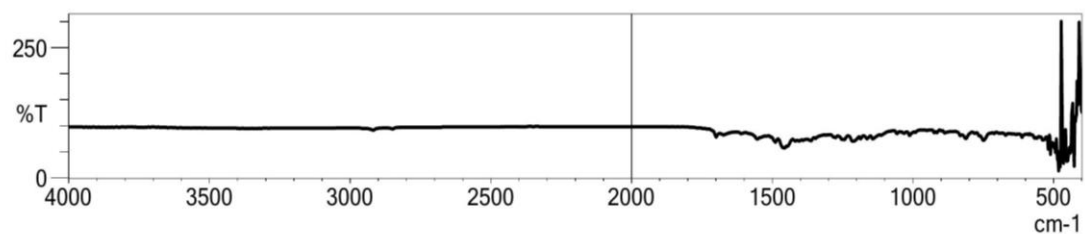


**Figure 5.40.** IR spectrum of the compound *3j*



Current Data Parameters  
NAME AF-TA-C11  
EXPNO 10  
PROCNO 1

F2 - Acquisition Parameters  
Date\_ 20220606  
Time\_ 14.24 h  
INSTRUM spect  
PROBHD zg30  
PULPROG zg30  
TD 65536  
SOLVENT DMSO  
NS 128  
DS 2  
SWH 8012.820 Hz  
FIDRES 0.244532 Hz  
AQ 4.0894465 sec  
RG 88.37  
DW 62.400 usec  
DE 6.50 usec  
TE 296.5 K  
D1 1.00000000 sec  
TD0 1  
SF01 400.1324708 MHz  
NUC1 1H  
F1 8.00 usec  
PLW1 10.94900036 W

F2 - Processing parameters  
SI 65536  
SF 400.1300000 MHz  
WDW EM  
SSB 0  
LB 0.30 Hz  
GB 0  
PC 1.00

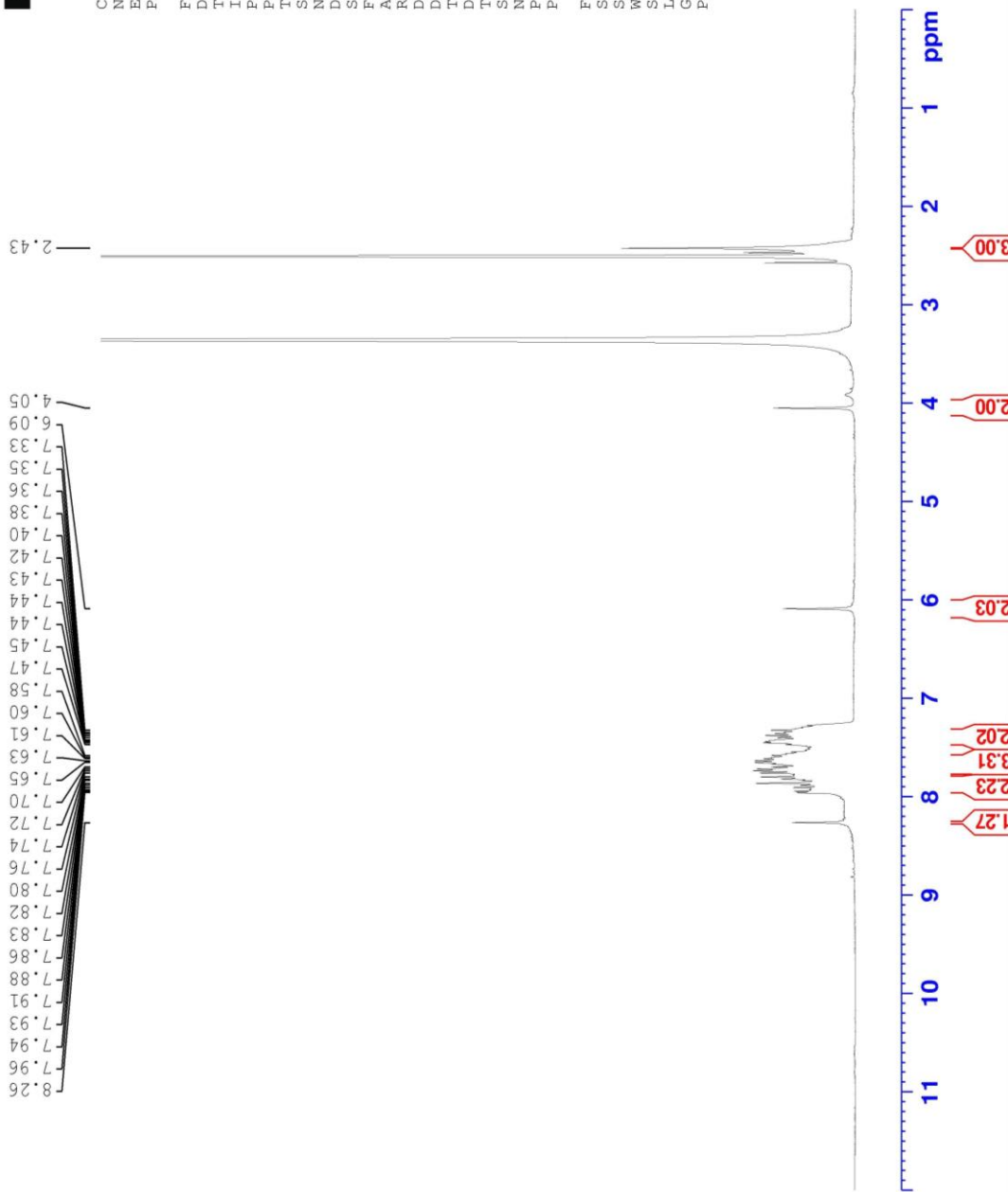


Figure 5.41. <sup>1</sup>H-NMR spectrum of the compound 3j



Current Data Parameters  
NAME AF-TA-C11  
EXPNO 12  
PROCNO 1

F2 - Acquisition Parameters  
Date\_ 20220621  
Time 15.53 h  
INSTRUM spect  
PROBHD Z866401\_0004 (   
PULPROG zgpg30  
TD 65536  
SOLVENT DMSO  
NS 4096  
DS 4  
SWH 24038.461 Hz  
FIDRES 0.733596 Hz  
AQ 1.3631488 sec  
RG 31.19  
DM 20.000 usec  
DE 6.50 usec  
TE 296.4 K  
D1 2.00000000 sec  
D11 0.03000000 sec  
TD0 1  
SFO1 100.6228296 MHz  
NUC1 13C  
F1 15.00 usec  
PLW1 90.2969707 W  
SFO2 400.1316005 MHz  
NUC2 1H  
CPDPRG2 waltz16  
PCPD2 90.00 usec  
PLW2 10.94900036 W  
PLW12 0.08651100 W  
PLW13 0.04351400 W

F2 - Processing Parameters  
SI 32768  
SF 100.6127690 MHz  
WDW EM  
SSB 0  
LB 1.00 Hz  
GB 0  
PC 1.40

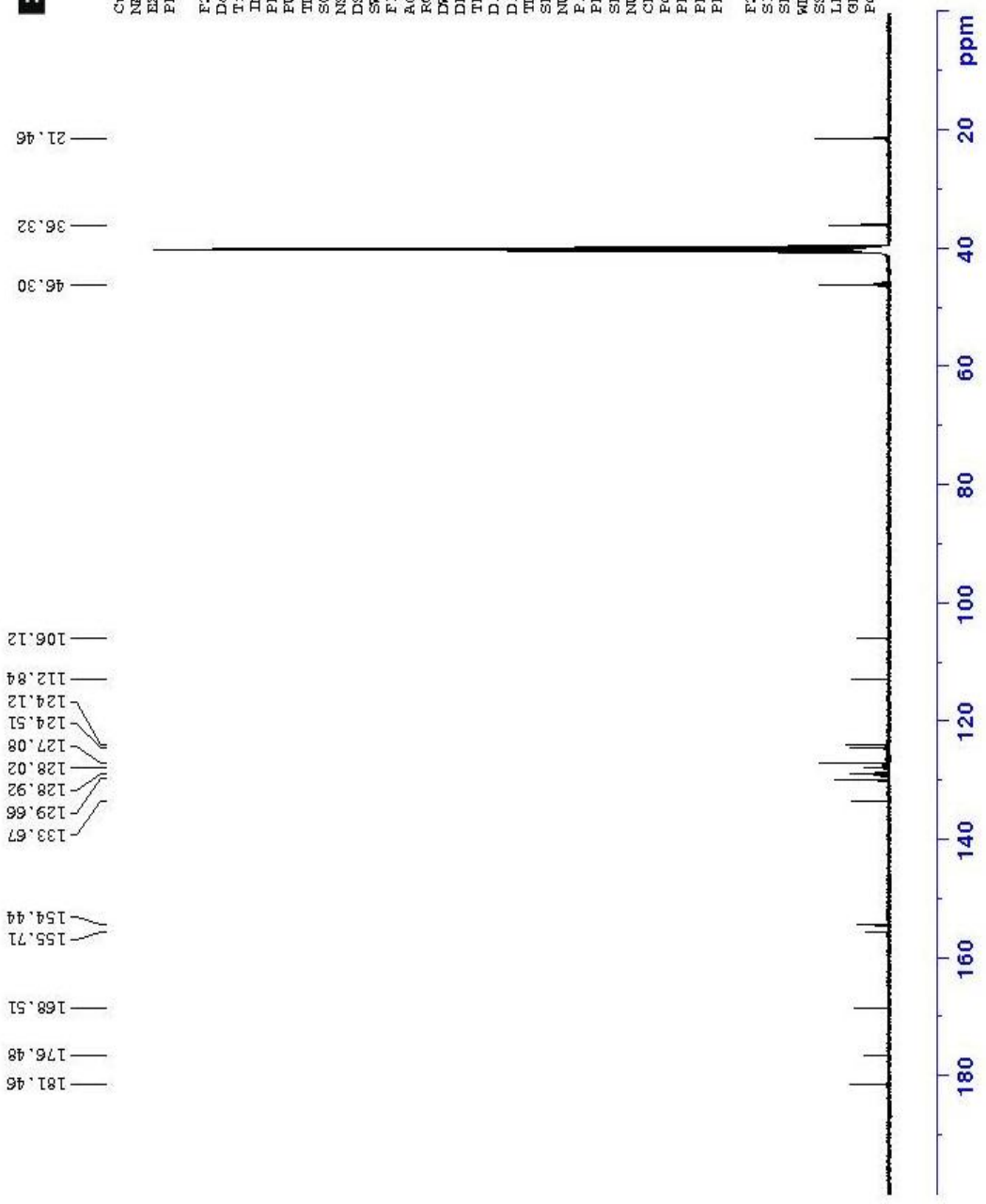


Figure 5.42. <sup>13</sup>C-NMR spectrum of the compound 3j

Data File: C:\LabSolutions\Data\Analiz\Asaf\AF-TA-C-11\_241.lcd

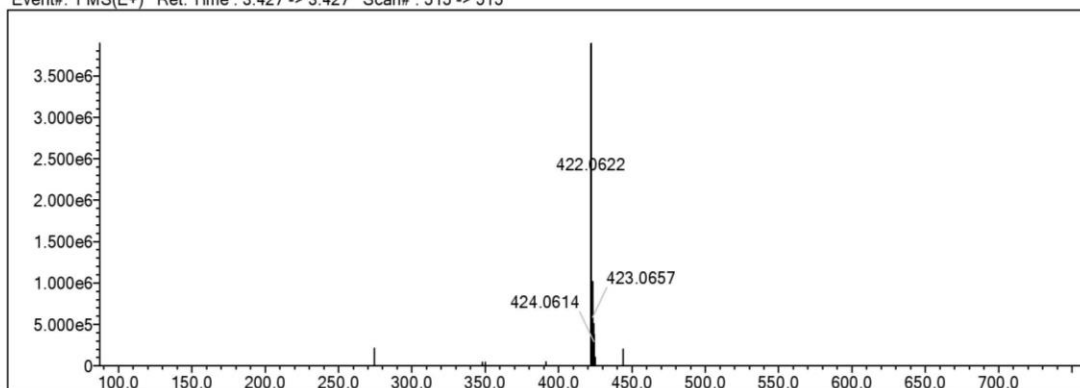
Elmt	Val.	Min	Max	Elmt	Val.	Min	Max	Elmt	Val.	Min	Max	Elmt	Val.	Min	Max	Use Adduct
H	1	9	26	O	2	0	4	Cl	1	0	0	I	3	0	0	H
B	3	0	0	F	1	0	0	Br	1	0	0					
C	4	7	37	P	3	0	0	Ru	2	0	0					
N	3	2	6	S	2	0	2	Pd	2	0	0					

Error Margin (ppm): 10  
 HC Ratio: unlimited  
 Max Isotopes: 3  
 MSn Iso RI (%): 10.00

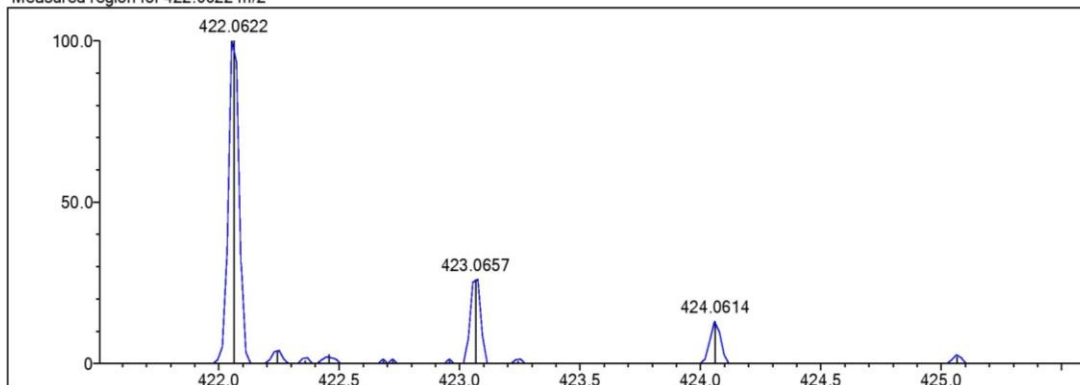
DBE Range: 5.0 - 20.0  
 Apply N Rule: yes  
 Isotope RI (%): 1.00  
 MSn Logic Mode: AND

Electron Ions: both  
 Use MSn Info: yes  
 Isotope Res: 9000  
 Max Results: 50

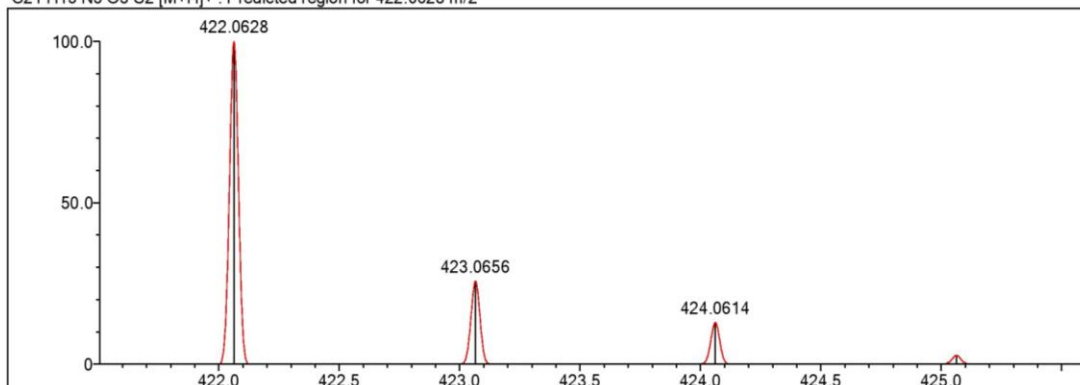
Event#: 1 MS(E+) Ret. Time : 3.427 -> 3.427 Scan# : 515 -> 515



Measured region for 422.0622 m/z



C21 H15 N3 O3 S2 [M+H]<sup>+</sup> : Predicted region for 422.0628 m/z



Rank	Score	Formula (M)	Ion	Meas. m/z	Pred. m/z	Df. (mDa)	Df. (ppm)	Iso	DBE
1	98.95	C <sub>21</sub> H <sub>15</sub> N <sub>3</sub> O <sub>3</sub> S <sub>2</sub>	[M+H] <sup>+</sup>	422.0622	422.0628	-0.6	-1.42	100.00	16.0

Figure 5.43. Mass spectrum of the compound 3j

## 5.2. Chemical Analysis Results

### 5.2.1. IR spectrometry

The IR spectra of the synthesized compounds with hybrid benzothiazole and thiazolinone rings have shared stretching bands that appeared at (3061-2918)  $\text{cm}^{-1}$  related to the aromatic C-H bond, while the stretching bands appeared at (2970-2848)  $\text{cm}^{-1}$  related to the aliphatic C-H bond. The C=O stretching bands appeared at (1703-1660)  $\text{cm}^{-1}$ . On the other hand, C=N and C=C stretching bands revealed at (1595-1402)  $\text{cm}^{-1}$ , between (827-800)  $\text{cm}^{-1}$  out of plane bending bands appeared for the compounds **3b**, **3c**, **3e**, **3f**, and **3g** with 1,3-disubstituted benzene.

### 5.2.2. $^1\text{H-NMR}$ analysis results

The structure of the synthesized 2-[(5-methylbenzothiazol-2-yl)(2-oxo-2-(substituent)ethyl)amino]thiazolinone derivatives basically have a shared thiazolinone ring and benzothiazole ring. Benzothiazole ring has methyl substituent at position 5 and connected with the thiazolinone ring by amine bridge to which the different substituent link, all derivatives have shared the (N-CH<sub>2</sub>-C=O) structure connected to different substituent.

In the  $^1\text{H-NMR}$  spectrum, the protons of the methyl substituent located at position 5 of the benzothiazole ring appeared as singlet peak between (2.42-2.43) ppm. The other protons found in the benzothiazole ring located at positions; C<sub>4</sub>-H appeared as a singlet peak at (7.85-7.88) ppm, C<sub>6</sub>-H appeared at (7.34-7.36) ppm, and C<sub>7</sub>-H appeared at (7.61-7.69) ppm.

The methylene protons at position 5 of the thiazolinone ring appeared as singlet peak at (4.04-4.05) ppm.

The peak of the protons of (N-CH<sub>2</sub>-C=O) are highly de-shielded and appeared downfield at a range (6.09-6.32) ppm as a singlet peak.

The protons of the phenyl ring in compounds **3b**, **3c**, **3e**, **3f**, **3g** substituted by various substituents at position 4 appeared at range (7.16-8.42) ppm as they are shifted up or downfield according to the type of the substituent on the phenyl ring. For example, the strong electron-withdrawing group C≡N in compound **3g** caused the protons of the phenyl ring to shift downfield and appeared at (8.14-8.32) ppm. However, the calculated *J* values were between 8 and 12 Hz, which is consistent for aromatic hydrogens.

The protons of the methyl substituent at position 4 of the phenyl ring in compound **3b** appeared as singlet peak at (2.45) ppm. In contrast the protons of (O-CH<sub>3</sub>) substituent at position 4 of the phenyl ring in the compound **3c** are shifted downfield and appeared as singlet peak at (3.91) ppm.

### 5.2.3. <sup>13</sup>C-NMR analysis results

The <sup>13</sup>C-NMR spectrums of the synthesized compounds were examined, the peaks were observed as expected and the total carbon number was counted and related to that expected number of peaks.

The synthesized derivatives of 2-((5-methylbenzothiazol-2-yl)[2-oxo-2-(substituent)ethyl]amino)thiazolinone have shared thiazolinone and benzothiazole skeleton and a peak between (21.23-21.46) ppm was observed in all derivatives which is related to the carbon of the methyl substituent at position 5 of benzothiazole ring. C<sub>5</sub> of the thiazolinone ring appeared at (31.24-31.25) ppm for the compounds **3a**, **3b**, **3c**, **3g**, and **3h**, while the carbon of the methylene bridge between N and C=O are more deshielded and appeared at (36.25) ppm for the same compounds. On the other hand, C<sub>5</sub> of the thiazolinone ring appeared at a range between (35.58-36.51) ppm for compounds **3d**, **3e**, **3f**, **3i**, and **3j**, while the carbon of the methylene bridge between N and C=O appeared between (46.30-52.59) ppm for the same compounds because of the effect of a different substituents.

The carbon of amide carbonyl (N-C=O) at position 4 of the thiazolinone ring appeared at a range between (162.78-188.77) ppm in all the synthesized compounds, while the carbon of the carbonyl group at the structure (N-CH<sub>2</sub>-C=O) appeared between (166.12 and 191.23) ppm.

The carbon of the methyl substituent at the para position of the phenyl ring appeared at (21.79) ppm at compound **3b**. Whereas, at compound **3c** the carbon of the methoxy substituent at the para position of the phenyl ring appeared downfield at (56.27) ppm.

### 5.2.4. Mass spectrometry

Mass spectra of the synthesized compounds were obtained in negative and positive modes by electrospray ionization method (ESI) analyzed using the ionization technique [90]. M+1 peaks were detected in the mass spectra for all the analyzed compounds.

### 5.3. Results and Discussion of Aromatase Inhibition Activity

The synthesized compounds 2-((5-methylbenzothiazol-2-yl)[2-oxo-2-(substituent)ethyl]amino)thiazolinone were investigated for their aromatase inhibition activity, and the results are represented in **Table 5.1**.

The compounds were tested at concentrations of  $10^{-3}$  and  $10^{-4}$  M, and the results represented as inhibitory percent % and compared with letrozole as a standard drug. Moreover, the  $IC_{50}$  (the concentration needed for 50% inhibition) was measured.

In general, the synthesized compounds showed aromatase inhibition activity. The compound **3b** showed the most potent inhibition activity to aromatase enzyme by more than 90% in both the  $10^{-3}$  and  $10^{-4}$  M concentrations comparable to letrozole and  $IC_{50}$  value  **$0.041 \pm 0.002$   $\mu$ M**.

The compound **3i** has shown inhibition by more than 70% ( $72.397 \pm 1.608$ ) at the  $10^{-3}$ M concentration. In contrast, the compounds **3e** and **3g** exert inhibition by around (67% and 64%) respectively, at the same concentration. All the compounds showed inhibition by around (20%-29%) in the more diluted solvent concentration of  $10^{-4}$ M.

Almost all the synthesized compounds exert inhibition to aromatase enzyme by around 40% and more at  $10^{-3}$ M dilution.

**Table 5.1.** The % of inhibition of the synthesized compounds against aromatase enzyme at  $10^{-3}$  and  $10^{-4}$ M concentrations and  $IC_{50}$  ( $\mu$ M) values

Compound	Aromatase enzyme inhibition %		
	$10^{-3}$	$10^{-4}$	$IC_{50}$
<b>3a</b>	42.546 $\pm$ 0.836	23.459 $\pm$ 0.752	>1000
<b>3b</b>	<b>94.358<math>\pm</math>1.863*</b>	<b>90.729<math>\pm</math>2.375*</b>	<b>0.041<math>\pm</math>0.002*</b>
<b>3c</b>	46.184 $\pm$ 1.041	27.163 $\pm$ 0.864	>1000
<b>3d</b>	39.821 $\pm$ 0.727	21.841 $\pm$ 0.711	>1000
<b>3e</b>	<b>67.131<math>\pm</math>1.334</b>	29.364 $\pm$ 0.836	>100
<b>3f</b>	42.427 $\pm$ 0.955	22.458 $\pm$ 0.755	>1000
<b>3g</b>	<b>64.396<math>\pm</math>1.295</b>	24.927 $\pm$ 0.957	>100
<b>3h</b>	41.920 $\pm$ 0.841	24.664 $\pm$ 0.667	>1000
<b>3i</b>	<b>72.397<math>\pm</math>1.608</b>	26.814 $\pm$ 0.839	>100
<b>3j</b>	45.167 $\pm$ 0.863	20.789 $\pm$ 0.958	>1000
<b>Letrozole</b>	98.246 $\pm$ 2.654	95.344 $\pm$ 1.768	0.026 $\pm$ 0.001

### 5.4. Pharmacokinetic Profile

Prediction of the absorption, distribution, metabolism, and elimination (ADME profile) of the drug molecule are not less important than its interaction with the enzyme receptor. The physicochemical parameters of the synthesized derivatives were estimated

by *in silico* method using (SwissADME) program [91]. The most important physicochemical properties to be determined are molecular weight (Mw), hydrogen bond acceptors (HBA), hydrogen bond donors (HBD), topological polar surface area (TPSA), lipophilicity descriptor (LogP), water solubility descriptor (LogS), gastrointestinal absorption (GIA), and the drug-likeness based on Lipinski's "Rule of Five" [92], which correlate the physicochemical properties to pharmacokinetic of drugs. All were determined for the synthesized compounds **3a-3j** and compared with the reference letrozole. The results are in **Table 5.2**.

**Table 5.2.** *The in silico physicochemical parameters*

	Physicochemical parameters				Pharmacokinetic properties			Drug likeness
	Mw	HBA	HBD	TPSA	LogP	LogS	GIA	
<b>3a</b>	381.47	4	0	116.17	3.83	-6.61	High	5/5
<b>3b</b>	395.5	4	0	116.17	4.15	-6.99	High	5/5
<b>3c</b>	411.5	5	0	125.4	3.75	-6.77	High	5/5
<b>3d</b>	431.53	4	0	116.17	4.61	-7.91	High	4/5
<b>3e</b>	399.46	5	0	116.17	4.09	-6.71	High	5/5
<b>3f</b>	415.92	4	0	116.17	4.27	-7.26	High	4/5
<b>3g</b>	406.48	5	0	139.96	3.53	-6.82	Low	4/5
<b>3h</b>	450.36	4	0	116.17	4.84	-7.92	High	4/5
<b>3i</b>	450.36	4	0	116.17	4.84	-7.92	High	4/5
<b>3j</b>	421.49	5	0	129.31	4.19	-7.65	Low	4/5
<b>Letrozole</b>	285.3	4	0	78.29	2.32	-4.03	High	5/5

**HBA:** Hydrogen bond acceptors, **HBD:** Hydrogen bond donors, **TPSA:** Topological polar surface area (Å<sup>2</sup>), **Log P:** Lipophilicity indicator, **Log S:** Water solubility indicator, **GIA:** Gastrointestinal absorption, **Mw:** Molecular weight g/mol

The calculated molecular weight of the compounds **3a-3j** ranged between (381.47-450.36) g/mol, higher than letrozole 285.3 g/mol. All the compounds showed HBA character from 4 to 5 and no HBD similar to letrozole.

Topological polar surface area values were calculated between (116.17-139.96) Å<sup>2</sup>.

The highest calculated value of LogP is 4.84 for the compounds **3h** and **3i** and the lowest value is 3.53 for the compound **3g**, the nearest value to that of letrozole.

The absorption from the GI tract is high for most compounds except **3g** and **3j** as they have a higher number of hydrogen bond accepting groups, thus a higher hydrophilic character. According to the Lipinski rule of five, this poor absorption affects the drug-likeness potentiality of these compounds.

The physicochemical parameters of the most active compound **3b** are comparable to that of standard letrozole. It obeys the five rules of Lipinski and exhibits a high GI absorption suggesting it can be used orally and acts as HBA and HBD the same as

letrozole does. The HBA character is important for aromatase inhibition activity because the natural ligand androstenedione act as HBA. These similarities in the ADME profile of the compound **3b** with letrozole add additional value to its reported AI activity.

However, the *in silico* ADME study gives a preliminary idea of the potentiality of the drug to be effective. Still, it does not determine whether the compounds comply with the rule, but they have a better chance of reaching the market because they are less likely to be eliminated during clinical trials.

### 5.5. Molecular Docking Analysis

Computational chemistry plays a critical role in determining the biological activity of derivatives, validating the results of a SAR study, and understanding the possible interaction modes of the most active molecules with the active binding site.

Studying structural details of aromatase enzyme assists in better understanding the possible interactions between ligand and enzyme active site. The X-ray crystal structure of the aromatase enzyme (PDB ID: 3EQM) was retrieved from the protein data bank server.

The human monomeric aromatase enzyme is part of the endoplasmic reticulum consisting of heme attached to a long polypeptide chain consisting of 503 amino acids. The distal cavity of the heme-binding pocket is the active binding site of the aromatase enzyme. By investigation of the crystal structure of the aromatase-androstenedione complex, it is clear that it binds with  $\beta$ -face to orient the C19 methyl group toward the iron of the heme at a distance of 4.0Å, and to orient, the C17 and C3 keto groups toward the amino group of Met374 and Asp309 residue of the recognition site to form a hydrogen bond which is important for ligand localization. The van der Waals interactions formed by androstenedione are important for its interaction with a catalytic cleft, the amino acid residues namely, Leu477, Ile133, Met374, Arg115, Phe134, Phe221, Ala306, Thr310, Trp224, Val370, and Val373, were found at the active site of the aromatase enzyme [93, 94].

In the molecular docking study of NSAIs (letrozole) the most important amino acid involved in its interaction with enzyme were M374, R115, I133, W224, L228, I305, A306, V370, L372, V373, F134, D309, R435, T310, L477 as well as heme iron [95].

The 2D pose and 3D pose of the most active compound **3b** obtained from docking studies are presented in **Figure 5.44** and **Figure 5.45**.

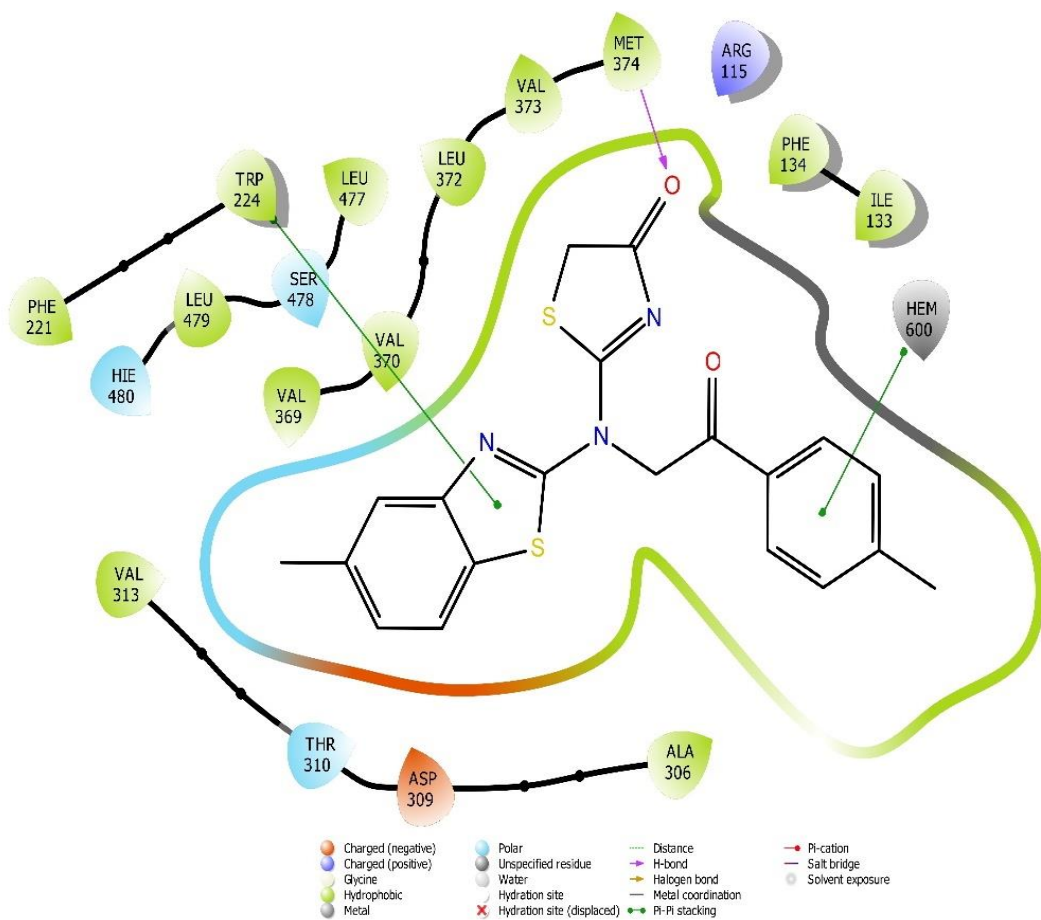


**Figure 5.44.** The 2D pose of the compound **3b** with aromatase enzyme

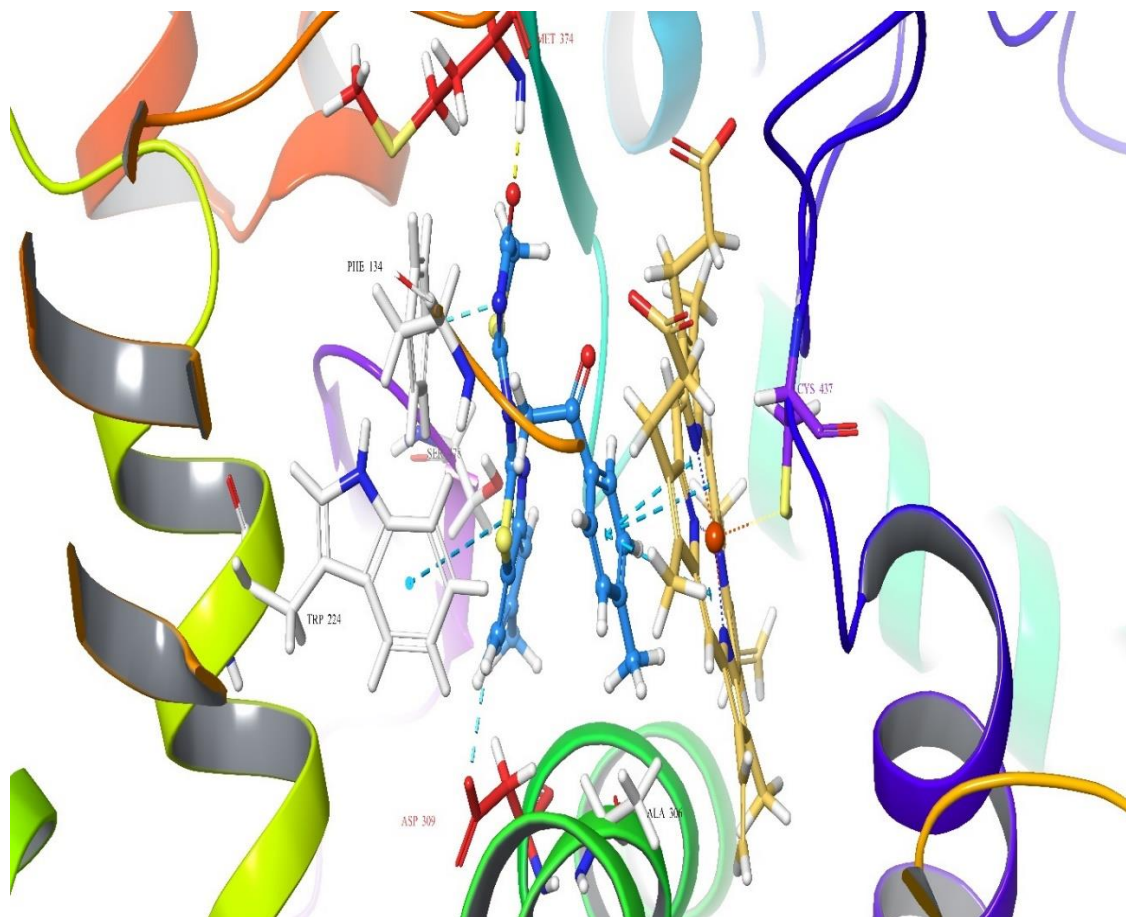


**Figure 5.45.** The 3D pose of the compound **3b** with aromatase enzyme

Molecular docking study of the 2D pose of the compound **3b** reveals that the interaction between the enzyme active binding site and the drug molecule results from three intermolecular interactions:  $\pi$ - $\pi$  interaction between benzothiazole ring and indole of the Trp224,  $\pi$ - $\pi$  interaction between the aromatic phenyl ring and the Hem600, and the hydrogen bonding between the oxygen (a proton acceptor) of the carbonyl group and amino residue of the Met374. At the same time, the 3D pose showed an additional hydrogen bond with Asp309 amino acid residue. The two hydrogen bonds with Met374 and Asp309 are essential for ligand recognition and positioning.

According to the results from both *in vitro* (aromatase inhibition assay) and *in silico* (docking study), compound **3b** fits well with the aromatase enzyme and inhibits the enzyme by making different intermolecular interaction bonds with the most important amino acid residues reported in the enzyme active interaction sites (recognition site and the heme core of activity).

## 5.6. Structure Activity Relationship Study

SAR studies are extremely valuable and necessary, helping to understand the activity of a molecule, designing new compounds, and eliminating and clarifying the adverse effects of current medications.

The active binding site of the aromatase enzyme must recognize the substrate at particular positions similar to its natural ligand. The recognition site has an amino acid residue Met374 that forms a hydrogen bond with the (C=O, -OH) at the C17 of androstenedione and testosterone, respectively, and the (C=O) group at C3 acts as an acceptor for hydrogen bonding with Asp309 residue, thus availability of hydrogen bond acceptors are essential for the affinity of the ligand [33, 96].

The ligand's positioning to the aromatase enzyme cleft is ensured by the hydrophobic interaction made by a hydrophobic portion of the molecule, similar to that of a natural steroid [97].

The oxidation of the methyl group at C19 by the oxygen of active Hem causing aromatization of ring A and synthesis of estrogen is the most important site to be blocked for inhibition activity to the aromatase enzyme. This blockage is done by the coordination of electron pairs of azole heteroatom with an empty orbital of the ferrous (Fe)<sup>+2</sup> of Hem600 and preventing the access of Hem600 to the C19 and the subsequent aromatization [98].

The azole which also act as an acceptor for hydrogen bonding and other H-bond acceptor functionalities must be of a certain distance to each other, like that between C19 and C17 or C3 of the endogenous ligand which is calculated to be around 10.25Å [96].

The hydrophobic pocket in the active binding site is small, explaining the high inhibitory result achieved by compound **3b** with methyl substituent (optimum lipophilic group and small in size). Similarly, compound **3e** with fluoro substituent at the para position of the phenyl ring showed around 67% of inhibition because it has a small size. The 3',4'-disubstitution in compound **3i** showed 72% of inhibition which is more favorable than 2',4'-disubstitution shown in compound **3h**. The lowest inhibition value was reported to compound **3d** with bulky aryl substitution.

Additionally, the electronic effect of substituent also affects the aromatase inhibition activity. Most studies reported that the electron-withdrawing substituent is preferred for inhibition activity, and almost all the clinically available NSAIs (fadrozole, anastrozole, and letrozole) have a cyano substituent on the para position of the aryl group.

This finding was confirmed by activity achieved by the derivative **3g** with an inhibitory percent around 64%, which has a CN group also located at the para position of the phenyl ring. This is explained by the electron-withdrawing group at the para position may be involved in some electronic or  $\pi$ - $\pi$  interactions with the enzyme [33, 99].

The structural requirements for the aromatase inhibition activity are concluded as follows:

1. Theazole containing heterocycles are essential for aromatase inhibition activity to coordinate with  $\text{Fe}^{+2}$  part of heme.
2. The hydrophobic aryl group is essential for the activity to interact with enzyme active binding site by hydrophobic interaction and to improve binding affinity.
3. The presence of hydrogen bond acceptors is essential for the recognition and localization of ligands.
4. The shape and the size of the molecule lead to favorable steric interaction with the target.
5. The size and electronic effect of different substituents also affect activity.

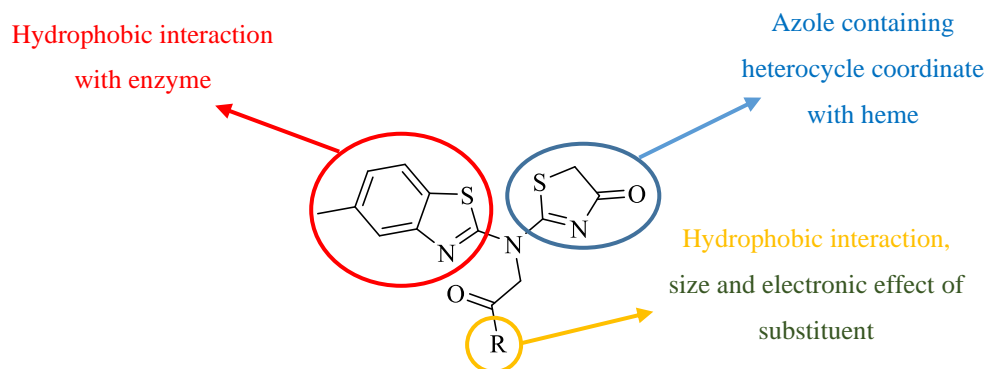


**Figure 5.46.** *The general requirements for aromatase inhibition activity*

## 6. CONCLUSION AND RECOMMENDATIONS

Within our research framework, ten compounds of thiazolinone derivatives were synthesized by efficient procedures from the starting benzothiazole ring and purified. Their chemical structures were elucidated and confirmed by infrared spectroscopy (IR), high-resolution mass spectroscopy (HRMS), proton nuclear magnetic resonance ( $^1\text{H-NMR}$ ), and carbon-13 nuclear magnetic resonance ( $^{13}\text{C-NMR}$ ) analysis methods. After their structures were elucidated, they were investigated for inhibition of aromatase enzyme.

The compound **3i** showed  $72.397 \pm 1.608$  % of inhibition at concentration  $10^{-3}\text{M}$ , and the compounds **3e** and **3g** showed ( $67.131 \pm 1.334$ ,  $64.396 \pm 1.295$ ) % of inhibition, respectively, at the same dilution. These inhibitory presents are insufficient for these compounds to have  $\text{IC}_{50}$  value but indicate they are good candidates for further optimization.

While the compound **3b** (2-((5-methylbenzothiazol-2-yl)[2-oxo-2-(p-tolyl)ethyl]amino)thiazol-4(5H)-one) revealed the highest activity in the *in vitro* study (aromatase inhibition assay) with  $\text{IC}_{50}$  value  $0.041 \pm 0.002$   $\mu\text{M}$ , which is about 1.6 fold lower in activity compared to the drug letrozole. The *in silico* study of the compound **3b** displayed it fits well to the enzyme pocket and interacted with the most important amino acid residues in the active binding site (Hem600, Met374, Asp309, and Trp224). In conclusion, compound **3b** docking result goes parallel with the *in vitro* result of enzyme test.

The physicochemical parameters of the most active compound **3b** were studied by *in silico* method and the results were comparable to that of standard letrozole, as it fully obeys the drug-likeness rules and exhibited a high absorption through the GI tract suggesting its oral administration.

In general, the synthesized compounds were projected to have a greater inhibitory effect on aromatase enzyme when compared to the available medications and similar structures in the literature. On the basis of molecular docking studies, future investigations should focus on the antifungal and anticancer activities, which are predicted to be promising for these derivatives. The synthesis of derivatives with diverse substituents on benzothiazole-thiazolinone skeleton based on bio-isosteric modification and SAR studies till the optimum blocker is reached.

## REFERENCES

- [1] Roberts, K., Rickett, K., Greer, R., Woodward, N. (2017). Management of aromatase inhibitor induced musculoskeletal symptoms in postmenopausal early Breast cancer: A systematic review and meta-analysis. *Crit Rev Oncol Hematol*, 111, 66-80.
- [2] Hyder, T., Marino, C.C., Ahmad, S., Nasrazadani, A., Brufsky, A.M. (2021). Aromatase Inhibitor-Associated Musculoskeletal Syndrome: Understanding Mechanisms and Management. *Front Endocrinol (Lausanne)*, 12, 713700.
- [3] Hu, Z., He, B., Ma, L., Sun, Y., Niu, Y., Zeng, B. (2017). Recent Advances in Ergosterol Biosynthesis and Regulation Mechanisms in *Saccharomyces cerevisiae*. *Indian J Microbiol*, 57 (3), 270-277.
- [4] Trosken, E.R., Fischer, K., Volkel, W., Lutz, W.K. (2006). Inhibition of human CYP19 by azoles used as antifungal agents and aromatase inhibitors, using a new LC-MS/MS method for the analysis of estradiol product formation. *Toxicology*, 219 (1-3), 33-40.
- [5] Zarn, J.A., Brusweiler, B.J., Schlatter, J.R. (2003). Azole fungicides affect mammalian steroidogenesis by inhibiting sterol 14 alpha-demethylase and aromatase. *Environ Health Perspect*, 111 (3), 255-261.
- [6] Wouters, W., De Coster, R., Goeminne, N., Beerens, D., van Dun, J. (1988). Aromatase inhibition by the antifungal ketoconazole. *J Steroid Biochem*, 30 (1-6), 387-389.
- [7] Mayhoub, A.S., Marler, L., Kondratyuk, T.P., Park, E.J., Pezzuto, J.M., Cushman, M. (2012). Optimization of the aromatase inhibitory activities of pyridylthiazole analogues of resveratrol. *Bioorg Med Chem*, 20 (7), 2427-2434.
- [8] Yahiaoui, S., Fagnere, C., Pouget, C., Buxeraud, J., Chulia, A.J. (2008). New 7,8-benzoflavanones as potent aromatase inhibitors: synthesis and biological evaluation. *Bioorg Med Chem*, 16 (3), 1474-1480.
- [9] Shah, R., Rosso, K., Nathanson, S.D. (2014). Pathogenesis, prevention, diagnosis and treatment of breast cancer. *World J Clin Oncol*, 5 (3), 283-298.
- [10] Fisusi, F.A., Akala, E.O. (2019). Drug Combinations in Breast Cancer Therapy. *Pharm Nanotechnol*, 7 (1), 3-23.

- [11] Sandhu, R., Parker, J.S., Jones, W.D., Livasy, C.A., Coleman, W.B. (2010). Microarray-Based Gene Expression Profiling for Molecular Classification of Breast Cancer and Identification of New Targets for Therapy. *Lab Med*, 41 (6), 364-372.
- [12] Azawi, S., Liehr, T., Rincic, M., Manferrari, M. (2020). Molecular Cytogenomic Characterization of the Murine Breast Cancer Cell Lines C-127I, EMT6/P and TA3 Hauschka. *Int J Mol Sci*, 21 (13)
- [13] *Cochrane Database of Systematic Reviews*,
- [14] Gu, G., Dustin, D., Fuqua, S.A. (2016). Targeted therapy for breast cancer and molecular mechanisms of resistance to treatment. *Curr Opin Pharmacol*, 31, 97-103.
- [15] Bodmer, A., Castiglione-Gertsch, M. (2011). Role of hormonal manipulations in patients with hormone-sensitive metastatic breast cancer. *Eur J Cancer*, 47 Suppl 3, S28-37.
- [16] Beresford, M., Tumor, I., Chakrabarti, J., Barden, J., Rao, N., Makris, A. (2011). A qualitative systematic review of the evidence base for non-cross-resistance between steroidal and non-steroidal aromatase inhibitors in metastatic breast cancer. *Clin Oncol (R Coll Radiol)*, 23 (3), 209-215.
- [17] Burstein, H.J., Lacchetti, C., Anderson, H., Buchholz, T.A., Davidson, N.E., Gelmon, K.A., Giordano, S.H., Hudis, C.A., Solky, A.J., Stearns, V., Winer, E.P., Griggs, J.J. (2019). Adjuvant Endocrine Therapy for Women With Hormone Receptor-Positive Breast Cancer: ASCO Clinical Practice Guideline Focused Update. *J Clin Oncol*, 37 (5), 423-438.
- [18] Early Breast Cancer Trialists' Collaborative, G. (2015). Aromatase inhibitors versus tamoxifen in early breast cancer: patient-level meta-analysis of the randomised trials. *Lancet*, 386 (10001), 1341-1352.
- [19] Nowaczyk, A., Kowiel, M., Gzella, A., Fijalkowski, L., Horishny, V., Lesyk, R. (2014). Conformational space and vibrational spectra of 2-[(2,4-dimethoxyphenyl)amino]-1,3-thiazolidin-4-one. *J Mol Model*, 20 (8), 2366.
- [20] Ramsh, S.M., Smorygo, N.A., Ginak, A.I. (1984). Structure of 2-amino-4-thiazolinone. *Chem Heterocycl Com*, 20 (8), 865-869.
- [21] Qiu, K.M., Wang, H.H., Wang, L.M., Luo, Y., Yang, X.H., Wang, X.M., Zhu, H.L. (2012). Design, synthesis and biological evaluation of pyrazolyl-thiazolinone

- derivatives as potential EGFR and HER-2 kinase inhibitors. *Bioorg Med Chem*, 20 (6), 2010-2018.
- [22] Chen, S., Chen, L., Le, N.T., Zhao, C., Sidduri, A., Lou, J.P., Michoud, C., Portland, L., Jackson, N., Liu, J.J., Konzelmann, F., Chi, F., Tovar, C., Xiang, Q., Chen, Y., Wen, Y., Vassilev, L.T. (2007). Synthesis and activity of quinolinyl-methylene-thiazolinones as potent and selective cyclin-dependent kinase 1 inhibitors. *Bioorg Med Chem Lett*, 17 (8), 2134-2138.
- [23] Al-Ansary, G.H., Ismail, M.A., Abou El Ella, D.A., Eid, S., Abouzid, K.A. (2013). Molecular design and synthesis of HCV inhibitors based on thiazolone scaffold. *Eur J Med Chem*, 68, 19-32.
- [24] Xiao, M., Xu, L., Lin, D., Lian, W., Cui, M., Zhang, M., Yan, X., Li, S., Zhao, J., Ye, J., Liu, A., Hu, A. (2021). Design, synthesis, and bioassay of 4-thiazolinone derivatives as influenza neuraminidase inhibitors. *Eur J Med Chem*, 213, 113161.
- [25] Dwivedi, J., Devi, K., Asmat, Y., Jain, S., Sharma, S. (2016). Synthesis, characterization, antibacterial and antiepileptic studies of some novel thiazolidinone derivatives. *J Saudi Chem Soc*, 20, S16-S20.
- [26] Haouas, B., Saied, T., Ayari, H., Arfaoui, Y., Benkhoud, M.L., Boujlel, K. (2016). Electrogenated base-promoted synthesis and antimicrobial activity of 2-imino-1,3-thiazolidin-4-one derivatives. *J Sulfur Chem*, 37 (4), 391-400.
- [27] Liu, H.-L., Lieberzeit, Z., Anthonsen, T. (2000). Synthesis and Fungicidal Activity of 2-Imino-3-(4-arylthiazol-2-yl)-thiazolidin-4-ones and Their 5-Arylidene Derivatives. *Molecules*, 5 (12), 1055-1061.
- [28] Rostamizadeh, S., Aryan, R., Ghaieni, H.R., Amani, A.M. (2009). Solvent-free chemoselective synthesis of some novel substituted 2-arylbenzimidazoles using amino acid-based prolinium nitrate ionic liquid as catalyst. *Journal of Heterocyclic Chemistry*, 46 (1), 74-78.
- [29] Ali, Y., Alam, M.S., Hamid, H., Husain, A., Dhulap, A., Hussain, F., Bano, S., Kharbanda, C. (2016). Molecular modeling and synthesis of some new 2-imino-4-thiazolidinone derivatives with promising TNF- $\alpha$  inhibitory activity. *New J Chem*, 40 (1), 711-723.
- [30] Raghdah, M.A., Raheem Jameel, M., Basim Jasim, H. (2019). Synthesis, characterization and pharmacological activity of new 2-imino-thiazolidine-4-one derivatives. *Int J Res Pharm Sci*, 10 (3), 1763-1769.

- [31] Ottana, R., Maccari, R., Barreca, M.L., Bruno, G., Rotondo, A., Rossi, A., Chiricosta, G., Di Paola, R., Sautebin, L., Cuzzocrea, S., Vigorita, M.G. (2005). 5-Arylidene-2-imino-4-thiazolidinones: design and synthesis of novel anti-inflammatory agents. *Bioorg Med Chem*, 13 (13), 4243-4252.
- [32] Singh, N., Tripathi, A.C., Tewari, A., Kumar, R., Saraf, S.K. (2014). Ulcerogenicity devoid novel non-steroidal anti-inflammatory agents (NSAIDs): syntheses, computational studies, and activity of 5-arylidene-2-imino-4-thiazolidinones. *Med Chem Res*, 24 (5), 1927-1941.
- [33] Adhikari, N., Amin, S.A., Saha, A., Jha, T. (2017). Combating breast cancer with non-steroidal aromatase inhibitors (NSAIs): Understanding the chemico-biological interactions through comparative SAR/QSAR study. *Eur J Med Chem*, 137, 365-438.
- [34] Asiri, Y.I., Alsayari, A., Muhsinah, A.B., Mabkhot, Y.N., Hassan, M.Z. (2020). Benzothiazoles as potential antiviral agents. *J Pharm Pharmacol*, 72 (11), 1459-1480.
- [35] Sharma, P.C., Bansal, K.K., Deep, A., Pathak, M. (2017). Benzothiazole Derivatives as Potential Anti-Infective Agents. *Curr Top Med Chem*, 17 (2), 208-237.
- [36] Aggarwal, S., Paliwal, D., Kaushik, D., Gupta, G.K., Kumar, A. (2018). Pyrazole Schiff Base Hybrids as Anti-Malarial Agents: Synthesis, In Vitro Screening and Computational Study. *Comb Chem High Throughput Screen*, 21 (3), 194-203.
- [37] Racane, L., Pticek, L., Sedic, M., Grbcic, P., Kraljevic Pavelic, S., Bertosa, B., Sovic, I., Karminski-Zamola, G. (2018). Eco-friendly synthesis, in vitro anti-proliferative evaluation, and 3D-QSAR analysis of a novel series of monocationic 2-aryl/heteroaryl-substituted 6-(2-imidazoliny)benzothiazole mesylates. *Mol Divers*, 22 (3), 723-741.
- [38] Haroun, M. (2019). Novel Hybrids of Pyrazolidinedione and Benzothiazole as TZD Analogues. Rationale Design, Synthesis and *In vivo* Anti-Diabetic Evaluation. *Med Chem*, 15 (6), 624-633.
- [39] Husain, A., Madhesia, D., Rashid, M., Ahmad, A., Khan, S.A. (2016). Synthesis and *in vivo* diuretic activity of some new benzothiazole sulfonamides containing quinoxaline ring system. *J Enzyme Inhib Med Chem*, 31 (6), 1682-1689.

- [40] Zheng, X.J., Li, C.S., Cui, M.Y., Song, Z.W., Bai, X.Q., Liang, C.W., Wang, H.Y., Zhang, T.Y. (2020). Synthesis, biological evaluation of benzothiazole derivatives bearing a 1,3,4-oxadiazole moiety as potential anti-oxidant and anti-inflammatory agents. *Bioorg Med Chem Lett*, 30 (13), 127237.
- [41] Stevens, M.F., McCall, C.J., Lelieveld, P., Alexander, P., Richter, A., Davies, D.E. (1994). Structural studies on bioactive compounds. 23. Synthesis of polyhydroxylated 2-phenylbenzothiazoles and a comparison of their cytotoxicities and pharmacological properties with genistein and quercetin. *J Med Chem*, 37 (11), 1689-1695.
- [42] Kanafani, Z.A., Perfect, J.R. (2008). Antimicrobial resistance: resistance to antifungal agents: mechanisms and clinical impact. *Clin Infect Dis*, 46 (1), 120-128.
- [43] Trosken, E.R., Scholz, K., Lutz, R.W., Volkel, W., Zarn, J.A., Lutz, W.K. (2004). Comparative assessment of the inhibition of recombinant human CYP19 (aromatase) by azoles used in agriculture and as drugs for humans. *Endocr Res*, 30 (3), 387-394.
- [44] Santen, R.J., Petroni, G.R., Fisch, M.J., Myers, C.E., Theodorescu, D., Cohen, R.B. (2001). Use of the aromatase inhibitor anastrozole in the treatment of patients with advanced prostate carcinoma. *Cancer*, 92 (8), 2095-2101.
- [45] Cannarella, R., Condorelli, R.A., Barbagallo, F., La Vignera, S., Calogero, A.E. (2021). Endocrinology of the Aging Prostate: Current Concepts. *Front Endocrinol (Lausanne)*, 12, 554078.
- [46] Kmetova Sivonova, M., Jurecekova, J., Tatarkova, Z., Kaplan, P., Lichardusova, L., Hatok, J. (2017). The role of CYP17A1 in prostate cancer development: structure, function, mechanism of action, genetic variations and its inhibition. *Gen Physiol Biophys*, 36 (5), 487-499.
- [47] Patel, V., Liaw, B., Oh, W. (2018). The role of ketoconazole in current prostate cancer care. *Nat Rev Urol*, 15 (10), 643-651.
- [48] Batalo, M., Nagaiah, G., Abraham, J. (2011). Cognitive dysfunction in postmenopausal breast cancer patients on aromatase inhibitors. *Expert Rev Anticancer Ther*, 11 (8), 1277-1282.
- [49] Hurria, A., Patel, S.K., Mortimer, J., Luu, T., Somlo, G., Katheria, V., Ramani, R., Hansen, K., Feng, T., Chuang, C., Geist, C.L., Silverman, D.H. (2014). The effect

- of aromatase inhibition on the cognitive function of older patients with breast cancer. *Clin Breast Cancer*, 14 (2), 132-140.
- [50] Tralongo, P., Di Mari, A., Ferrau, F. (2005). Cognitive impairment, aromatase inhibitors, and age. *J Clin Oncol*, 23 (18), 4243.
- [51] Blanchet, J., Zhu, J. (2004). Reeve's synthesis of 2-imino-4-thiazolidinone from alkyl (aryl) trichloromethylcarbinol revisited, a three-component process from aldehyde, chloroform and thiourea. *Tetrahedron Lett*, 45 (23), 4449-4452.
- [52] da Silva Santos, J., Junior, J.J., da Silva, F.M. (2018). 1,3-Thiazolidin-4-ones: Biological Potential, History, Synthetic Development and Green Methodologies. *Curr Org Synth*, 15 (8), 1109-1123.
- [53] Egan, R.S., Tadanier, J., Garmaise, D.L., Gaunce, A.P. (2002). Intermediates in the Hantzsch thiazole synthesis. *J Org Chem*, 33 (12), 4422-4426.
- [54] Babadjamian, A., Metzger, J., Chanon, M. (1975). Etude du mécanisme de la réaction de hantzsch des thiazoles. I. Mise en évidence et détermination des produits intermédiaires et de dégradation. *J Hetero Chem*, 12 (4), 643-649.
- [55] Reeve, W., Nees, M. (2002). Reactions of Aryl(trichloromethyl)carbinols with Sulfur Nucleophiles. Formation and Proof of Zwitterionic Structure of Iminothiazolidinones. *J Am Chem Soc*, 89 (3), 647-651.
- [56] Appalanaidu, K., Kotcherlakota, R., Dadmal, T.L., Bollu, V.S., Kumbhare, R.M., Patra, C.R. (2016). Synthesis and biological evaluation of novel 2-imino-4-thiazolidinone derivatives as potent anti-cancer agents. *Bioorg Med Chem Lett*, 26 (21), 5361-5368.
- [57] Abdu-Allah, H.H., Abdel-Moty, S.G., El-Awady, R., El-Shorbagi, A.N. (2016). Design and synthesis of novel 5-aminosalicylate (5-ASA)-4-thiazolinone hybrid derivatives with promising antiproliferative activity. *Bioorg Med Chem Lett*, 26 (7), 1647-1650.
- [58] Sahin, Z., Ertas, M., Berk, B., Biltekin, S.N., Yurttas, L., Demirayak, S. (2018). Studies on non-steroidal inhibitors of aromatase enzyme; 4-(aryl/heteroaryl)-2-(pyrimidin-2-yl)thiazole derivatives. *Bioorg Med Chem*, 26 (8), 1986-1995.
- [59] W, S.R., Saleh, E.M., Menon, V., Vazhappilly, C.G., Abdu-Allah, H.H.M., El-Shorbagi, A.A., Mansour, W., El-Awady, R. (2020). Induction of DNA damage, apoptosis and cell cycle perturbation mediate cytotoxic activity of new 5-

- aminosalicylate-4-thiazolinone hybrid derivatives. *Biomed Pharmacother*, 131, 110571.
- [60] Osmaniye, D., Gorgulu, S., Saglik, B.N., Levent, S., Ozkay, Y., Kaplancikli, Z.A. (2021). Design, synthesis, in vitro and in silico studies of some novel thiazole-dihydrofuran derivatives as aromatase inhibitors. *Bioorg Chem*, 114, 105123.
- [61] Evren, A.E., Nuha, D., Dawbaa, S., Saglik, B.N., Yurttas, L. (2022). Synthesis of novel thiazolyl hydrazone derivatives as potent dual monoamine oxidase-aromatase inhibitors. *Eur J Med Chem*, 229, 114097.
- [62] Osmaniye, D., Levent, S., Sağlık, B.N., Karaduman, A.B., Özkay, Y., Kaplancıklı, Z.A. (2022). Novel imidazole derivatives as potential aromatase and monoamine oxidase-B inhibitors against breast cancer. *New J Chem*, 46 (16), 7442-7451.
- [63] Desai, N.C., Joshi, V.V., Rajpara, K.M. (2012). Synthesis of new quinoline-2-pyrazoline-based thiazolinone derivatives as potential antimicrobial agents. *Med Chem Res*, 22 (8), 3663-3674.
- [64] Stana, A., Vodnar, D.C., Tamaian, R., Pirnau, A., Vlase, L., Ionut, I., Oniga, O., Tiperciuc, B. (2017). Design, Synthesis and Antifungal Activity Evaluation of New Thiazolin-4-ones as Potential Lanosterol 14 $\alpha$ -Demethylase Inhibitors. *Int J Mol Sci*, 18 (1)
- [65] Lino, C.I., Goncalves de Souza, I., Borelli, B.M., Silverio Matos, T.T., Santos Teixeira, I.N., Ramos, J.P., Maria de Souza Fagundes, E., de Oliveira Fernandes, P., Maltarollo, V.G., Johann, S., de Oliveira, R.B. (2018). Synthesis, molecular modeling studies and evaluation of antifungal activity of a novel series of thiazole derivatives. *Eur J Med Chem*, 151, 248-260.
- [66] Eissa, S.I., Farrag, A.M., Abbas, S.Y., El Shehry, M.F., Ragab, A., Fayed, E.A., Ammar, Y.A. (2021). Novel structural hybrids of quinoline and thiazole moieties: Synthesis and evaluation of antibacterial and antifungal activities with molecular modeling studies. *Bioorg Chem*, 110, 104803.
- [67] Keri, R.S., Patil, M.R., Patil, S.A., Budagumpi, S. (2015). A comprehensive review in current developments of benzothiazole-based molecules in medicinal chemistry. *Eur J Med Chem*, 89, 207-251.
- [68] Bogert, M.T., Naiman, B. (2002). Researches on Thiazoles. XX. The Synthesis of Benzothiazoles from Aldehydes and Ortho-aminothiophenol. The Action of

- Aldehydes upon Zinc Ortho-aminothiophenolate and upon Related Thionated Aromatic Amines. *J Am Chem Soc*, 57 (9), 1529-1533.
- [69] Facchinetti, V., da R. Reis, R., R.B. Gomes, C., R.A. Vasconcelos, T. (2012). Chemistry and Biological Activities of 1,3-Benzothiazoles. *Mini-Rev Org Chem*, 9 (1), 44-53.
- [70] Fan, X., He, Y., Wang, Y., Xue, Z., Zhang, X., Wang, J. (2011). A novel and practical synthesis of 2-benzoylbenzothiazoles and 2-benzylbenzothiazoles. *Tetrahedron Lett*, 52 (8), 899-902.
- [71] Downer-Riley, N.K., Jackson, Y.A. (2007). Iodine-mediated cyclisation of thiobenzamides to produce benzothiazoles and benzoxazoles. *Tetrahedron*, 63 (41), 10276-10281.
- [72] Shi, D.F., Bradshaw, T.D., Wrigley, S., McCall, C.J., Lelieveld, P., Fichtner, I., Stevens, M.F. (1996). Antitumor benzothiazoles. 3. Synthesis of 2-(4-aminophenyl)benzothiazoles and evaluation of their activities against breast cancer cell lines in vitro and in vivo. *J Med Chem*, 39 (17), 3375-3384.
- [73] Solomon, V.R., Hu, C., Lee, H. (2009). Hybrid pharmacophore design and synthesis of isatin-benzothiazole analogs for their anti-breast cancer activity. *Bioorg Med Chem*, 17 (21), 7585-7592.
- [74] Tzanopoulou, S., Sagnou, M., Paravatou-Petsotas, M., Gourni, E., Loudos, G., Xanthopoulos, S., Lafkas, D., Kiaris, H., Varvarigou, A., Pirmettis, I.C., Papadopoulos, M., Pelecanou, M. (2010). Evaluation of Re and (99m)Tc complexes of 2-(4'-aminophenyl)benzothiazole as potential breast cancer radiopharmaceuticals. *J Med Chem*, 53 (12), 4633-4641.
- [75] Makowska, A., Wolff, L., Saczewski, F., Bednarski, P.J., Kornicka, A. (2019). Synthesis and cytotoxic evaluation of benzoxazole/benzothiazole-2-imino-coumarin hybrids and their coumarin analogues as potential anticancer agents. *Pharmazie*, 74 (11), 648-657.
- [76] Zhao, S., Zhao, L., Zhang, X., Liu, C., Hao, C., Xie, H., Sun, B., Zhao, D., Cheng, M. (2016). Design, synthesis, and structure-activity relationship studies of benzothiazole derivatives as antifungal agents. *Eur J Med Chem*, 123, 514-522.
- [77] Luo, B., Li, D., Zhang, A.L., Gao, J.M. (2018). Synthesis, Antifungal Activities and Molecular Docking Studies of Benzoxazole and Benzothiazole Derivatives. *Molecules*, 23 (10)

- [78] Ballari, M.S., Herrera Cano, N., Wunderlin, D.A., Feresin, G.E., Santiago, A.N. (2019). One-pot sequential synthesis and antifungal activity of 2-(benzylsulfonyl)benzothiazole derivatives. *RSC Advances*, 9 (50), 29405-29413.
- [79] Havrylyuk, D., Mosula, L., Zimenkovsky, B., Vasylenko, O., Gzella, A., Lesyk, R. (2010). Synthesis and anticancer activity evaluation of 4-thiazolidinones containing benzothiazole moiety. *Eur J Med Chem*, 45 (11), 5012-5021.
- [80] Prabhu, P.P., Panneerselvam, T., Shastry, C.S., Sivakumar, A., Pande, S.S. (2015). Synthesis and anticancer evaluation of 2-phenyl thiazolidinone substituted 2-phenyl benzothiazole-6-carboxylic acid derivatives. *J Saudi Chem Soc*, 19 (2), 181-185.
- [81] Patel, R.V., Park, S.W. (2014). Catalytic N-formylation for synthesis of 6-substituted-2-benzothiazolylimino-5-piperazinyl-4-thiazolidinone antimicrobial agents. *Res Chem Intermediat*, 41 (8), 5599-5609.
- [82] Çevik, U.A., Osmaniye, D., Levent, S., Sağlık, B.N., Çavuşoğlu, B.K., Özkay, Y., Kaplancıklı, Z.A. (2020). Synthesis and characterization of a new series of thiadiazole derivatives as potential anticancer agents. *Heterocycl Commun*, 26 (1), 6-13.
- [83] DEODHAR\*, M.N., , A.C.D.a.S.D.K. (2012). Analgesic and Antiinflammatory Activity of Derivatives of 2-Aminobenzothiazole. *Asian J Chem*, 24
- [84] Omar, Y.M., Abdel-Moty, S.G., Abdu-Allah, H.H.M. (2020). Further insight into the dual COX-2 and 15-LOX anti-inflammatory activity of 1,3,4-thiadiazole-thiazolidinone hybrids: The contribution of the substituents at 5th positions is size dependent. *Bioorg Chem*, 97, 103657.
- [85] Acar Çevik, U., Kaya Cavusoglu, B., Sağlık, B.N., Osmaniye, D., Levent, S., Ilgin, S., Ozkay, Y., Kaplancikli, Z.A. (2020). Synthesis, Docking Studies and Biological Activity of New Benzimidazole- Triazolothiadiazine Derivatives as Aromatase Inhibitor. *Molecules*, 25 (7)
- [86] (2020): Schrödinger Release 2020-3, Maestro Schrödinger, LLC, New York, NY, USA.
- [87] (2020): Schrödinger Release 2020-3, LigPrep 2020 Schrödinger, LLC, New York, NY, USA.
- [88] (2020): Schrödinger Release 2020-3, Glide Schrödinger, LLC, New York, NY, USA.

- [89] Li, W.-Y., Song, Y., Chen, H.-B., Yang, W.-L. (2014). Synthesis of 2-amino-5-mercapto-1,3,4-thiadiazole derivatives. *Heterocycl Commun*, 20 (1)
- [90] Pavia, D.L., Lampman, G.M., Kriz, G.S., Vyvyan, J.R. (2015). *Introduction to Spectroscopy*, Fifth Edition.
- [91] Daina, A., Michielin, O., Zoete, V. (2017). SwissADME: a free web tool to evaluate pharmacokinetics, drug-likeness and medicinal chemistry friendliness of small molecules. *Sci Rep*, 7, 42717.
- [92] Lipinski, C.A., Lombardo, F., Dominy, B.W., Feeney, P.J. (1997). Experimental and computational approaches to estimate solubility and permeability in drug discovery and development settings. *Adv Drug Deliver Rev*, 23 (1-3), 3-25.
- [93] Ghosh, D., Griswold, J., Erman, M., Pangborn, W. (2010). X-ray structure of human aromatase reveals an androgen-specific active site. *J Steroid Biochem Mol Biol*, 118 (4-5), 197-202.
- [94] Hong, Y., Li, H., Yuan, Y.C., Chen, S. (2009). Molecular characterization of aromatase. *Ann N Y Acad Sci*, 1155, 112-120.
- [95] Suvannang, N., Nantasenamat, C., Isarankura-Na-Ayudhya, C., Prachayasittikul, V. (2011). Molecular Docking of Aromatase Inhibitors. *Molecules*, 16 (5), 3597-3617.
- [96] Banting, L., Smith, H.J., James, M., Jones, G., Nazareth, W., Nicholls, P.J., Hewlins, M.J., Rowlands, M.G. (1988). Structure-activity relationships for non-steroidal inhibitors of aromatase. *J Enzyme Inhib*, 2 (3), 215-229.
- [97] Adhikari, N., Baidya, S.K., Jha, T. (2020). Effective anti-aromatase therapy to battle against estrogen-mediated breast cancer: Comparative SAR/QSAR assessment on steroidal aromatase inhibitors. *Eur J Med Chem*, 208, 112845.
- [98] Wood, P.M., Woo, L.W., Labrosse, J.R., Thomas, M.P., Mahon, M.F., Chander, S.K., Purohit, A., Reed, M.J., Potter, B.V. (2010). Bicyclic derivatives of the potent dual aromatase-steroid sulfatase inhibitor 2-bromo-4-[(4-cyanophenyl)(4h-1,2,4-triazol-4-yl)amino]methyl}phenylsulfamate: synthesis, SAR, crystal structure, and in vitro and in vivo activities. *ChemMedChem*, 5 (9), 1577-1593.
- [99] Doiron, J., Soultan, A.H., Richard, R., Toure, M.M., Picot, N., Richard, R., Cuperlovic-Culf, M., Robichaud, G.A., Touaibia, M. (2011). Synthesis and

structure-activity relationship of 1- and 2-substituted-1,2,3-triazole letrozole-based analogues as aromatase inhibitors. *Eur J Med Chem*, 46 (9), 4010-4024.